Metal-organic framework based nanomaterials: An advanced review of their synthesis and energy storage applications

Jhalak Gupta[1], Faiza Habib[2*], Akram Alfantazi[3*], Mohd Zahid Ansari[4*], Zubair Ahmad[4*] and Mudasir A Yatoo[5*]

[1]*Department of Physics, Aligarh Muslim University, Aligarh, 202002, India*
[2]*Department of Chemistry, University College London, WC1H 0AJ, UK*
[3]*Department of Chemical Engineering, Khalifa University, Abu Dhabi 127788, UAE*
[4]*School of Chemical Engineering, Yeungnam University, Gyeongbuk 38541, Republic of Korea*
[5]*Department of Materials, Faculty of Engineering, Imperial College London, SW7 2AZ, UK*

ABSTRACT

Metal-organic frameworks (MOFs) have emerged as a versatile class of porous materials with enormous potential for various applications, including energy storage devices. In this review, we present a comprehensive analysis of the recent advancements and applications of MOFs in the field of energy storage. We begin by providing a brief overview of the fundamental aspects of MOFs, including their synthesis, structural diversity, and tuneable properties.

We then focus on the utilisation of MOFs in advanced energy storage systems with a particular focus on supercapacitors. MOFs can be employed as electrode materials, separators, and catalysts, offering enhanced electrochemical performance, improved charge/discharge rates, and prolonged cycling stability. The unique tunability of MOFs allows for the rational design of tailored materials with desired properties, such as high specific capacity, excellent conductivity, and superior cycling stability. We will further discuss in detail the recent developments in MOF-based electrochemical capacitors, highlighting the significant progress made in achieving high energy and power densities. The exceptional charge storage capacity of MOFs combined with their facile synthesis and scalability make them promising candidates for next-generation energy storage technologies.

The review further sheds light on the challenges and opportunities in the practical implementation of MOFs in energy storage devices with an eye on future research and development in the MOFs for energy applications. The manuscript discusses perspectives and future directions and, we believe, the insights presented are timely and will be of particular help to young and early-stage researchers.

Corresponding authors: Faiza Habib, faiza.habib@ucl.ac.uk; Akram Alfantazi, akram.alfantazi@ku.ac.ae; Zahid Ansari, zahid.smr@yu.ac.kr; Zubair Ahmad, zubair7157@yu.ac.kr and Mudasir A. Yatoo, m.yatoo15@imperial.ac.uk.

1. INTRODUCTION

Almost everything around us requires energy to be built and kept in working order. However, two-thirds of all greenhouse gas emissions worldwide are caused by the production and consumption of energy. As a result of mankind's excessive use of fossil fuels, fossil fuel sources have been rapidly depleted, and air pollution has increased, causing long-lasting and possibly irreparable harm to our climate. For society to develop sustainably, it is imperative to address the problem of climate change. At the same time, it is crucial to guarantee access to energy to promote economic growth and improve quality of life, particularly in less developed regions of the world. The globe is currently moving toward renewable energy sources like solar energy, wind energy, and so on. To effectively gather and store the energy produced by renewable sources is difficult in moving away from fossil fuels. Unfortunately, renewable energy sources are sporadic in nature and not entirely exploitable at the time of production. Therefore, there is a critical need for effective energy storage systems to utilise green energy in the future. There are many different types of effective energy conversion and storage devices on the market right now, including batteries, conventional capacitors, electrochemical capacitors, fuel cells and hydrogen storage systems [1, 2, 3]. Fuel cells including solid oxide fuel cells because of their superior efficiency and fuel flexibility too are being investigated heavily by the scientific community [4, 5, 6]. Due to their superior electrochemical characteristics, which include a high specific power, rapid charging/discharging rate and outstanding cycling life, supercapacitors or electrochemical capacitors (ECs) have garnered significant attention among them. In contrast to batteries, modern supercapacitors still have low specific energy. The Ragone plot for several energy storage systems, including fuel cells, supercapacitors, traditional batteries and regular capacitors is shown in Figure 1.1. This graph shows the amount of particular energy (Wh/kg) and specific power (W/kg) for each device as a function of discharging time (E=Pt). Batteries may provide a lot of energy (100–200Wh/kg), but because they take longer to recharge, their specific power performance suffers [7]. Due to their higher specific power (500–10,000 W/kg) compared to batteries and their satisfying specific energy (1–10 Wh/kg) compared to conventional capacitors, supercapacitors are recognised as important members of the energy storage family [8]. It is also important to note that supercapacitors have an increased cycle lifespan and can be fully charged/discharged at a fast rate [9]. Two key strategies have been thoroughly investigated for boosting the specific energy to get beyond this restriction: (i) fabricating high specific

capacitance advanced supercapacitors, and (ii) expanding the potential window from the electrolyte chosen [10-13].

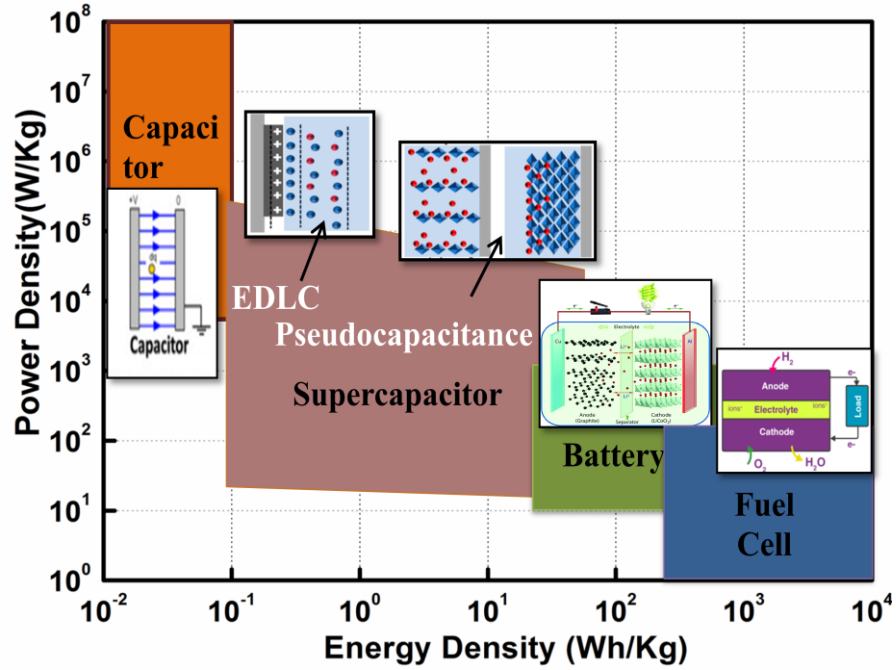

Figure 1.1. Ragone plot for different energy storage systems.

Two electrodes that are segregated make up the basic supercapacitor design. A separator, a type of semi-permeable membrane, is used to protect against electrical contact between electrodes [14]. The membrane is slightly porous to allow for high ionic conductivity and ionic charge transport with low thickness, high electrical impediment, and conductivity combining to produce the best results. The separator and electrodes are then submerged in an electrolytic solution, that is by allowing the flow of current between electrodes, you can stop cells from discharging. This permits the electronic current from flowing across the electrodes by allowing the flow of ionic current instead. removing the cells' charge [15].

The overall charge that can be held in a supercapacitor is limited by the kind of electrolyte and electrode surface area as compared to a battery's entire electrode and total active mass. Supercapacitors operate similarly to traditional capacitors. Supercapacitors have increased capacitance (F/g, F/cm^2) because their electrodes have a large surface area and new electrode materials, and electrolytes can boost supercapacitors' energy density. There are three types of

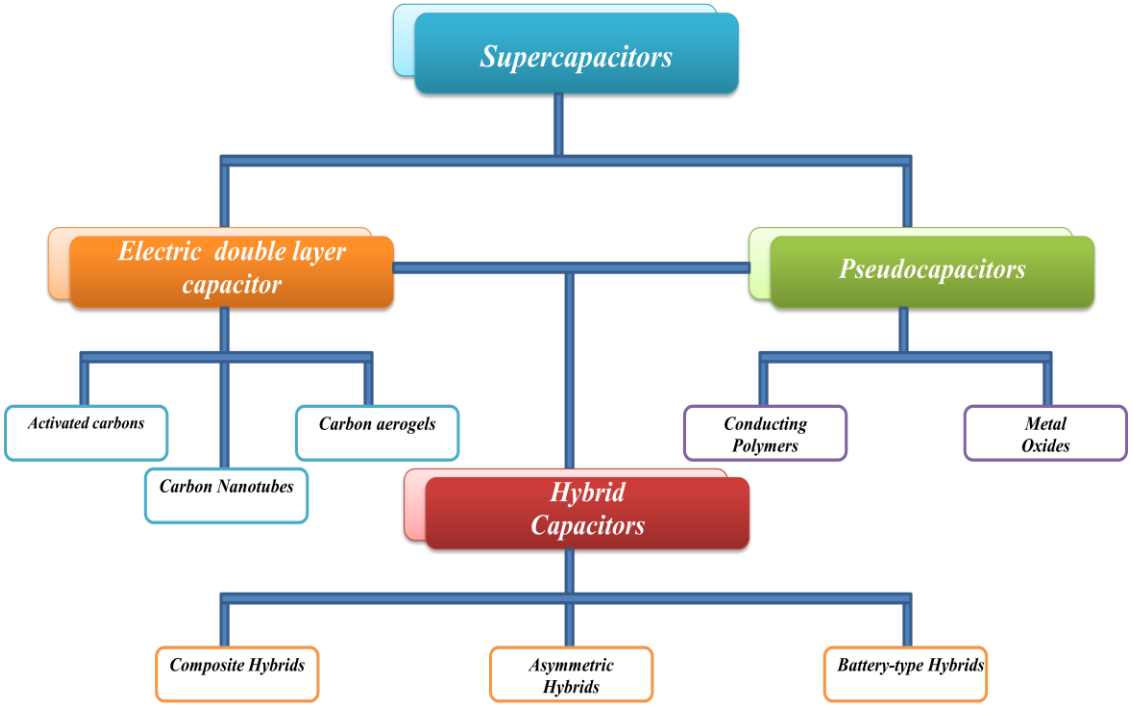

Figure 2.1 Classification of supercapacitors.

supercapacitors – electrochemical double-layer capacitors (EDLCs), pseudocapacitors, and hybrid capacitors – depending on the charge storage mechanism [14]. The electrochemical double-layer capacitors, sometimes referred to as EDLCs, are devices that electrostatically store charge at the junction of an electrode and electrolyte, resulting in positive and negative ions' double layers. In pseudo capacitance, energy is stored by the redox process, but in EDLCs, energy is stored through ions adsorption between electrode and electrolyte. Highly porous materials are used in the fabrication of electrodes for EDL capacitors. The Faradic reaction at the electrode-electrolyte interface is the source of the energy storage mechanism in pseudocapacitors (PCs) (Figure 1.2) [16].

PC electrodes are typically built using metal oxides and conducting polymers. The electrode material's surface area and increased micropore volume affect SC efficiency. Although conducting polymers and metal oxides have relatively high surface areas, the electrolyte has relatively limited access to the active surface area. Metal oxide and carbon-based composites are not affected by this problem. Third-generation hybrid SCs are these types [17].

Material made from MOFs has recently received great attention for energy storage applications. Aside from their relatively poor conductivity and lack of chemical/structural robustness, pristine

MOFs have important properties like high specific surface area, acceptable porosity, electrochemical activity, tuneable morphology, stability, multi functionalities and conductivity. These items can inherit the primary [18], inheriting only the fundamental compositional and structural properties from their precursors of MOFs [19]. In the construction of hollow nano/ micro structured materials with prolonged interior space and shells that are functional, MOFs are frequently utilised as sacrifice templates and metal precursors [20]. SCs have numerous applications in energy backup, hybrid electric vehicles, automation, and portable electronics such as UPS and IT, phones [21]. Energy is stored in SCs using two different processes. Pseudo capacitance is the second and the first is referred to as electrochemical double-layer capacitance (EDLC) [22].

2. ENERGY STORAGE MECHANISMS IN SUPERCAPACITORS

Theelectrolyte either develops a thin layer or penetrates the pores of the electrode surface in the absence of voltage [23]. Figure 2.1 shows the general operating mechanism in SCs. When voltage is given to an electrode, counter ions are attracted while comparable ions are repelled [24]. The cation/anion ratio changes throughout this process, allowing the electrode to charge. However, due to Coulomb interaction at the electrode, adsorbed species still contain both kinds of ions, and this procedure causes counter ions to enter extremely restricted locations [25]. An equal amount of potential is stored on each electrode in a system with two electrodes. Charged double layers in a capacitor caused the charge-discharge process, which resulted in reversible electrostatic accumulation of charged species on the electrode surface [26]. Both electrodes function as anodes and cathodes, respectively.

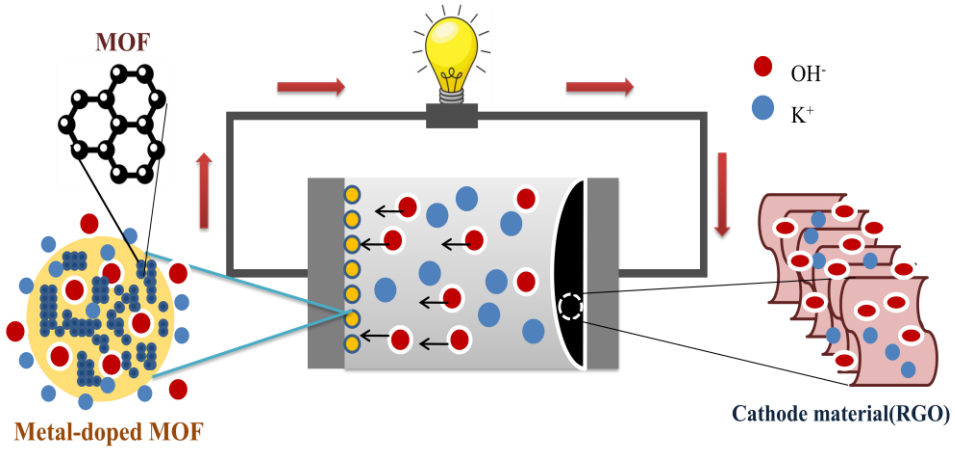

Figure 2.1. Working mechanism of MOF-based supercapacitors.

Cathode and anode emit positive and negative ions, respectively, when the potential is applied. These ions condense into a layer that is parallel to the electrode surface. The SC's overall capacitance is computed as:

$$^1/_C = {}^1/_{C_C} + {}^1/_{C_A} \qquad (2.1)$$

where C is the total capacitance, C_C is the cathode capacitance and C_A is the anode capacitance.

Materials innovation and design have been one important route to obtaining better-performing SCs. MOFs are one class of material being investigated vigorously and these materials have primarily been utilised as supercapacitor electrodes [27]. The effectiveness, dependability, structural stability, and design and construction methods of the electrodes have all been covered. The study's results are evaluated critically, and the significance of upcoming challenges is highlighted.

3. SYNTHESIS OF MOF NANOSTRUCTURES

An organic linker and a metal ion or cluster form coordination bonds to produce MOFs, a subclass of supramolecular porous coordination polymers. As a result, they have compositions that can be controlled and are highly adaptable to three-dimensional architectures. Additionally, they serve as essential templates for the creation of derived materials with morphologies that are greatly optimised. Yaghi's and Li's groups first developed MOFs in the 1990s. MOF materials are frequently created by co-precipitation, solvothermal, mechanochemical, liquid phase diffusion, microwave assistance, electrochemical, sonochemical, or stacking of metal ion connective species with bridging ligands that are frequently organic. Different synthetic processes can result in different crystallisation speeds, particle sizes, size distributions, adsorption characteristics, and morphologies, all of which have a direct impact on the features of the resulting MOF material and its by-products.

Materials with a variety of particular porosities and surface areas, adsorption abilities, electrochemical and catalytic performances, chemical and functional behaviours, and more, can be attained thanks to the remarkable versatility and practicality of MOFs structures and compositions. The oxygen reduction reaction (ORR), oxygen evolution reaction (OER), hydrogen evolution reaction (HER), and carbon dioxide reduction are only a few electrochemical

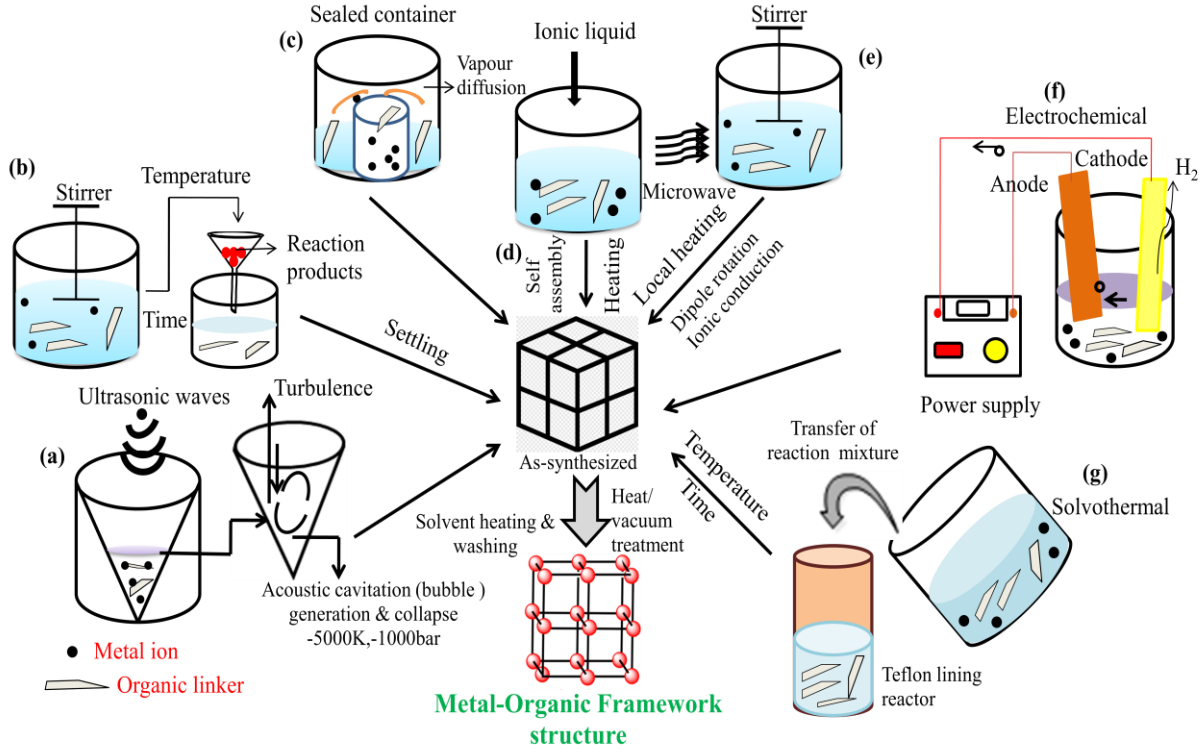

Figure 3.1. List of the different MOF synthesis techniques: (a) sonochemical synthesis (b) conventional solution (c) diffusion (d) ionothermal process (e) microwave-assisted synthesis (f) electrochemical synthesis and (g) solvothermal synthesis. Reproduced with permission from [39].

reactions that can have their MOF properties changed. They might also be used as electrode materials in equipment like supercapacitors, batteries, and fuel cells. We can investigate their potential capacitive and Faradaic capabilities in energy conversion and storage devices thanks to their distinctive porous architectures consisting of organic connectors and metal ions that resemble Prussian Blue-like materials. However, the electronic and hopping charge-diffusion performs less effectively than anticipated because of structural instability and generally weak electrical conductivity. As a result, methods to enhance these characteristics while enhancing the electrochemical characteristics were investigated, resulting in MOF-derived materials.

By evaluating the characteristics and structures of pure MOF, it may be possible to produce framework structures with desirable characteristics, such as a family of MOFs with the same symmetry (IRMOF): IRMOF-1 through IRMOF-16. [28, 29]. According to the institution where they were discovered, groups of MOFs are categorised, including HKUST-1 (Hong Kong University of Science and Technology), MIL-1 (Materials Institute Lavoisier), and UiO-1 (Universitetet I Oslo) [30]. Fe, Cu, Zn, Co, and other metal ions are encircled by nitrogen-based

tetrahedra and connected to imidazole rings, that can serve several purposes. The ZIF (zeolite imidazolate framework) is a number and acronym that can be used to create these MOFs [31]. Among the several other categories, researchers classify synthesised MOFs as MOP-1, F-MOF-1, and CPL [30]. Additionally, larger pore width benefits increased porosity and longer organic ligands, resulting in a longer connection between inorganic SBU [32]. As molecular building blocks, MOFs can modify their physical and chemical characteristics because they can be produced with a range of metal centres and ligands [33]. The enormous specific surface area and pore volume of MOFs make them well-suited for immobilising molecular catalysts on conductive substrates [34]. Additionally, it is possible to modify these materials to enhance their high selectivity for particular chemical reactions. The optical band gap of MOF semiconductors can be set between 1.0 and 5.5 eV, according to theoretical simulations [30, 35].

As formerly said, two main parts make up MOFs: linkers, also known as bridging elements or metal ions, and organic linker ligands. Metal ions and organic linkers are typically combined to create MOFs in a mild environment. Certain conditions must be satisfied to produce a crystalline and porous surface. As shown in Figure 3.1, several MOF compounds have been produced during the past 20 years using a range of synthetic techniques [36, 37, 38]. The different MOFs-based nanostructures' synthesis routes are shown in Table 3.1.

3.1. Conventional synthesis routes: The most widely used conventional approach for MOF synthesis is called the "solvo/hydrothermal method," in which the metal salt, organic linker, and frequent templates are dissolved in an organic solvent or solution in a reaction vessel. To produce the desired MOF, the reaction mixture is heated for a short period at a particular temperature under enhanced pressure in an autoclave or sample vial.

Without parallelization in the standard synthesis routes, Standard electric heating was used to carry out the synthesis processes. An important consideration in the preparation of MOFs is reaction temperature. The type of reaction setup is determined by the solvothermal (SVT) and non-solvothermal (non-SVT) temperature ranges. In isolated containers, SVT reactions are conducted above the solvent’s boiling point at ambient pressure and temperature (Figure 3.1(g)). However, non-SVT reactions occur at the solvent's boiling point or a lower boiling point under a reasonable amount of pressure, simplifying the synthesis process' requirements. [40, 41]. Using water as a solvent is referred to as the "hydrothermal (HDT) approach." For a given structure,

adjustments are made to solvent composition, pressure, reagent concentration, temperature, and other synthesis variables [42]. Only mixing the initial components enabled the preparation of well-known MOFs such as MOF-5, HKUST-1, MOF-74, ZIF-8 and MOF177 at standard temperature [43, 44, 45, 46]. The direct precipitation method, which uses this technique, shows how the crystallisation of a small number of MOFs essentially takes place quickly. Surprisingly, a few of these MOFs, including ZIF-8, have exceptional chemical and thermal stabilities. The formation of the product is greatly affected by the reaction temperature. As a result, structures become more condensed at higher temperatures [47, 48]. The crystalline morphological structure is, however, highly impacted by temperature variations, and a protracted response time can also result in MOF failure [49].

3.2. Microwave-Assisted Route: Microwave-assisted (MWA) synthesis is based on the core idea of combining electromagnetic radiation with mobile electronic carriers. These carriers can be electrons or ions in solids or polar molecules or ions in liquids. As shown in Figure 3.1(e), MOFs are frequently synthesised by MWA at temperatures more than 100 ºC and reaction periods no longer than 60 minutes [50]. A few papers discuss how to alter the composition and reaction parameters, such as process temperature, solvent, reactant quantity, irradiation intensity, and irradiation time among others, to optimise reaction conditions. Smaller crystals can be synthesised more quickly with MW irradiation than with conventional electric heating (CEH) [50, 51]. The advantages of MW-assisted MOF synthesis, such as crystallisation acceleration, nanoparticle formation, and improved product purity, are connected to the solution's quick boiling and nucleation rate [50].

Using the MWA synthesis method, a large number of metal carboxylate-based MOFs (M = Fe, Cr, Ti, Ce, Zn etc.) were produced. The first MOF, CrMIL-100, was produced with a 44% yield by MW irradiation at 220 ºC for 4 hours [52, 53]. The MW irradiation-based synthesis of CrMIL-101 led to uniform nanoscale size. CrMIL-101 nanocrystals with diameters of around 50 nm were created by lowering the quantity or raising the pH of the reactants, yielding 37% without the use of hydrofluoric acid (HF) [54]. Using DMF as the solvent, in 10 minutes at 150ºC, 200 nm-diameter FeMIL-101 crystalline nanoparticles were produced [55]. With a yield of 27%, in 10 minutes at 95 ºC, cubic-structured IRMOF-1 (isoreticular MOF) crystals with lengths ranging from 2 to 4 lm were created. A further study found that decreasing the H2BDC content in the

preparatory solution decreased the highly crystalline IRMOF-1's size (down to 1 lm in diameter) and shape [56]. HKUST-1/MW@H3PW12O40 was synthesised by Zou *et al.* utilising a more effective microwave irradiation technique at 395 K for 20 min. The synthetic HKUST-1/MW (10-20 lm diameter) had a large surface area of 1405 m^2g^1, a pore capacity of 0.58 cm^3g^1, exceptional chemical stability, and a limited ability to synchronise H_2O compounds. The build-up of polyoxometalate (H3PW12O40), which filled the MOFs nanopores, improved the stability of HKUST-1/ MW in water [57]. Ni-CPO-27 (crystal size: 22 to 28 nm) was made via MWA synthesis at reaction temperatures of 90 to 130 ºC for 60 minutes of irradiation. Lee *et al.* investigated the effects of irradiation time and response temperature on the pore size and shape of this material [58].

3.3. Electrochemical synthesis: Due to its benefits, such as gentle reaction conditions and quick synthesis times, electrochemical synthesis has a significant position in the field of material research. About MOF synthesis specifically, this method enables real-time adjustment of MOF structure, direct deposition of MOF thin films with adjustable characteristics on various chosen substrates and obviates the requirement for counter anion separation of metals because no metal salts are employed. Additionally, because electrochemical processes are confined, MOF thin film production can be controlled without surface pre-treatment.

MIL-100(Al), HKUST-1 and NH2MIL-53(Al) are examples of prototypical MOFs that were prepared utilising electrochemical cells through anodic dissolution. According to Joaristi *et al.*, several reaction parameters, such as temperature, solvents, current density (J_C), and electrolytes have an impact on the conclusion of the production process and the surface characteristics of the MOF that is generated [59] (Figure 3.1(f)). To generate Ni-MOFs in situ in nickel form, Cao *et al.* created a scalable and inexpensive ELC method (NF). With no additional processing, the resulting Ni-MOFs rod-like array self-assembled into a structure that is flower-shaped while retaining its function as an electrode material without binders. It also possessed a massive specific capacity of 5.10 Ccm^2 at J_C of 2.0 $mAcm^2$ [60].

By developing an ELC synthesis procedure for several Zn and Cu-based MOFs, Mueller *et al.* published a ground-breaking work. In their report, many fusions of electrode components (Co, Zn and Cu) and linkers (H_2BDC, $H_2BDC(OH)_2$, and 1,2,3-H_3BTC) were described, enabling to scale-up of the synthesis process. These mixtures could be used to produce a large number of Cu

and Zn-based compounds with large pores and high surface areas [61]. To contrast the impacts of the various procedures on the properties of the molecule, Schlesinger *et al*. synthesised HKUST-1 using ELC and SVT methodologies at ambient pressure. When using the ELC method, adding conducting salts or linkers inside the porous areas after crystallisation produced a subpar result. At room temperature and air pressure, using the ELC synthesis technique, Wei *et al.* successfully created an ultra-stable UiO-66-NH2 (Zr-based MOFs). Surprisingly, synthetic UiO-66-NH2 outperformed UiO-66-NH2 created via the SVT method for fluorescence detection of Fe^{3+} ions in water [62]. An ELC method was employed to create the bi-ligand Zn (1, 3-BDC)0.5 MOF (bzim). The purity and yield of the products were influenced by the processing time as well as the J_C. The best yield (87%) and purest MOFs were created under the optimal circumstances of 60 mA current for two hours [63].

3.4. Mechanochemical route for synthesis: Mechanical force can cause a wide variety of physical phenomena and chemical reactions. When two solid materials are ground together, the mechanical energy disrupts the crystalline structure's order, creating fissures and new surfaces, leading to a complex series of transformations. When two solids meet, they deform and sometimes even melt, generating hot spots where molecules can undergo extraordinarily intense vibrational excitation, breaking bonds, and producing several products [64]. Pichon *et al.* performed the first mechanochemical (MCL) synthesis of a porous MOF, Cu (INA)2 (isonicotinic acid, INA), without the use of any solvents. The results showed robust 3D linkage and could be measured by grinding Cu-acetate and isonicotinic acid for 10 minutes without applying heat [65]. A complete analysis of solvent-free MCL synthesis using combinations of a few metals (Ni, Cu, or Zn with various counter ions) and carboxylate-based linkers were also published by the same group. The XRPD results showed that [66] combinations were measurable and [67] combinations gave rise to crystalline molecules. HKUST-1 and Cu $(INA)_2$, among other well-known and novel co-ordination polymers, created nanoporous combinations [68]. The rising interest in mechanically induced MOF synthesis can be attributed to several factors. Since procedures can be performed without the use of solvents at room temperature., this has a favourable effect on the environment [69].

Additionally, metal-oxides can be used in place of metals as starting materials, producing H_2O as a by-product. It has been shown that ZnO is suitable for making pillared-layered MOF. Metal

oxides were hardly ever used in established solution procedures because of their poor solubility [70, 71]. A collection of three-dimensional MOFs joined by direct linkers and diamine pillars and including di-nuclear paddle wheel components were successfully produced and thoroughly classified by Chun *et al*. The architecture was unaffected by the anisotropic alteration of the linkers and pillars made possible by the metal-diamine-dicarboxylate co-ordination. Two-dimensional layers were formed using linear linkers like 1,4-bdc and tmbdc, while perpendicular connections between the sheets were made by diamine ligands like DABCO and BPY connected at the edges of Zn_2 sweeping wheel entities. The side groups of the 1,4-bdc derivatives were used to create the exposed frameworks [Zn_2(1,4-bdc) (tmbdc) (dabco)] and [Zn_2(1,4-bdc)$_2$ (dabco)], which both possessed various diameters of open apertures and nanopores [72].

3.5. Sonochemical synthesis: Sonochemical procedures (SCL), which use homogenous and rapid nucleation, can produce substantially smaller particles and have a faster crystallisation duration than traditional SVT technologies [73, 74]. Once a reaction combination is subjected to high-energy ultrasound, SCL is produced. Although it is frequently claimed that ultrasound is sound above the range at which the human ear can perceive it, ultrasound falls within the entire range of audible sound. As shown in Figure 3.1(a), sound can be divided into three categories: Ultrasound can be categorized as low frequency (20 to 100 kHz), middle frequency (100 kHz to 1 MHz), and high frequency (above 1 MHz) (1 to 10 MHz) [75]. Acoustic cavitation, the emergence and dissolution of bubbles created in a solution during sonication, results in extremely high local temperatures and pressures (greater than 1000 $K.s^1$), as well as rapid heating and cooling rates, which are necessary to create crystallites [76, 77]. In 30 minutes, the SCL technique using 1-methyl-2-pyrrolidone (NMP) as the solvent produced outstanding MOF-5 nanocrystals with sizes ranging from 5 to 25 lm [78]. After thorough analysis and comparison, it was discovered that the sample's physical characteristics were almost identical to those of a regularly generated sample. After 5 min of reaction time, HKUST-1 formed nanocrystalline powder (10 to 40 nm) using a DMF/EtOH/H_2O mixed solution, and longer reaction times produced crystals with greater sizes (50 to 200 nm) and higher yields. However, the product only partially disintegrated as a result of the ongoing reaction [79].

The production of nanoporous Fe-fumarate (MIL-88A), with crystals 100 nm in size, was facilitated through ultrasound. Iron (III) chloride hexahydrate and fumaric acid were combined in

a sealed glass flask and heated to 50 ºC in an ultrasonic bath. The reaction parameters, shape, crystalline nature, and yield of generated products were specifically influenced by the Fe content synthesis time, and the base contents [80]. Without the use of a solution phase surfactant, catalyst, or template, according to Tehrani and co-workers, $Zn_3(BTC)_2$ nanorods may be generated under ultrasonic conditions [81]. In a further study, the combinations of the iso structures Ln(BTC)(H_2O) were created utilising (BTC)3 as the linker (Ln = Ce, Tb, or Y). Tb substance was previously produced by ordinary heating, however, by using ultrasonication, the reaction temperature and time may be reduced to 20 minutes and 40 ºC, respectively. 23 lm-long highly crystalline particles were produced. Based on N_2 sorption investigations [82], these compounds also displayed exceptional physical properties. NaOH and triethylamine were used in a sonochemical process with pH-adjusted synthesis conditions to create ZIF-8. In brief, 50 mL of DMF, 0.7 mL of triethylamine, 2 mM zinc nitrate hexahydrate, and 2 mM HMeIm were mixed. The resulting mixture was transferred to a 70 mL reactor using a power-regulating ultrasonicator. The ZIF-8 samples were synthesised and then immersed in DMF, deposited in methyl alcohol, and dried at 80 ºC [83].

3.6. Ionic liquids as a synthesis means: Because of their distinctive characteristics, such as their nearly insignificant vapour pressure, recyclability, improved solubility capabilities, and increased thermal stability, ionic liquids (ILs) have gained great attention as a solvent for chemical reactions [84]. Inorganic solvents or water are typically used to make MOFs, although recently, ILs have become more popular. The most popular IL for making MOFs is 1-alky-3-methyl imidazolium. While deep eutectic solvents (fusions of two or more combinations with melting points lower than any components) were used to create MOFs (Figure 3.1(d)) [85], exhibiting solvent behaviours comparable to ILs. Based on thermal stability, in the SVT synthesis of the co-ordination polymer [Cu(I) (bpp)], Jin *et al.* investigated the characteristics of an IL, [bmim][BF4] (bmim = 1-butyl 3-methylimidazolium; bpp = 1,3-bis (4-pyridyl) propane).BF4. Additionally, the structure of the synthesised polymer was unique from that of polymers made using conventional techniques. According to this study's findings, ILs may be a promising new type of pure and active solvent for the synthesis and crystallisation of co-ordination polymers [86].

Ionothermal conditions were used to generate poly-oxometalate-based MOFs (POMFs), such as (CH_2L_{12})[(CuL12) ($PMoV_{I9}MoV_3O_{40}$]. Single-crystal data set with an original intuitively linked molecular structural design were produced [87]. They consist of 2D interconnected polyrotaxane layers with distinctive cyclophanes that result in H-bonded 3D supermolecules. An ionothermal method was presented by Liu *et al.* to produce extremely stable NH_2MIL-53(Al) MOF NPs. Two crucial characteristics of the as-prepared NH_2-MIL-53(Al) included free amine functionalization, which served as a crucial proton carrier, and the formation of 1-ethyl-3-methyl-imidazolium IL complexes, which served as proton-conducting channels. Furthermore, NH_2-MIL53(Al) has an extraordinarily high proton conductivity of 3 $\times 10^5$ S. cm1 at 80 ºC because of its structural thermal endurance (>400 ºC), proving that these MOFs might be utilised to produce proton-conductive materials in anhydrous environments [88]. Wu *et al.* investigated a novel magnesium MOF known as $[Amim]_2$ $[Mg_3(1,4\text{-}NDC)_4$ $(MeIm)_2$ $(H_2O)_2]$ in an ionothermal system using an IL, 1-propylene-3-methyl imidazolium chloride (AmimCl), as both a reactant and a solvent. The connected MeIm was produced in situ during the ionothermal synthesis by AmimCl breaking down [89]. Several [Co-BDC] MOFs, $[RMI]_2[Co_3(BDC)_3X_2]$, were made using an ionothermal reaction and 8 different kinds of 1-methyl-3alkylimidazolium halide [RMI]. A comparable negative 2D $[Co_3(BDC)_3X_2]$ framework have 2 frames with RMI^+ in the interlayer space[90].

3.7. Microfluidic MOF synthesis route: Over the past few decades, high-screening biological and biochemical studies have extensively used droplet-based microfluidic technology. The microfluidic approach to material synthesis has several benefits, including the ability to monitor material production in-situ using optical microscopy and extremely effective mixing into constrained droplets that increases the reaction rate. Additionally, the microdroplets use as opposed to continuous flow enables the avoidance of a crucial problem such as channel obstruction in the presence of solid particles. Before being encapsulated in nanolitre droplets conveyed by the non-polar oil carrier, both organic and metallic precursors are first dissolved in a polar solvent.

Recently, the synthesis of HKUST-1 was studied using a microfluidic system. Cu (OAc) is used to make the aqueous phase. H3BTC was dissolved in 1-octanol at 60 ºC and then combined with $2H_2O$ and polyvinyl alcohol in water at room temperature to produce the organic ligand complex. They used syringe pumps to deliver immiscible liquids to T-junction where they mixed

Table 3.1. Synthesis of different MOF-based nanostructures.

Synthesis Routes	MOF based materials	Metal precursors	Ligands	Solvent	Conditions	Reference
SVT	HKUST-1	$Cu(NO_3)_2.3H_2O$	H_3BTC	EtOH and H_2O	50ºC, 3h	[45]
	ZIF-8	$ZNCl_2$	Hmim	$NaHCO_2$	130ºC, 4h	[96]
	MOF-5	$Zn(NO_3)_2.6H_2O$	H_2BDC	DMF	120ºC,16h	[98]
	Cu-FMOF-4B	$Cu(NO_3)_2.3H_2O$	3-methyl pydridine	DMF and DEF	85 ºC,96h	[97]
	UiO-66	$ZrCl_4$	H_2BDC	DMF	120ºC,24h	[99]
	MIL-101	$Cr(NO_2)_3.9H_2O$	H_2BDC	HF & H_2O	210ºC,60min	[53]
	Mg-MOF-74	$Mg(NO_3)_2.6H_2O$	H_4DOBDC	DMF, EtOH and H_2O	125ºC,24h	[100]
	FeMIL-101	FeCl3	BDC	DMF	150ºC,15min	[55]
MWA	IRMOF-1	$Zn(NO_3)_2.6H_2O$	BDC	DMF	150ºC,24h	[56]
	HKUST1	$Cu(NO3)2.6H_2O$	H_3BTC	Ethanol	120ºC,10min	[57]
	MOF-5	$Zn(NO_3)_2.4H_2O$	H_2BDC	NMP	100ºC,15min	[102]
	ZIF-8	$Zn(NO_3)_2.6H_2O$	MIm	DMF	120ºC,1 min	[101]
ELC	Cu-MOF	Cu plates	BTC	MeOH	1.3A,12V,150 min	[61]
	HKUST-1	Cu rod	BTC	TBAH and H_2O	1.3A,19V,5min	[103]
	Zn-MOF	Zinc plate	1,3-H_2BDC,Hbzim	DMF and EtOH	60mA, 60V,2h	[63]
	UiO-66-NH_2	Metal zirconium	TABA	DMF and acetic acid	2A,4V,1h	[62]
	HKUST-1	$Cu_2(OAc).4(H_2O)_2$	H_3BTC	DMF and EtOH	40kHz,30min	[79]
SCL	MIL-88A	$FeCl_3.6H_2O$	Fumaric acid	MeOH, EtOH and DMF	20kHz,2h	[105]
	Mg-MOF-74	$Mg(NO_3)_2.6H_2O$	2,5-H_4dhtp	DMF,H_2O and EtOH	500W,20kHz,1 h	[104]

to produce an aqueous solvent and an organic combination. These droplets passed through hydrophobic polytetrafluoroethylene tubes before being collected in ethanol, producing the HKUST-1 MOF [91]. It is feasible to create three different core-shell MOF composites: $[Co_3BTC_2]$@$[Ni_3BTC_2]$, MOF-5@diCH_3MOF-5, and Fe_3O_4@ZIF-8 using a new two-step integrated microfluidic synthesis technology in a continuous flow way. In the presence of moisture, MOF-5@diCH_3-MOF-5 demonstrated higher mechanical strength compared to bare MOF-5. By using Knoevenagel condensation, the catalytic activity of Fe_3O_4@ZIF-8 was studied. The time-efficient production of excellent MOF composites having various morphological features was made possible by microfluidics technology [92].

3.8. Dry gel conversion MOF synthesis: A secure technique for producing porous materials is the dry-gel conversion (DGC), which converts amorphous gel powder into crystalline zeolite when it comes into contact with water vapour or volatile amines. Zeolite membranes and zeolites have been produced using it. DGC provides significant advantages over traditional hydrothermal synthesis, including little waste disposal, reduced template consumption, and the potential for continuous production. During the Dry Gel Conversion (DGC) synthesis, an unstructured, dried alumino-silicate gel is transformed into crystal-like zeolite by interacting with water and volatiles [93]. The ecologically friendly DGC synthesis method was used to produce ZIF-8 and Fe-MIL-100. To form ZIF-8, the water steams on the surface of the eutectic mixture of the substrate ($Zn(OAc)_2H_2O$ and HmIM) along with extra HmIM [94]. The DGC approach was used to quickly create FeMIL-100 from Fe^o (metallic iron) and H_3BTC at 165^oC for 4 days [95].

4. NANOMATERIALS MOFs

Using controlled self- and external-templating processes, MOF precursors were converted into MOF-derived nanomaterials with 0D, 1D, 2D, and 3D structures [106, 107, 108]. The direct chemical or thermal modification of pure MOFs is related to self-meditating techniques [106, 109]. Due to the facilitated electron/mass movement, high stability created by strong structure, and an increased number of active sites, the structure and morphology of nanostructured materials greatly contribute to ESC applications[110, 111]. Numerous distinctive physical and chemical properties of MOF derivatives have been carefully examined in ESC. Due to their rich porosity topologies and the presence of both metals and organic linkers, pure MOFs are inherently feasible precursors for various nanostructured metal compounds, heteroatom-doped

carbons, and their composites[112]. Based on the conversion process's reaction mechanism, the synthesis of freestanding MOF derivatives can be divided into two groups: heat transformation and ion exchange [112].

Thermal transformation provides an efficient technique to make numerous freestanding MOF derivatives (e.g., air, N_2, or Ar) by directly pyrolyzing virgin MOFs at a set temperature under particular conditions. Different target derivatives are commonly linked to various pyrolysis temperatures and reactive environments [113]. The creation of nanostructured carbon or carbon-based composites formed from MOFs requires a high pyrolysis temperature (600 to 1000 ºC) in an N_2 or Ar environment [113-115]. The thermal transformation reaction is often carried out in ambient air at a relatively low pyrolysis temperature (250 to 450ºC) to produce nanostructured metal oxides or their composites made from MOFs. Ion exchange, a solid-liquid reaction, is a potent method for producing nanostructured MOF derivatives with adaptable forms and compositions in addition to thermal transformation. Additionally, if the interaction between the metal ion and organic linkers is weaker than that between the metal ion and other inorganic anions, the thermal transition may take place in mild conditions[116-118]. By maintaining the ion diffusion rate at an intermediate range during the conversion process, there are more opportunities to produce superior structural complexity, such as hollow, core-shell, yolk-shell, and multi-shell metal complexes. Overall, the reactant concentration gradient and temperature have a beneficial impact on the ion diffusion rate [118-120].

4.1. 0D MOF nanomaterials: A careful selection of organic ligands, metal nodes and controlled production conditions can be used to produce MOFs with controlled particle sizes and distinct morphologies. These MOF nanocrystals underwent chemical or thermal conversion, but their morphology was preserved, producing NPs with a polyhedral or hollow shape (Figure 4.1). To prevent failure before transformation, MOF-derived unique NPs were created by using crystalline MOF particles with extremely high thermal stability [121]. Different permeable C-based NPs were made using Zn-based MOF NPs with accurate rhombic dodecahedral structures and outstanding heat stability [122, 123]. A ZnO/C nanocomposite was created by partly annealing hydrolysed MOF-5 at various temperatures while nitrogen was present. The petaloid morphology was preserved by ZnO/C-600 and ZnO/C-700 aggregates of ZnO nanoparticles having a porous structure. The outcomes showed that ZnO/C-600 and ZnO/C700 had exceptional

adsorption and photocatalytic activity on the breakdown of methylene blue (MB) when exposed to sunlight [124]. Three zinc-based MOFs, MOF-74, MOF-5 and ZIF-8 were used to make porous ZnO/C nanocomposites. These materials were produced at high temperatures in a water-steam environment, and their photocatalytic H_2 evolution reaction (HER) and photodegradation of organic dye pollutants were evaluated [125]. Hussain *et al.* produced ZnO/C nanocomposites by heating MOF-5 to a high temperature in a single step and subjecting it to various carbonisation atmospheres.

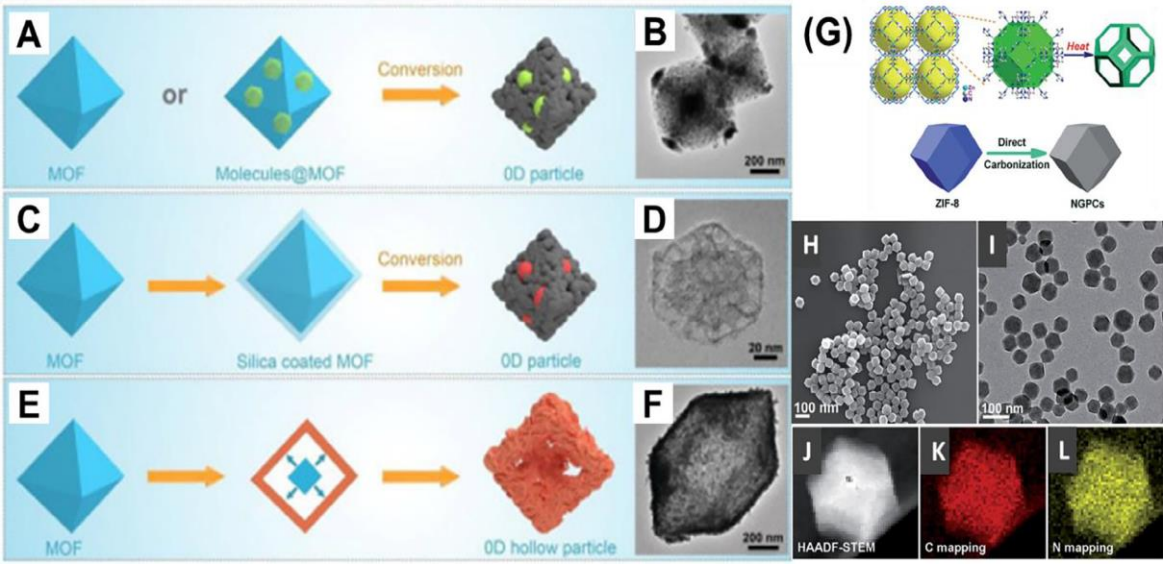

Figure 4.1. (A) 0D particles can be created via morphology-preserved conversion processes from MOF nanoparticles. (B) TEM images of porous MoC_x nano-octahedrons synthesised by method (A). (C) MOF nanoparticles covered with layers of silica prevented buildup during pyrolysis, producing 0D particles. (D) a porous Co/N co-doped carbon nano-framework created by method (C). (E) self-templates for the synthesis of 0D hollow particles. (F) TEM image of hollow Ni/Fe LDH polyhedrons synthesised utilising self-templates made of Fe-based MOF nanocrystals. (G) Nitrogen-doped porous carbon nanopolyhedra synthesised from templates using MOF nanomaterials. (H) and (I) Mono-dispersive ZIF-8 nanopolyhedra shown in SEM and TEM images respectively. The HAADF-STEM pictures of a single carbon polyhedron and the related elemental mapping of C and N are shown in (J), (K), and (L), respectively. A, C and E, reproduced with permission from [126], B reproduced with permission from [127], D reproduced with permission from [128], F reproduced with permission from [129], G to L reproduced with permission from [122].

Iron carbide nanoparticles integrated with carbon nanotubes were created using a dual-MOF restricted pyrolysis approach [130]. Iron carbide nanocrystalline integrated with carbon nanotubes encased in a porous carbon matrix were used to create a complex structured composite material using a unique MOF-in-MOF precursor formed of a Zn-based MOF polyhedron host and several absorbed Fe-based MOF nanorods. Wei *et al.* reported the development of a

molecularly designed and morphologically developed nanostructured electrocatalyst [131]. Using the common Co-based metal-organic framework ZIF-67, nanocrystals of varying sizes and forms were painstakingly created. ZIF-67 was pyrolyzed to produce nitrogen-doped carbon nano-polyhedrons that contained cobalt nanoparticles, and the carbonised by-products kept the nano-size and MOF precursor's shape. Sora *et al.* devised a straightforward technique for producing highly efficient heterogeneous catalysts (M@HCS, M = Au or Ag) by evenly encasing catalytically active Au or Ag nanocrystals within hollow carbon supports (HCS) [132]. To make these hybrid composites, polystyrene@ZIF-8 core-shell particles were pyrolyzed with either Au3+ or Ag+ ions added to the ZIF-8 shell [132].

4.2. 1D MOF nanomaterials: Due to their numerous advantages, one-dimensional nanomaterials like nanotubes, nanofibers, nanowires, and nanorods have gained interest recently in the field of ESC. MOFs with 1D morphologies or MOFs based on 1D external prototypes as precursors were used to creating MOF-derived 1D nanomaterials [133, 134]. When creating MOF-derived 1D nanomaterials, which would be employed as self-templates, the precise manufacture of 1D MOF regulated the morphology and preserved chemical or thermal transformation. One method for making 1D carbon nanorods uses 1D MOFs nanorods with unstable Zn-components as originators. The precursors of the MOFs were dissolved, and unstable Zn species were eliminated via a pyrolysis reaction at 1000 ºC using rod-shaped Zn-based MOFs as their template. 1D carbon nanorods were produced as a result, and they might be employed as electrode resources for SC applications [131]. A combination of very porous nitrogen-doped C and CNTs was made using a MOF-based technology. In this system, the Ni species acted as a catalyst, and the Zn-based MOF and injected urea functioned as nitrogen and carbon resources, respectively [136].

High lithium storage capacity, rate capability, and cycle stability are made possible by the mesoporous structure and 1D nanorod form, which provide a fast diffusion channel for electron/mass transfer while maintaining structural integrity during charged-discharge operations. One may also construct 1D carbon nanorods utilising 1D MOF nanorods and volatile Zn components as precursors [135]. 1D tubular MOF-based nanostructures were investigated for a variety of uses, including separation and sensing in catalysis. It was discovered that the MOF's hierarchical porosity and dimensionality increased the analyte's mass transport efficiency toward

the catalytic and adsorption sites. Due to their structural characteristics (hybrid nature, excellent tunability, large surface area, changeable pore diameters, etc.), MOFs have attracted a lot of interest in energy-related applications like SCs [137,138].

4.3. 2D MOF nanomaterials: Due to their quick electron mobility, quick ionic diffusion, a large number of active sites, and controlled manufacture, 2-dimensional materials are finding increasing use in the field of ESC [139-142]. The same internal or external templating techniques that can be used to create 1D MOF-derived nanomaterials may also be used to create 2D MOF-derived nanomaterials (Figure 4.3). According to Cao *et al.*, cobalt sulphide NPs and nitrogen-doped carbon were combined to form a combination with a 2D structure using porphyrin-based MOF NSs as self-templates. The self-templating method involves employing prototype MOFs having a 2D sheet structure directly, and then transforming those prototypes while maintaining the original structure. From MOFs with 2D morphologies, controlled processes can be employed to create 2D structures, such as the ion-assist SVT reaction [143]. 2D materials with MOFs were produced in situ on the NS substrate's surface using the external-templating approach. According to Zhong *et al.*, high-temperature pyrolysis of the MOF/graphene oxide NSs produced by the uniform growth of Zn-based MOFs on superficial graphene oxide NSs produced nitrogen-doped porous carbon NSs [144].

2D MOF nanosheets have caught the attention of researchers due to their exceptional physical and chemical characteristics, such as their ultrathin layer thickness, high specific surface area, high aspect ratio, an abundance of exposed unsaturated metal sites, adjustable chemical composition, discernible surface atomic structures [145]. It has been reported that the ultrathin layers of 2D MOF nanosheets, which possess an abundance of accessible unsaturated metal sites, favour reactant contact with active sites, rapid reactant and product diffusion, effective photogenerated charge carrier transfer and separation, and the transfer of electrolytes and electrons. Additionally, in electrocatalytic, photocatalytic, or thermocatalytic applications, they were said to have a superior catalytic activity to their 3D equivalents. Research on electrocatalysis and photocatalysis has so far shown a great deal of interest in 2D MOF-based catalysts [146, 147]. Utilizing both the top-down and bottom-up synthesis approaches, as shown in Figure 4.3(C), 2D MOF-derived materials were synthesised employing 2D MOF as self-templates [148]. To produce ultrathin Zn(bim)(OAc) MOF NSs with a yield of about 65% and a

thickness of about 5 nm, as well as their generated porous ultrathin carbon nanosheets with a thickness of about 3 nm, for use in energy storage applications, Zhao *et al.* developed a low-cost method [149]. The HT synthesis of Co-HPA MOF NSs (HPAhypoxanthine) was established by Gao *et al.* These NSs were then carbonised to create identical Co@NAC NSs [150].

With only one or a few atomic layers of thickness and a large proportion of unsaturated metal sites, which are frequently utilised as active sites, Metallenes, derived from MOFs, are recently created 2D metallic materials that are perfect for heterogeneous catalysis [151,152]. A greater amount of electron transfer occurs during catalysis, particularly electrocatalysis, because of the more linked atoms in metallenes than in conventional thin metal nanoparticles [153,154]. Additionally, metallenes can function independently without the aid of support or surfactant, opening up a wider range of applications [152, 155].

4.4. 3D MOF nanomaterials: The benefits of materials with 3D architecture include excellent carrier transport or diffusion speed and excellent electrolyte permeability. To produce 3D MOF-derived nanocomposites like frameworks, nanoarrays, and nanofoams, structured reactions are supported by coherent planning and manufacture of MOF precursors based on structural and chemical composition [156]. As depicted in Figure 4.4, during high-temperature pyrolysis, self-template MOFs are frequently linked with other molecules or salts to promote morphological change. Using thiourea and CoCl2 as precursors in an aluminium-based MOF, researchers came up with a novel method for creating porous 3D-honeycomb nanostructures (Figure 4.4(B)). The formation of a 3D-honeycomb structure was caused by the dissolution of the cobalt complex during pyrolysis, which resulted in the production of a significant amount of nitrogen and sulphur comprehending gases [157]. To produce web-like interconnected carbon networks for ORR electrocatalysis, Zn-based MOFs and NaCl compounds were pyrolyzed, as shown by Qian *et al.* It was hypothesised that during pyrolysis, melted NaCl stimulated the surface region of Zn-based MOF NPs, leading to the particles' association with 3D carbon networks [158]. To build 3D-ordered porous carbon, Zhao *et al.* investigated the utilisation of MOFs produced from high-energy ligands as precursors [159].

With the use of a 3D scaffold, Xu *et al.* created integrated tubular metal-organic framework structures [160] that were derived from nitrogen-doped carbon tubes (NCTs) with high salt adsorption capacities. NCTs demonstrated ultrahigh capacitive deionization (CDI) performance

when compared to other carbon materials, emphasising the value of 3D free-standing carbon structures in CDI applications [160]. Yang *et al.* produced granular $NiCo_2S_4$ nanowires coupled to NiCoZn-S nanosheets on carbon fibres to form 3D hierarchical nanoarrays (CF@NiCoZn-S/$NiCo_2S_4$). These three-dimensional architectural electrodes could be used for electrocatalysis, energy storage, and environmental applications [161].

There are a lot of publications that have been written about the manufacturing of 3D MOF-derived materials by an external-templating method. Cobalt-based MOF nanowire arrays on the surface of Cu foil could be directly synthesised and carbonised in an N2 atmosphere to create hybrid Co3O4/C porous nanowire arrays. The quick electron transit and coupling between the Co_3O_4/C nanowire array and copper foil, the numerous active sites, and the simple mass transfer were attributed to the good ELC activity and stability of the resulting Co_3O_4/C nanowire arrays for electrochemical OER [162]. According to Liu *et al.*, spongy C and CNT connections and copper hydroxide nanowires were interlaced and percolated during the construction of MOFs to create an independent thin film. To make MOF-CNT thin film composites, organic ligands were added to this independent thin film. The MOF-CNT thin film was then pyrolyzed at a higher temperature to produce MOF-derived porous C/CNT networks hybrid components for LSB[163].

5. MOF-BASED NANOMATERIALS FOR SUPERCAPACITORS

A unique class of crystalline porous materials called MOF by Yaghi [164,165] originally appeared in 1995 as a result of the potent interactions between organic ligands and metal ions and has since distinguished itself with persistent porosity and large surface areas [166]. Since the inorganic component in porous hybrid frameworks was either an isolated polyhedron or a small cluster, as in coordination chemistry, coordination polymers were the previous name for these materials. However, it was soon realised that porous hybrid materials might contain inorganic elements with increased dimensionality, leading to MOF, or multi-scale order frameworks [167, 168]. Porous materials were first created in 1989 by Hoskin and Robson, who combined octahedral or tetrahedral arrays of metal centres with organic moieties to create scaffolding-like structural three-dimensional frameworks [169]. Using single crystal XRD, a diamond-like structure called [N $(CH_3)_4$][$CuZn(CN)_4$] was successfully created and analysed [170]. A 3D MOF that demonstrated gas adsorption characteristics at room temperature was created in 1997 by Kitagawa *et al.* [171]. The synthesis of HKUST-1 [172] and MOF-5 [173] was published in

1999, and in the year that followed, they were among the most extensively explored MOFs. Beginning in 2002, F'erey *et al.* described the MIL-47 [174] and MIL-88 [175]/MIL-53 [176] porous MOFs, which are flexible and nonflexible, respectively.

One of the most well-known commercialised MOFs is Cu-BTC, commonly known as HKUST-1, which was created by BASF and distributed by Sigma Aldrich under the trade name BASOLITE® C300 [177, 178]. Toyota, Strem Chemicals, Ford Global, and MOF Technologies are just a few of the businesses that have patents for producing MOF on a wide scale. A review of the World Intellectual Property Organization (WIPO) database revealed a steady rise in the number of patents issued by the world's researchers. This shows that business applications for MOF are gaining a lot of traction. As seen in Figure 5.1, several research publications have been published during the past three decades. A key aspect of MOF synthesis is depicted in Figure 5.2.

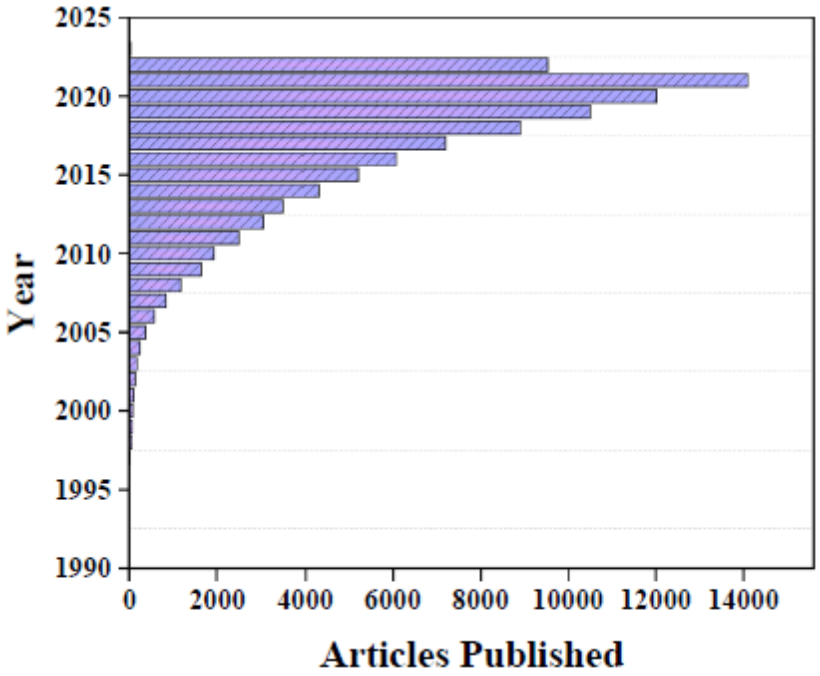

Figure 5.1. Number of articles related to MOFs published from 1991 to the present, (Web of Science). Reproduced with permission from [179].

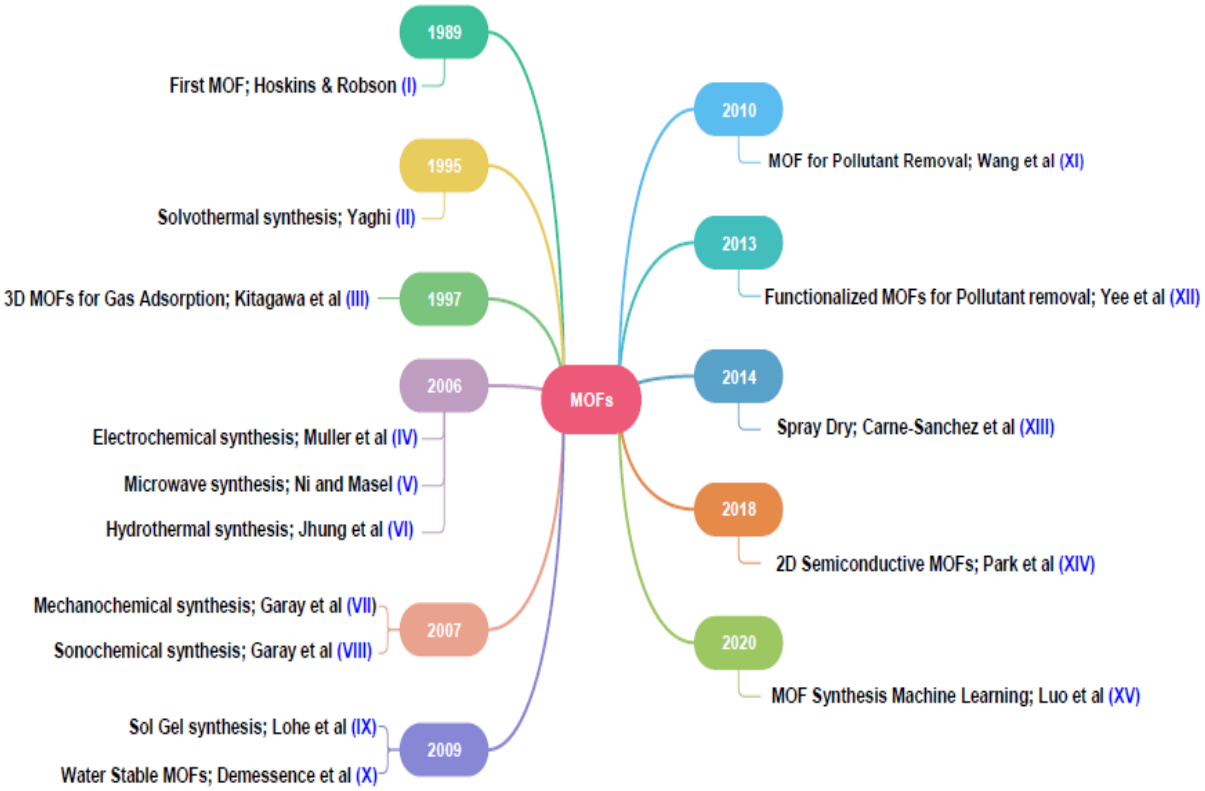

Figure 5.2. Landmark of MOF synthesis (I) [169] (II) [180] (III) [181] (IV) [182] (V) [183] (VI) [184] (VII) [185] (VIII) [185] (IX) [186] (X) [187] (XI) [188] (XII) [185] (XIII) [189] (XIV) [190] (XV) [191]. Reproduced with permission from [179].

A variety of uses for MOF include catalysis [192], gas separation [193], drug delivery systems [194, 195], imaging, sensing, molecular conductors [196], gas separation [197], energy storage [198] and structural determination [199, 200]. Due to its porous nature, MOF is a very significant class of material with an unequalled degree of tunability. The recent progress of using MOFs as SC can be categorised into two kinds [201, 202]. First MOFs are utilised as new patterns to create porous metal oxides or carbons with a large surface area (size: 0.6-2 nm) [203-205]. Second, and more difficult because of their flexibility, are MOFs used directly as SC electrodes (rear usage) [206]. Flexibility is converted to a distinct stable structure to overcome this restriction. R&D-based successful approach because there are numerous ways to produce MOF material The schematic diagram in Figure 5.3 that follows can help you understand the general procedure for developing MOFs.

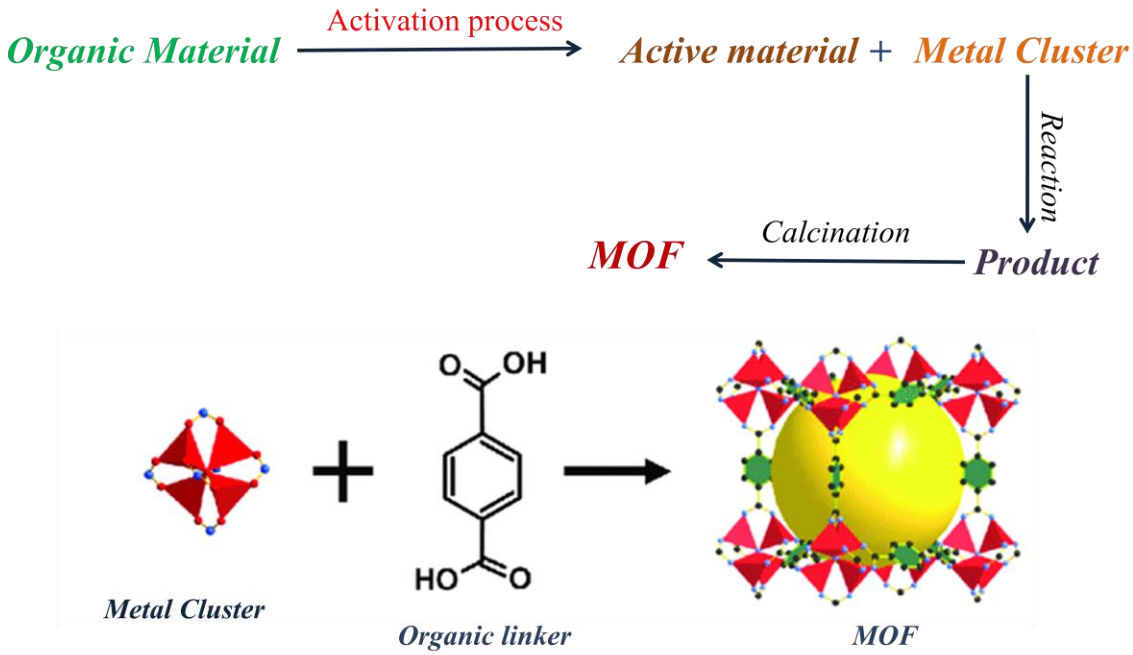

Figure 5.3 A typical synthesis process for MOFs.

For the development of MOF for SCs, several metals (Co, Zn, Cu, Ni, etc.) have been utilised [207]. Table 5.1 lists several materials derived from MOFs for application as SCs electrodes.

5.1. Cobalt metal in MOFs: A self-supported template consisting of nickel foam and Co-MOF@$CoCr_2O_4$ has been tested as a promising candidate for SCs. The SC displayed power density (2.34 $mWcm^2$) and specific capacitance (596.8 Cg^{1}) that retains 95% even after 5000 cycles in the presence of a PVA and KOH mixture as the electrolyte [245]. Youngho *et al.* created a bimetallic MOF that is reliable and economical for asymmetric SC. The material for the SC electrodes was created via a straightforward hydrothermal method. The electrode used in this experiment had a power density of 2000 W per kilogramme and testing up to 5000 cycles of charging and discharging was successful with an efficiency of 94% [210]. Porous Co_3O_4 nanostructure (nano hollow sphere, hallow nano tubes, etc.) formed from Co-MOF was described by Dandan Chen *et al.* Using a straightforward calcination technique, the porous material was removed from Co-MOF. The porous material performs well under cyclic conditions, having a good specific capacitance of 150 F g^{-1} at a current density of 1 A g^{-1} in 1 M KOH [246]. Nanotubes were produced for the same purpose by Wang *et al.* using the same procedure and material.

Table 5.1. Electrode materials for SC applications derived from MOFs.

Electrode material	Electrolyte	Specific Capacitance	Efficiency	Reference
Co–MOF@$CoCr_2O_4$–Ni	PVA & KOH	596.8 Cg^{-1}(0.4 Ag^{-1})	85% (5000 cycles)	[208]
Co/Mn MOF	1 M KOH	1176.59 F g^{-1} (3 mA cm^{-2})	94% (5000 cycles)	[210]
Co/Zn–S@ rGO	6 M KOH	1640 F g^{-1} (1 A g^{-1}	90% (8000 cycles)	[209]
Na_2Co-MOF	0.5 M Na_2SO_4	321.8 F g^{-1} (4 A g^{-1})	97% (5000 cycles)	[211]
Co-MOF	Acetonitrile	300 F g^{-1} (1 A g^{-1})	94% (1000 cycles)	[212]
Co_3O_4@$CoNi_2S_4$	2 M KOH	244.4 mA h g^{-1} (1 A g^{-1})	81% (10,000 cycles)	[213]
CoP–CoNC/CC	2 M KOH	975 F g^{-1} (1 mA cm^{-2})	87% (5000 cycles)	[214]
Co_3O_4@Co-MOF	3.0 M KOH	1020 F g^{-1} (1 A g^{-1})	97% (5000 cycles)	[216]
u-hl-MOF-Co1-xS@ C	3 M KOH	13.1 F cm^{-2} (1 mA cm^{-2})	97% (10,000 cycles)	[215]
$CoSe_2$/NC	6 M KOH	120.2 mA h g^{-1} (1 A g^{-1})	92% (10,000 cycles)	[217]
c-MOF(Ni_2[CuPc $(NH)_8$])-NSs	PVA/LiCl gel	18.9 mF cm^{-2} (0.4 mA cm^{-2})	91% (5000 cycles)	[219]
Co_3O_4@Co-MOF	3 M KOH	1020 F g^{-1} (0.5 A g^{-1})	97%(5000 cycles)	[218]
NiCo MOF	2 M KOH	94.3 F g^{-1} (0.5 A g^{-1})	80% (10,000 cycles)	[221]
Ni/Co-based MOFs	1 M KOH	1074.5 C g^{-1} (1 mA cm^{-2})	79% (5000 cycles)	[220]
NiCo-MOFs	3 M KOH	1126.7 F g^{-1} (0.5 A g^{-1})	93% (3000 cycles)	[222]
Ni_3(HITP)$_2$	Neutral	15.69 mF cm^{-2} (1 mA cm^{-2})	84% (10,000 cycles)	[224]
Ni-MOF/rGO)	6 M KOH	954 F g^{-1} (1 A g^{-1})	80% (4000 cycles)	[223]
NiCo-MOF	3 M KOH	4077.3 F g^{-1} (2.5 A g^{-1})	84% (5500 cycles)	[225]
Ni-MOF/rGO	6 M KOH	1154.4 F g^{-1} (1 A g^{-1})	90% (3000 cycles)	[227]
Ni-Co-O@CFP	PVA/KOH	2038 F g^{-1} (1.5 A g^{-1})	94% (5000 cycles)	[226]
Ni-MOF nanosheets	3 M KOH	680 C g^{-1} (1 A g^{-1})	68% (3000 cycles)	[228]
Ni/C/rGO-n	3 M KOH	1258.7 F g^{-1} (8 A g^{-1})	96% (5500 cycles)	[230]
Cu-MOF nanowire with	3 M KCl	252.1 mF cm^{-2} (1.1 mA g^{-1})	91% (8000 cycles)	[229]

polypyrrole				
Cu_2O/Cu@C nanosheets	1 M KOH	665 F g^{-1} (0.5 A g A g^{-1})	81% (5000 cycles)	[231]
Cu-Co-P(anode), $CuFeS_2$(cathode)	6 M KOH	2043.3 F g^{-1} (1 A g^{-1})	97% (8000 cycles)	[232]
rGO/Cu-MOF	1 M KCl	44.6 mF cm^{-2} (0.013 mA cm^{-1})	90% (100 cycles)	[234]
$Zn_2(bdc)_2(dabco)]_n$ crystals	$HClO_4$	3150 mF cm^{-2} (10 mA cm^{-2})	93% (1000 cycles)	[233]
Zn-MOF	6 M KOH	220 F g^{-1} (1 A g^{-1})	99% (10,000 cycles)	[235]
$MnNi_2O_4$	6 M KOH	2848 F g^{-1} (1 A g^{-1})	93% (5000 cycles)	[237]
Zn-MOF	1.0 M H_2SO_4	203 F g^{-1} (100 mA g^{-1})		[236]
$ZnMoO_4$ nanosheets	3 M KOH	1212 F g^{-1} (1 A g^{-1})	94% (5000 cycles)	[238]
Mn-MOF	2 M KOH	567.5 mA h g^{-1} (1 A g^{-1})		[239]
Al-MOF	1 M KOH	280 F g^{-1} (0.5 A g^{-1})	50% (5000 cycles)	[241]
zirconium-based MOF	6 M KOH	694 F g^{-1} (0.5 A g^{-1})		[240]
CeO_2/C/MoS_2	2 M KOH	1325.7 F g^{-1} (1 A g^{-1})	93% after 1000 cycles	[243]
Fe_3O_4 nano aggregates	3 M KOH	868.7 C g^{-1} (2 A g^{-1})	88.8% (3000 cycles)	[242]
α-Fe_2O_3 nano- octahedron	1 M LiOH	250.2 mA h g^{-1} (10 A g^{-1})	867% (6000 cycles)	[244]

An excellent contender for energy storage material is nanoporous material. According to Na Xin *et al.*, the Co/ Zn-S@ rGO bimetallic porous structure exhibits a power density of 800 W kg^{-1} and an energy density of 91.8 W h kg^{-1}. The material was tested in a variety of ways, and the highest specific capacitance measured was 1640 F g^{-1}. It's important to note that during testing at current density 10 A g^{-1}, activation of the electrode material led to capacitance starting to grow after 500 cycles and sustaining 90% of the initial capacitance after 8000 cycles. [247]. The electrochemical characteristics of a newly formed two-dimensional cobalt organic framework were described by Shankhamala Ghosh *et al.* Solvothermal synthesis was used to create the electrode material in a solution of water, ethanol, and DMF. The material was tested using a standard electrolyte of acetonitrile and a three-electrode setup. At a current density of 1 A g^1, the specific capacitance was 300 F g^1. Even after 1000 complete cycles, the capacitance maintained

94% of its original value [212]. For the SCs electrode, Richa Rajak *et al.* easily produced new hetero metallic Na/Co-based materials at room temperature using a slow diffusion technique. Very high supercapacitance (321.8 F g ^{1} at 4 A g ^{1}) and great cyclic stability up to 5000 cycles with 97% efficiency were revealed by electrochemical experiments. The production of various heterometallic MOFs for evaluating their electrochemical potential is made possible by the current synthesis method [211]. Dandan Han *et al.* developed Co_3O_4@$CoNi_2S_4$ porous material that can enhance the electrochemical activities of SCs. They provided some really interesting results, such as sp. capacitances of 244.4 mA h g^{-1} at current densities of 1 A g^{-1} and an exceptional rate capability of 86% at 16 A g^{-1} after 1000 cycles [213]. According to a review article by Jayesh Cherusseri *et al.,* MOF-based electrodes for SCs are very potential options because they have excellent power and energy densities. Co_3O_4@Co-MOF electrochemical activities were 1020 F g^{-1} at 0.5 A g^{-1} with efficiency remaining 97% for 5000 cycles [216]. Cobalt phosphide and cobalt nanoparticles (CoP-CoNC/CC) produced by the precipitation technique were implanted into N-doped nonporous carbon by Vijayakumar Elayappan *et al.* The material performed better electrochemically as it was being made, having a specific capacitance of 975 F g^{-1} at 1 mA cm ^{2} in a 2 M KOH electrolyte [214]. For the electrode material of SCs, Chang Soo Lee *et al.* produced u-hl-MOF@Co1xS@ C (u-hl-MSC) with a core-shell structure. With a three-electrode setup, the material exhibits areal specific capacitance of 13.1 F cm^2, energy density of 270 mW h cm^2, and power density of 0.6 W cm^2 [215].

Exceptional electrochemical characteristics of the $CoSe_2$/NC electrode are studied by Chenxu Miao *et al.* After 10,000 cycles, they reported a great cyclic ability of 92% and a high capacity of 120.2 mA h g ^{1} [217]. Shasha *et al.* developed and tested Nano cubes (Co_3O_4@Co-MOF) in an alkaline solution hydrothermal process. For 15 days, the as-prepared sample exhibited outstanding stability in an alkaline solution. The composite material, as manufactured, demonstrated a high specific capacitance of 1020 F g^{-1} at 0.5 A g^{-1}, extremely stable cycling (97%) energy density of 21.6 mW h cm^{-3} and up to 5000 cycles at 5 A g^{-1} [218].

5.2. Nickel metal in MOFs: Through ball milling exfoliation procedure, Mingchao Wang *et al.* produced 2D c- MOF (Ni_2[CuPc$(NH)_8$]) nanosheets based on phthalocyanine. The material has great power density (168 mW cm^2), stability, and specific capacity (91% efficiency), among other qualities [72]. Ni-Co-based hybrid MOF with good capabilities as SCs electrodes were

described by Fang Xu *et al.* Due to its low cost and favourable fabrication circumstances, its commercial-scale manufacturing is extremely encouraging. The power density of this material is the highest ever recorded (8000 W kg^1), and its 79% efficiency lasts for 5000 charging and discharging cycles [220]. For the first time, manufacturing porous Ni-Co nanotubes with a second layer of hydroxide for metal-organic frameworks has just been described. This particular structure has exceptional electrochemical potential since it has a specific capacitance of 94.3 Fg^{-1} at 0.5 A g^{-1}, an energy density of 118 W h kg^{-1} at a power density of 108 W kg^{-1}, and outstanding stability with no capacitance loss even after 10,000 charge-discharge cycles [221]. A brand-new, promising material for SCs was produced in 2019 by Yuxue Zhong. The hydrothermal technique was used to develop the composite Ni-MOF/rGO, which was then tested as an electrode for SCs. Excellent results included a specific capacitance of 954 F g^{-1} at a current density of 1 A g^{-1} and 80% efficiency at 5 A g^{-1} of current density. The Ni-MOF/rGO-300/activated carbon asymmetric super capacitor produced positive electrochemical results, according to the scientists [223]. Jie Sun *et al.* produced three NiCo-MOF morphologies (nano spheres, hollow spheres and rhombus sheets) by changing the solvent alone. All three samples have electrochemical characteristics and were sarcastic. When compared, it can be seen that the most recent sample had a specific capacitance of 1126.7 F g^{-1} at 0.5 Ag^{-1} current density and that its efficiency remained at 93% at 10 Ag^{-1} current density after 3000 cycles [222]. NiCo-MOF bimetallic hetero structure nanosheets were mentioned as a good candidate for making SC electrodes last year. The material as created also finds numerous uses in sensors, batteries, catalysts and fuel cells. It has an energy density of 76.3 Whg^{-1} and a super capacitor capacity of 244 Fg^{-1}. The nanocomposite also exhibits a high specific capacitance of 4077.3 F g^{-1} at a current density of 2.5 A g^{-1} [225]. $NiCo_2O_4$@CFP ultrathin nanosheets without a binder were created, and they were evaluated as a cathode with carbon nanosheets doped with nitrogen. The electrode system's specific capacitance achieved 2038 F g^{-1} at 1.5 Ag^{-1} after 5000 cycles at a current density of 20 Ag^{-1}, with a 94% efficiency. In a PVA/KOH hydrogel electrolyte, the electrode exhibits remarkable flexibility and outstanding electrochemical properties [226]. Ni-MOF and graphene oxide solution were produced hydrothermally by Jeonghyun Kim *et al.* With 90% efficiency remaining after 3000 cycles, this material's electrodes display 1154.4 F g^{-1} at 1 A g^{-1} in 6 M KOH with current densities ranging from 0.66 to 3 A g^{-1} [227]. As an emerging electrode material, 2D hybrid nano sheets of Ni MOF and carbon nanotubes have been discovered. The Ni-MOF/C-CNTs material

that has been developed shows good stability and a specific capacity of 680 C g^{-1} at 1 Ag^{-1}. At a power density of 440 W kg^{-1}, the electrode is said to be capable of holding an energy density of 44.4 W h kg^{-1}. [228] .Ni/C/rGO-n is a high-performance electrochemical material that has been claimed to have a specific heat capacitance of 1258.7 F g^{-1} over a broad current density range of 8–20 A g^{-1} and a capacitance of 1087.1 F g^{-1} having 86% efficiency [230].

5.3. Copper metal in MOFs: A highly conducive material was synthesized by Ruizuo Hou *et al.* in 2020 utilising Cu-CAT-NWAs and PPy membrane by an easy hydrothermal procedure. For solid-state flexible SCs, this material might be employed without restriction as linked and self-standing electrodes. Cyclic voltammetry was used to assess the built electrodes' long-term survivability in terms of flexibility, temperature, capacitance, and stability under flat, different bending angles, and twisted situations. Electrodes have a high capacity for energy storage, a long lifespan, and a 91% efficiency rate of up to 8000 cycles. To enhance the capacitive performance of various organic/inorganic hybrid conductive MOFs, this material's increased electrochemical characteristics may be employed [229]. According to Na Wu *et al.*, Cu_2O/Cu@C nano sheets electrochemical electrodes have specific capacitance, current density, efficiency, and cyclic stability of 665 F g^{-1}, 0.5 Ag^{-1}, 83%, and 5000 cycles, respectively [231]. Cu-Co-P hollow spheres and $CuFeS_2$ nano sheets were combined to create an assembly that was tested as an SCs electrode with remarkable electrochemical characteristics. The positive electrode was found to have a specific capacitance of 2043.3 F g^{-1} and the negative electrode to have a capacitance of 654.3 F g^{-1}. Despite having low-efficiency values, both electrodes were sturdy and kept working after 8000 cycles at 97% and 95%, respectively [232]. Crystalline $Cu_3(HHTP)_2$ NWAs electrochemical material was produced using the chemical vapour deposition process, and the test outcomes were very positive. For instance, the greatest capacitance reported was 41.1 F cm^{-2}, and it persisted at a 55% level with current densities increasing from 0.25 to 5 A g^{-1}. The electrode maintained 80% of its initial capacitance after a lengthy 5000-cycle procedure [248]. Hexahydroxytriphenylene (HHTP) with nanowire arrays (NWAs) Reduced graphene oxide (rGO) fibres and conductive $Cu_3(HHTP)$ (hexahydroxytriphenylene)$_2$ nanowire arrays work together to produce SCs with notable electrochemical performance. The conductive properties of rGO fibres and Cu MOF enable quick electron transfer during the electrochemical reaction. Due to the Cu-MOF nanowires' high surface area, the electrode and electrolyte have a sizable contact

area. This system's areal capacitance was found to be 44.6 mF cm^2 and its energy density to be 0.51 mW h cm^2 [234].

5.4. Zinc metal in MOFs: The ternary composite $[Zn_2(bdc)_2(dabco)]_n$ material was prepared by Ehsani *et al.* to investigate electrochemical characteristics as an electrode for SCs. The nanocomposite that was reported had an incredibly long life. The electrode maintained 93% of its initial specific capacitance during 1000 cycles at a current density of 10 mA cm^2 [233]. With 99% efficiency, the material had a capacity of up to 220 F g^{-1} and could run 10,000 times at 1 A g^{-1}. The manufacturing procedure makes it possible to create porous material for enhanced energy storage [235]. With his team, Soonsang Hong developed porous materials for energy storage technologies. The substance they synthesised was successful. A specific capacitance of 164-203 F g^{-1} at a scan rate of 10 mV s^{-1} is one example [236]. Xiaowei Xu *et al.* successfully fabricate $ZnMoO_4$ Nano sheet arrays and study the electrochemical material for SC electrodes. The material performs electrochemically excellent rate capability, a specific capacitance of 1212 F g^{-1} at 1 A g^{-1} current density. When the current density increased to 20 A g^{-1}, the capacitance decreased to 523 F g^{-1}. The maximum value for this material was tested at 94% performance over 5000 continuous charge-discharge cycles [238].

5.5. Manganese metal in MOFs: According to published research, manganese nickelate ($MnNi_2O_4$) porous nanosheets were made utilising a technique deriving from MOFs. The material was tested by measuring its capacitance, which was 2848 F g^{-1} at 1 A g^{-1}, and its high stability, which was 93% over the course of 5000 life cycles. $MnNi_2O_4$ that had already been produced was employed as the positive electrode whereas active carbon as the negative electrode. At a power density of 800 W kg^{-1}, the pair of electrodes displayed an energy density of 142.8 W h kg^{-1} [237]. For electrochemical applications, MOFs $[Mn(BDC).{}_n\ DMF]_n$ (Mn-MOFs) were made in 2020 using a hydrothermal procedure. With a specific capacity of 567.5 mA hg^{-1} at a current density of $1Ag^{-1}$, the experimental results were incredibly high. Reduced graphene oxide served as the anode and Mn-MOFs served as the cathode in this capacitor device. Over 10,000 cycles, the capacity retained 82% of the load [239].

5.6. Aluminium, Zirconium and Iron metal MOFs: To investigate its electrochemical characteristics, Mandira Majumder *et al.* synthesized an aluminium and reduced graphene-based MOF using the conventional thermal method. These thin SC electrodes were put to the test, and

they showed the best results: 3655 W kg^{-1} (power density), 280 F g^{-1} (sp. capacitance), and 50% efficiency that lasted for 5000 cycles [241]. For their energy storage applications, Chen Wang *et al.* reported zirconium-based MOF, $Zr_6(3\text{-}O)_4(3\text{-}OH)_4(OH)_6(H_2O)_6(HCHC)$. The material has a specific capacitance of 694 F g^{-1} at a current density of 0.5 A g^{-1}, respectively, according to calculations [240]. By using a hydrothermal technique, porous iron-based MOF (nano aggregates) with carbon polyhedrons were produced. The creation of active electrode material for SCs was the goal of this endeavour. The computed specific capacitance was 868.7 C g^{-1} at 2 A g^{-1}. A 3 M KOH electrolyte was used. Within 3000 cycles at 2 A g^{-1}, the electrode material preserved 771.8 C g^{-1} [242]. Defects like poor conductivity and volume expansion during charge and discharge processes were improved when oxygen vacancies were supplied to -Fe_2O_3 Nano-octahedrons. At a power density of 900 W kg^{-1}, the material had a specific capacity of 250.2 mA h g^{-1} and an energy density of 63 W h kg^{-1}. The results of this research provide new opportunities for its use in energy storage [244].

5.7. Rare earth metal MOFs: Jun-Hong Li *et al.* created a remarkable hybrid (CeO_2/C/MoS_2) material for electrochemical applications. The material's specific capacitance of 1325.67 F g^{-1} and good cyclic stability with an efficiency of 93% after 1000 cycles show that it is successful when compared to CeO_2/C (727.49 F g^{-1}) or MoS_2 (300.33 F g^{-1}) at 1 A g^{-1}. Furthermore, this substance was said to be similarly suited for asymmetric super capacitors [243].

6. COMPOSITE MOFs FOR SUPERCAPACITORS

6.1. MOFs/polymers composites: Because conductive polymers have significant intrinsic pseudocapacitive performance, combining a practical alternative is to combine MOFs with other high capacitance materials to enhance conductivity and function as hybrid supercapacitor electrodes. Impressively, Wang *et al.* originally proposed the approach for mixing pure MOFs and conductive polymers to achieve high capacitance in 2015 [249].In particular, ZIF-67 was first chosen to electrochemically deposit polyaniline (PANI) on carbon fabric (Figure 6.1). The produced PANI-ZIF-67-CC electrode has a high capacitance of 2146 mF cm^2 in 3 M KCl. The extraordinary performances are attributable to the PANI chains' capacity to join and connect the isolated ZIF-67, which enhanced the passage of electrons between the internal surface of ZIF-67 and the external circuit. This research offers a desirable method for improving MOFs' capacitive performances by entangling MOFs crystals with conductive polymers, even though the

symmetric supercapacitors constructed with PANI-ZIF67-CC electrodes only produce a modest amount of capacitance retention (near 20% loss after 2000 cycles). In later research projects, the same mixing approach has been used.

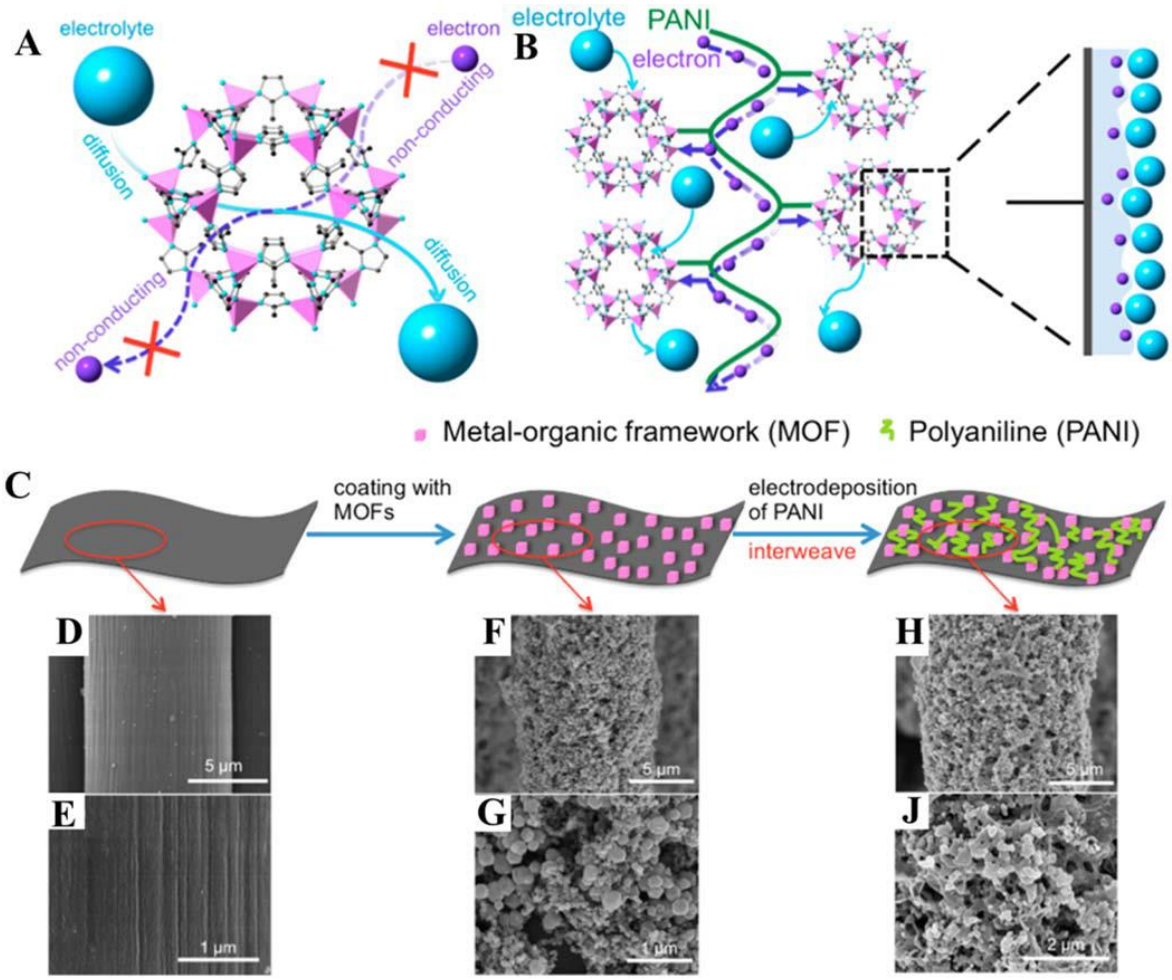

Figure 6.1. Schematic showing the transit of electrons and electrolytes to (A) ZIF-67 crystals and (B) PANI-ZIF-67. (C) Carbon textile fabrication technique aided by PANI-ZIF-67. SEM images of PANI-ZIF-67-CC, (D-E) carbon cloth fibre, and (F-G) ZIF-67 crystals supported by carbon cloth fibre. Reproduced with permission from [249].

To create MOF composites, a range of MOFs, including UIO-66 and MIL-101, have been investigated one after another [250, 251]. Redox polymer polypyrrole (PPy) has also been utilised to link MOF particles like ZIF-67 crystals and Cu-CAT nanowires and boost the overall conductivity of hybrid electrodes[252, 253]. The outcomes demonstrate that the cycling performances and capacitances are superior to those of pure MOFs and polymers. Peroxidised Polyacrylonitrile Nanofibers (PPNFs), in addition to conductive polymers, have also been found

to be effective supports for MOFs electrode materials. In 2020, Tian *et al.* employed the hydrothermal method to produce bimetallic M-Ni MOFs (M=Co, Cu, Zn, Fe) flower-shaped nanosheets supported by PPNFs as hybrid electrodes [254]. The rate performance and capability of the PPNF@M-Ni MOF (where M stands for Co, Zn, Fe and Cu) are in the following order: Zn< Cu< Fe< Co. A noteworthy finding is that for PPNF@Co-Ni MOF after 10,000 cycles in KOH electrolyte, there is essentially no discernible decrease from the initial capacitance.

Using the techniques of chemical polymerization, electrochemical polymerization, or photopolymerization, to improve Faradaic processes over the interface, 3-D conductive networks made of polymers and MOFs particles can be constructed. This is the general core idea for designing this type of hybrid electrode. Unfortunately, it is unclear how much real capacitance MOFs and polymers, respectively, contributed to these composites-based electrodes. Additionally, little attention is paid to the synergistic effects of each component at the micro level. The pseudocapacitance is entirely given by the MOFs when using a polymer as a support for MOFs like PPNF, and related research is uncommon.

6.2. MOFs/metal oxide composites: Another sort of often used pseudocapacitive substance is metal oxides. Depositing metal oxides, on the target MOFs is a workable method for producing hybrid MOF supercapacitor electrodes. Zhang and colleagues developed a straightforward method to increase capacitance by in situ self-transformation based on the presumption that the performances can be improved by creating close connections between the MOFs and metal oxides [255]. The researchers particularly selected the MOF-manganese hexacyanoferrate hydrate ($Mn_4Fe(CN)_{62.66715}.84H_2O$) nanocubes as the target MOFs for generating manganese oxides. NH_4F can be used to spread the resulting MnO_x with nanoflowers structure on the surface of each Mn MOFs nanocube. When compared to pure Mn-MOFs, in a Na_2SO_4 electrolyte, the MOFs-MnOx nanocomposites exhibit a threefold increase in pseudocapacitance, with a specific capacitance of 1200 Fg^{-1}. Furthermore, the electrode built with MnO_x-MOFs exhibits good capacitance retention at 94.7% after 10,000 cycles at $10Ag^{-1}$. Designing conductive MOFs/MnO_2 hybrid electrodes has also followed this integration method to increase capacitance and rate performance. For instance, a variety of Ni-HHTP/MnO_2 nanoarrays with various lengths of Ni-HHTP nanorods were created by Duan *et al.* [256] The charge storage mechanism for Ni-HHTP/MnO_2 is co-controlled by diffusion and non-diffusion, according to CV analysis, which

implies that both capacitor and battery behaviours are at play. With an increase in scan rating, the capacitive contribution rises. Ni-HHTP may significantly increase the conductivity by creating excellent nanorod arrays on the surface of MnO_2 along [001], providing a good capacity of 368.2F g^{-1} at 1 Ag^{-1} in KOH for this hybrid electrode. Numerous redox active sites are provided by the ultrathin MnO_2 nanosheets to generate high pseudo-capacitance.

Similar to MOFs/conductive polymer composites, MOFs/metal oxide composites offer hybrid capacity and incorporate both MOFs and metal oxides. For this type of supercapacitor electrode, there is no universal design advice. Pseudocapacitance, electric double-layer capacitance, and battery behaviour may all be implicated in the charge-discharge process in such an electrode. Additionally, not all MOFs can be used to mix metal oxides for hybrid electrodes, thus it is significant to focus on the ideal ratio of MOFs to metal oxides.

6.3. MOFs-based composites: Composites made from MOFs also perform very well at storing and converting energy [257-259]. It has been shown that MOFs can act as a class of perfect precursors for the controlled carbonization in an inert atmosphere required to synthesise carbon or doped carbon materials with capacitance. Typically, during carbonization, the structuring of the carbon network always occurs concurrently with the destruction of MOFs [260, 261]. On ZIF-8 and ZIF-67, several investigations on carbons generated from MOFs are based. Yusuke's group originally revealed the direct carbonization method in 2012, using ZIF-8 and ZIF-67 as the initial precursors to create nanoporous carbon materials [262, 263]. After being subjected to acid treatment, the resulting porous carbons essentially maintained ZIF-8 and ZIF-67's initial shape and both displayed pseudocapacitive behaviour in H_2SO_4 aqueous electrolyte (Figure 6.2A - 6.2F). Higher graphitic walls could be achieved for ZIF-67-derived carbon, indicating that different derived carbon materials might have different amounts of graphite due to the diverse metal components in MOFs. The ability to precisely control the morphology of MOFs is noteworthy because it may be used to control the capacitance of generated porous carbon.

Even with a low scan rate (125F g^{-1} at 5 mV/s), severe aggregation would be simple for the small, derived carbon particle sizes, further leading to low capacitance. The resultant ZIF-8's uniform 3D large-sized polyhedron carbon structure has a significantly larger capacitance

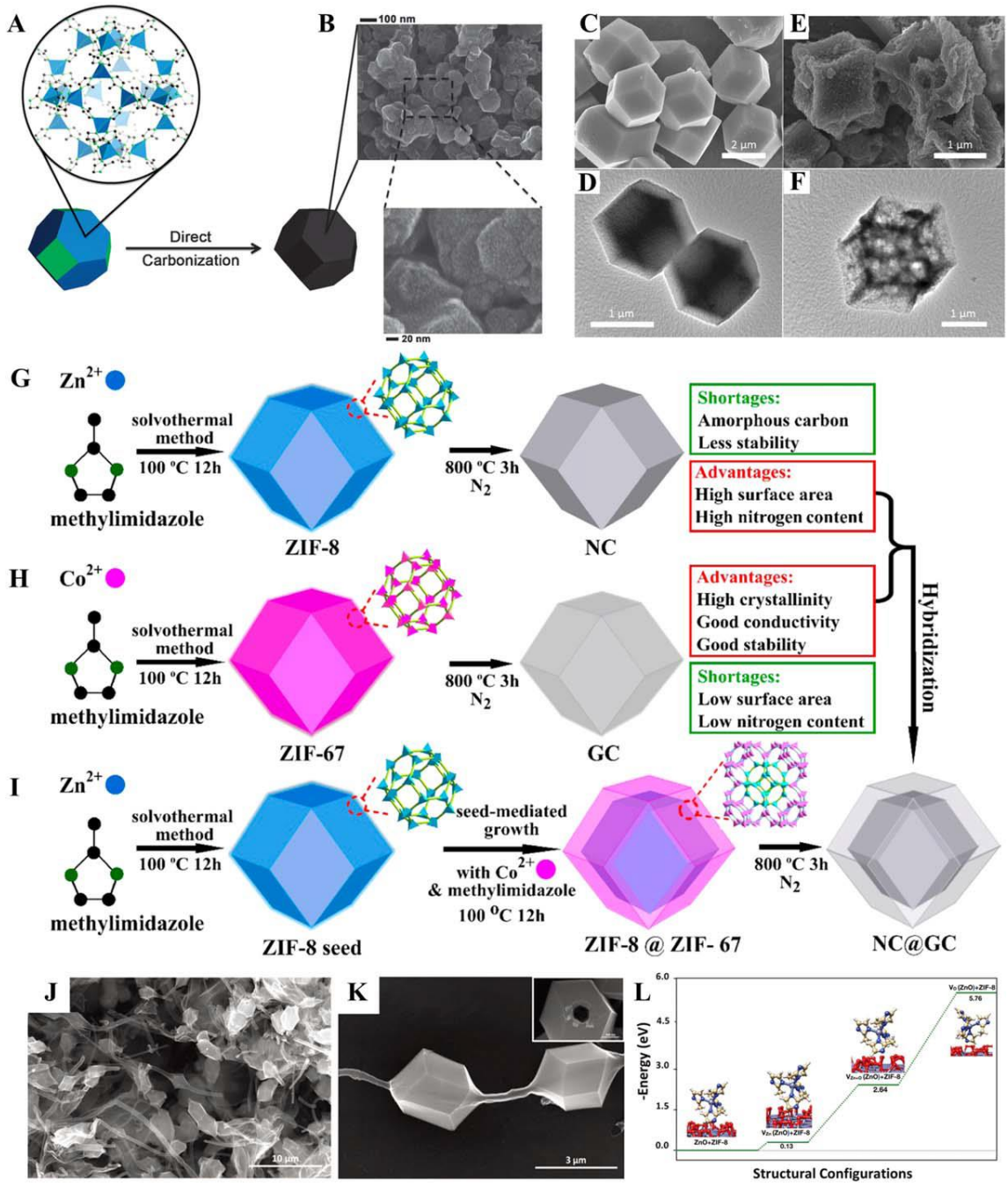

Figure 6.2. (A) ZIF-8's crystal structure for direct carbonization (B) SEM of carbon produced from ZIF-8. ZIF-67 images in (C) SEM and (D) TEM. (E) SEM and (F) TEM images. Process for producing (G) non-porous carbon (NC), (H) graphitic carbon (GC), and (I) core-shell NC@GC generated from ZIF-8@ZIF-67 crystals. (J) and (K) SEM of NTC obtained from ZIF-8/ZTP, (L) the relative energy for ZIF-8 on the ZTP surface with vacancies for O, Zn, and Zn+O. A and B, reproduced with permission from [235]; C, D, E and F, reproduced with permission from [262]; G, H and I, reproduced with permission from [264]; and J, K and L reproduced with permission from [265].

thanks to open porous designs that allow for the insertion and deinsertion of ions. In general, graphitized carbon frameworks and lower nitrogen concentrations are always present in ZIF-67-derived carbon, but high nitrogen contents and amorphous carbon can be found in ZIF-8-derived carbon. Given that ZIF-8 and ZIF-67 have similar coordination structures and lattice characteristics, a carbonising bimetallic ZIF made of ZIF-67 and ZIF-8 might incorporate the advantages of porous carbon generated from MOFs. Bimetallic MOFs will create a core-shell structure when ZIF-8 is used as a seed for the growth of ZIF-67 shells [266]. After carbonization, the resulting carbon is composed of a highly graphitic shell and a core with a large surface area (Figures. 6.2G - 6.2I). The $Co^{2+/}Zn^{2+}$ molar ratio can be adjusted to achieve the ideal capacitance. It is feasible to get a maximum capacitance of 270F g-1 at 2 Ag-1 when the Co2+/Zn2+ molar ratio is 0.05. In addition to this, new advancements in ZIF-8 pyrolysis have been made. By pyrolyzing hybrid ZIF-8/ZnO tetrapods (ZIF-8/ZTP), Yuksel *et al.* created an N-doped tubular carbon material (NTC) that resembles a necklace in 2020. (Figures. 6.2J and 6.2K) [267]. The authors discover that oxygen vacancies in the defect regions can cause ZIF-8 polyhedra to develop on the surface of ZTP (Figure 6.2L). Because of continuous polyhedral 3D hollow morphologies, the resulting supercapacitor is based on NTC and has a promising cycle life (91.5% capacitance retention after 50000 cycles). Carbonizing MOFs crystals also provide the resulting carbon with different morphologies in addition to a nanoporous structure. The production of carbon nanorods with 1D architectures could be induced by the thermal transformation of MOF-74 nanorods, as shown in Figure 6.3 by Xu's team [268]. The carbon nanorods may also undergo additional sonochemical processing and chemical activation to change into six-layered graphene nanoribbons. The as-fabricated graphene nanoribbons have a high specific surface area of 1500 m^2 g^{-1} and a capacitance of 189 Fg^{-1} at 0.1 A/g in H_2SO_4, both of which are greater than those of microporous carbon and carbon nanorods. The easier availability of ions between the layers of the graphene nanoribbons is responsible for the increased capacitance.

Overall, the majority of the nanoporous carbon produced using MOF as sacrificial templates has a very low capacitance. However, it should be emphasised that materials formed from MOFs that are carbon/metal oxides, metal oxides, or other metal compounds can be produced using a variety of multi-step techniques. The electrical conductivity, surface area, and cycle life of metal oxide nanostructures produced via MOF are frequently low. In comparison to pure metal oxides

produced from MOFs, carbon/metal oxides exhibit better performance [269]. By reaching 500 ºC through the use of an iron-based MOF (Fe-MIL-88B-NH2) crystal in an N_2 gas environment, for instance, a porous Fe_3O_4/carbon composite can be created, and the carbon layer produced from Fe-MOFs is amorphous [270]. However, the capacitance of the composite electrode is noticeably low. Different MOFs and annealing circumstances would result in very different derivatives. By annealing MIL-88-Fe formed on the oxidised carbon nanotube fibre (S—Fe_2O_3@C/OCNTF) at 350 °C in the air for 2 h, Zhou *et al.* discovered spindle-like carbon integrated -Fe_2O_3 [271]. With a high areal pseudocapacitance of 1232.4 mF cm^2 at 2 mA cm^2, the S-Fe_2O_3@C/OCNTF anode retains capacitance at a rate of 63% at 20 mA cm^2. Some carbon/metal composites generated from MOFs exhibit battery supercapacitor characteristics, which is an intriguing conclusion. To create MFOs-derived composites, as the precursor, Wang *et al.* selected a specific type of two-dimensional MOF $[Ni(ATA)_2(H_2O)_2](H2O)$. A hemihydrate of 3-amino-1H-1,2,4 triazole-5-carboxylic acid is known as ATA. [276]. They find that carbonising this MOF can produce Ni/N co-doped carbon (Ni@NC) core-shell rings. The battery mode is demonstrated by the Ni@NC composites made at different annealing temperatures (Ni@NC1 for 800 °C and Ni@NC1 for 900 °C). The produced A-Ni@NC1 material exhibits pseudocapacitance behaviour in the potential window of 1 to 0V after being treated with HCl for Ni@NC1 composites. The hybrid energy device has the highest energy density of 33.0 Whkg-1 and the highest power density of 375.1 Wkg-1 among comparable devices thanks to the usage of Ni@NC1 and A-Ni@NC1 composites as the positive and negative electrodes, respectively. According to recent research, supercapacitors can use metal phosphides produced from MOFs as both positive and negative electrode materials. Wei *et al.* used $Co_3[Co(CN)_6]_2$ and $Fe_4[Fe(CN)_6]_3$ as the precursors in 2021 to create Fe_2O_3 and Co_3O_4 nanocubes, which were then phosphorised to create FeP_4 and CoP nanocubes. In a KOH electrolyte, the FeP_4 and CoP nanocubes both exhibit pseudocapacitance behaviour and exhibit specific capacitances of 345 and 600 Fg^{-1}, respectively. Making hierarchical NiCoP-MOF heterostructures is another design technique to improve pseudocapacitive characteristics. He and his colleagues used the hydrothermal-localized phosphorisation transformation approach to create lamellar brick stacked Ni/Co-MOF/NiCoP. (Figures. 6.4A and 6.4B) [244]. Additionally, in KOH, Ni/Co-MOF/NiCoP heterostructures exhibit battery-capacitor behaviour. Such NiCoP-MOF-based supercapacitors have a capacity of 226.3C g^{-1} and virtually 100% capacity retention over 10000 cycles (Figure 6.4C). But

regrettably, the researchers have not looked deeper into what causes this remarkable stability. Additionally, several multicomponent materials generated from MOFs, such as $Cu(NiCo)_2S_4/Ni_3S_4$ and Co/Ni/B/S composites, have enhanced faradaic capability [273, 274].

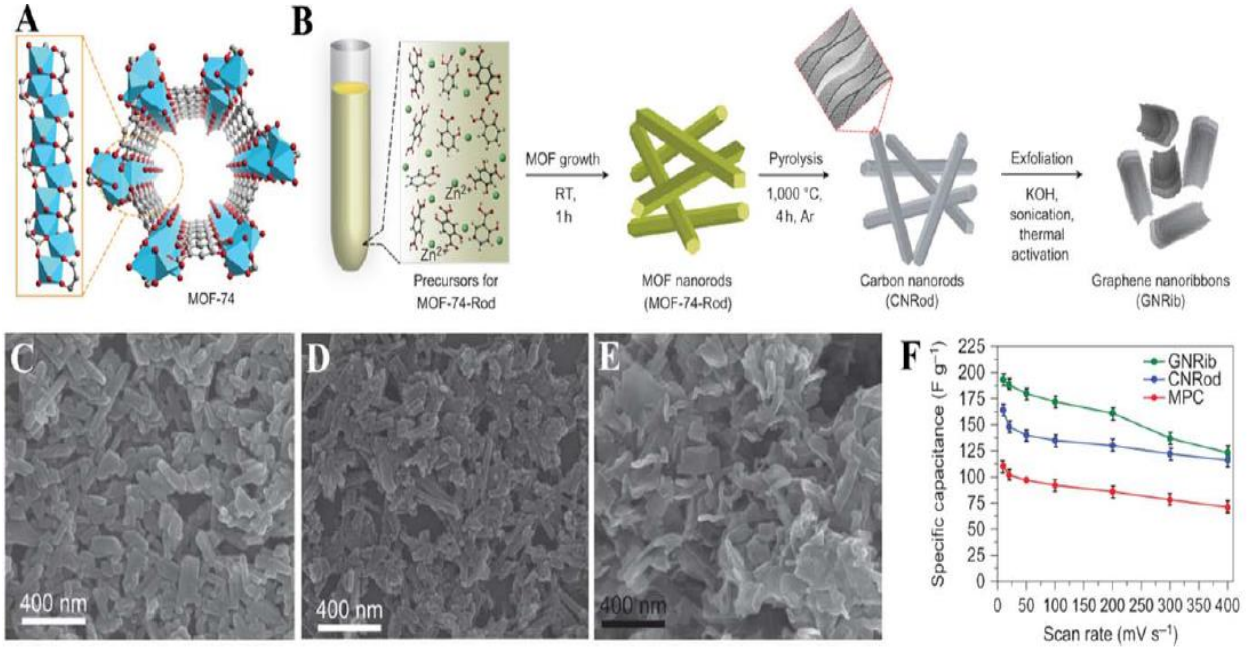

Figure 6.3. (A) The crystal structure of MOF-74. (B) The process of producing graphene nanoribbons by thermally transforming MOF-74 rods. Carbon nanorods (D), MOF-74 nanorods (C), and graphene nanoribbons (E) as shown in SEM pictures. (F) Special capacitance for graphene nanoribbons, carbon nanorods, and microporous carbon. Reproduced with permission from [268].

The majority of the above-mentioned derivatization research focuses on MOFs in powder form. Direct derivatisation of MOFs grown on freestanding substrates to produce self-supported electrodes is another derivatization technique. Yang *et al.* (1999) reported CF@NiCoZn-LDH nanosheet arrays using a ZIF8 nanosheet array on carbon fibre cloth (CF@Zn-MOF) as the template (Figure 6.4D).

Different LDH hybrids would develop when Co and Ni addition levels were controlled. And to improve the electrochemical performance, the authors used the $CF@Ni_2Co_1Zn$-LDH. Notably, via selective vulcanization, Co_9S_8 quantum dots (Co9S8 QDs) can be incorporated into the $CF@Ni_2Co_1Zn$-LDH interlayer to create CF@NiCoZn-LDH/Co9S8-QDs (Figure 6.4E and 6.4F). The capacitive performance is effectively improved by the created Co9S8 QDs with

plentiful active sites, and their capacity can reach 2504 Fg^{-1} at 1 Ag^{-1} (Figure 6.4G). 8000 cycles in KOH can likewise result in a 95.3% capacity retention. Another study on the creation of hybrid electrodes produced from self-supported MOFs is equally intriguing. NiCo-LDH was applied to carbon fibre by Wang *et al.* as a precursor for the development of NiCo-MOFs [276]. The authors find that under terephthalic acid (PTA) vapour environment, Co-PTA@$CoNiO_2$ core/shell nanosheet arrays can develop on the surface of carbon fibre. Additionally, the Co-PTA MOFs shell and $CoNiO_2$ give the double-layer capacitance and battery type capacity, respectively. In KOH, final hybrids had a capacity of up to 757.2 Fg^{-1}. The authors note that an

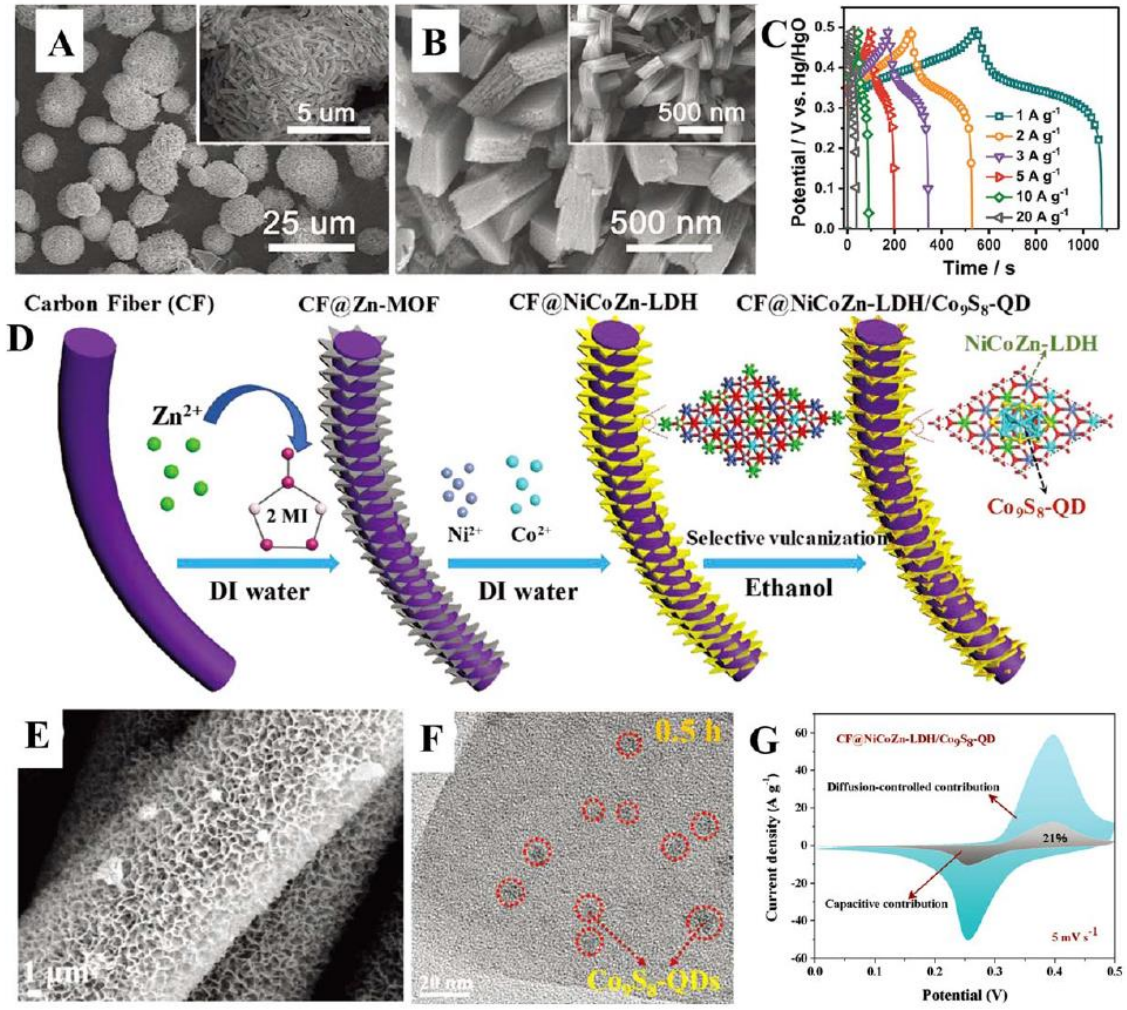

Figure 6.4. NiCoP-MOF SEM images from (A) to (B). (C) The NiCoP-MOFs electrode's charge-discharge curve. (D) The method used to create hybrid CF@NiCoZn-LDH/Co9S8-QDs. CF@NiCoZn-LDH/Co9S8-QDs SEM in (E). CF@NiCoZn-LDH/Co9S8-QDs SEM in (F). (G) CV of the electrodes CF@NiCoZn-LDH/Co9S8-QDs. Reproduced with permission from [271].

excessively thick MOF shell's restricted ability to diffuse ions results in impaired capacitance.

One unexplored area of research is the pyrolysis and other processing of MOFs to yield carbon, carbon/metal combinations, or metal compounds with various nanostructures as supercapacitor electrodes. The core of hybrids is a logical design, which aims to maximise power density and energy density by optimising capacitance or incorporating battery behaviour. The key concern is how the micro/nano porosity structure of virgin MOFs changes as a result of annealing or other treatment procedures. Different micro/nano geometrical models could be created in conjunction with electrochemical impedance spectroscopy (EIS), which offers some theoretical support for morphology design, to investigate the general diffusion and Faradic reaction behaviour of these micro/nano structures.

7. ELECTROLYTES USED IN MOF-BASED SUPERCAPACITORS

Figure 7.1 demonstrates a general classification of electrolytes for electrochemical supercapacitors. In SCs, electrolytes are just as crucial as electrodes. The capacitive performance, stability, and long life of SC require electrolytes that form an electrochemical double layer for a reversible redox process [277]. In the literature, various electrolyte types with varying strengths have been recorded. Despite their limited operating voltage range, aqueous electrolytes were among them and were used in the majority of cases [278]. Water in salt electrolytes or neutral electrolytes like Na_2SO_4 can be used to remedy this problem, but only a few combinations have been documented [279–284].

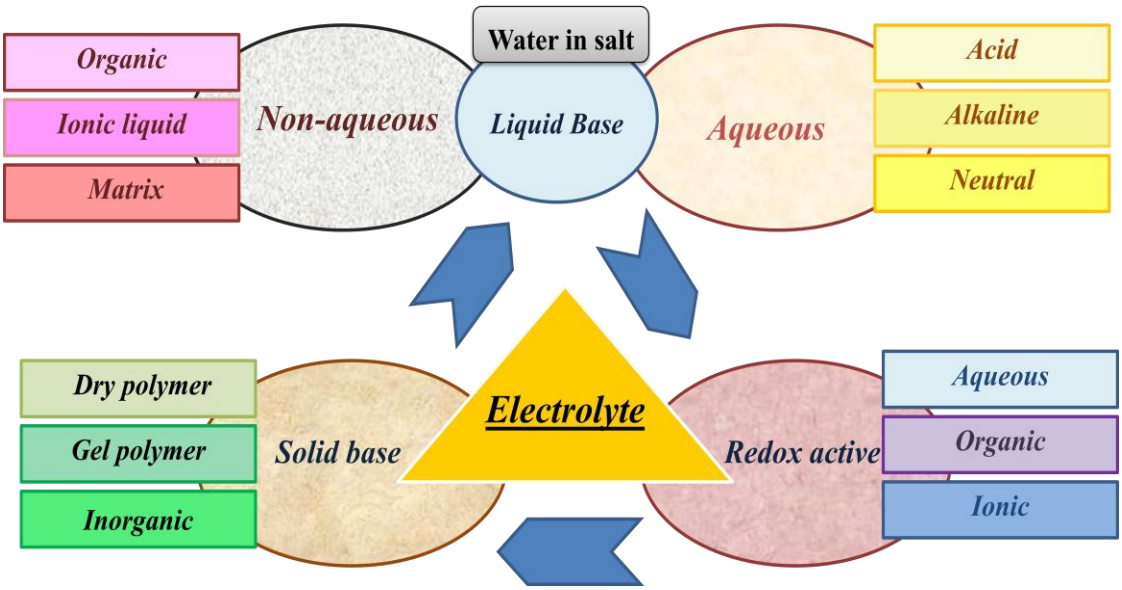

Figure 7.1. Classification of electrolytes for electrochemical supercapacitors.

Non-aqueous electrolytes produce steady operating potential values over a large range [285, 286]. Low specific capacitance is nonetheless produced by low ionic conductivity and slow mass diffusion, along with problems like toxicity and flame ability. There are also reports on solid state electrolytes [287–290]. Ion concentration, interface contact, ion size and type, solvent, cell voltage window and ions interaction are all factors that affect the overall electrolyte performance, including cycle stability, power density, energy density, and pseudo capacitance [291]. Conductivity compared to energy densities, long life, power densities, and performance are design factors for electrolyte synthesis [292]. The correct salt concentration and solvent mixture can increase efficiency [293-296]. Most often, aqueous KOH is employed in literature, with concentrations ranging from 1-6 M.

8. ROADMAP: MOF AS ELECTRODE MATERIALS FOR SUPERCAPACITORS

The development of metal-organic frameworks that met the requirements of large active sites, tuneable pore size, numerous robust structures with various chemical compositions, and high mechanical stability provided an insight into the development of electrochemical storage devices that took a new direction. In comparison to other standard materials, these acquired qualities increased the supercapacitor's capacitance, cycle life, and power density by enabling maximal charge accumulation in EDLC and accelerating the pace of redox reaction in pseudocapacitance. Even though MOFs are excellent energy materials, they lack electric conductivity, are difficult to manufacture, and lack catalytic activity in extremely acidic environments prevents them from being used in storage devices without additional work. Future possibilities and the evolution of MOF-based materials are shown in Figure 8.1.

One of the main issues with laboratory synthesis using the conventional solvothermal approach has been the ***large production of MOFs***. Given that the same procedure calls for high pressure and temperature, the prices of chemicals, when it is used on an industrial scale, the equipment, and operation substantially increase. For smaller crystalline MOF on the lab scale, techniques like spray drying, electrochemical, continuous flow, microwave, and mechanochemical production have evolved. The discovery of the aerogel and hydrogel processes, which generate a reasonably high yield of MOF at room temperature, partially addresses the issue of MOF's poor yield.

The insulating quality of MOFs also restricts their use in energy storage technologies. Many methods have been developed to give MOFs conductivity as well as ordered tenability and flexibility, including carbonization of MOF, the synthesis of 2-D MOF with conjugation or the control of - stacking in 3-D frameworks, and the use of redox-active or highly conjugated organic linkers in the matrix. In extremely basic or acidic fluids, they are still weak despite the enhanced conductivity.

The electrode's capacitance and energy density are reduced as a result of the **functional materials'** gradual degradation with time and the number of cycles. The support material utilised with MOFs must be inherent in the framework for the electrode to sustain high cycle rates. Therefore, it is important to extensively investigate the electrochemical activity of the MOFs and complementary materials used to construct electrodes to determine what variables are suppressing their activity. Along with simulation and theoretical computation, structural characterisation in situ or operando should be done to track the electrodes' chemistry as it changes in the electrolyte to better comprehend the underlying mechanism.

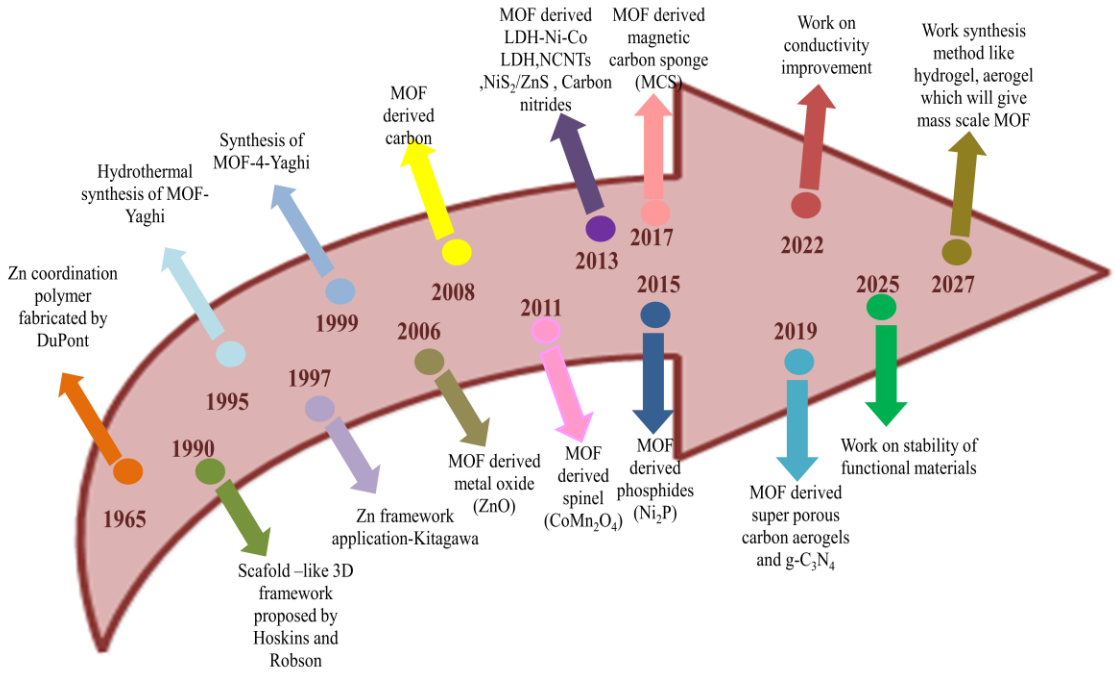

Figure 8.1. Roadmap and prospects for supercapacitor electrodes based on MOFs.

Despite obstacles and successes, MOFs have demonstrated remarkable performance as a precursor or sacrificial layer, as noted in the review. So, soon, we can expect to see a revolution in materials generated from metal-organic frameworks in the fields of renewable energy and electrochemical storage thanks to tenacious research and technical innovation.

CONCLUSION AND PERSPECTIVES

As a vital addition to batteries, supercapacitors are an essential component of any system for storing and transferring energy. The distinct electrochemical properties of supercapacitors, such as their rapid charging, high power density, and exceptional low-temperature performance, are wholly responsible for this phenomenon. A significant and promising study in this area is MOFs-based supercapacitors, which take advantage of the chemical geometry, programmable pore channels, and micro/nano structures of MOFs. For pure MOFs-based supercapacitors in particular, conductive MOFs give new possibilities. By using conductive MOFs with a sensible design, according to the latest research, capacitive performances can be favourably compared to those of commercial carbon materials.

Despite significant advancements, laboratory research on MOF-based supercapacitors is still in its infancy. Assuring the supercapacitor's performance balance is a necessary concern for practical implementation. Here are some directions for additional research on MOF-based electrode materials.

Three groups of electrode materials—pure MOFs, MOF composites, and compounds produced from MOFs—display various electrochemical characteristics. Despite numerous theoretical studies and experimental efforts devoted to comprehending the EDLCs mechanisms of porous carbon and MOFs, it is still necessary to establish a distinct and thorough connection between structures and performances for materials connected to MOFs. Particular attention should be paid to how the pores' characteristics, including hydrophobicity and confinement, affect ion dynamics and capacitance. Advanced MD simulation and numerous controlled experiments could be used to conduct a deeper and broader inquiry. However, to identify the mechanism of pseudo capacity for the electrode materials, some in situ physical characterization and electrochemical techniques must be introduced. These molecular-level insights into the response at the electrode

materials/electrolyte contact. Additionally, the electrode materials' matching capacitance attenuation law is also unclear.

It may be possible to promote cation-anion switching and facilitate ion transport by creating three-dimensional conductive MOF scaffolds with high crystallinity. This is because a molecular understanding of charge storage and dynamics for conductive MOF structures provides beneficial design advice for the electrode of pristine MOF-based supercapacitors. The design and production of novel organic ligands and single crystals of highly capacitive conductive 3D MOFs are thus significantly complicated. Another significant obstacle is the large-scale manufacture of the target MOFs. In the meanwhile, it is imperative to boost energy density as much as possible without reducing supercapacitor powder density.

A preferred strategy to increase the capacitance of the device is to introduce and combine several pseudocapacitive MOFs-based materials. However, current research does not have a good understanding of how MOFs interact with other pseudocapacitive materials such as conductive polymers and metal oxides. Design criteria are also lacking for the post-treatment of MOFs to produce derived materials. Therefore, it is essential to establish appropriate general fabrication and integration concepts and methodologies to optimise and balance the nonporous hybrid electrodes' performance in supercapacitors. Additionally, it might be easier to compare and estimate gravimetric capacitances rather than area capacitances.

Equally important to the design of the electrode materials is the selection of the proper electrolyte. The capacity of MOFs and MOF composites in organic and aqueous electrolytes always varies, and the electrolyte also affects the working voltage. The potential range of an aqueous electrolyte is typically highly dependent on the pH value because both the potential oxygen evolution reaction and the hydrogen evolution reaction are sensitive to pH. When using a neutral electrolyte, a broader voltage range for materials based on carbon and metal oxides is demonstrated by the higher overpotentials offered for the oxygen evolution reaction and the hydrogen evolution reaction as compared to electrolytes that are acidic or alkaline. However, MOFs' aqueous stability needs to be improved. In contrast, clean MOFs are better suited to organic electrolytes or ionic liquids with redox-active species. High MOF stability in the electrolyte under polarization is also necessary for this. The optimal electrolyte for the corresponding electrode materials still needs research.

REFERENCES

[1] Y. Shao, M. F. ElKady, J. Sun, Y. Li, Q. Zhang, M. Zhu, H. Wang, B. Dunn, R. B. Kaner, Design and Mechanisms of Asymmetric Supercapacitors, *Chem. Rev*. 2018, 118, 18, 9233-9280.

[2] Mudasir A Yatoo, Faiza Habib, Akhtar Hussain Malik, Mohsin Jahan Qazi, Sharique Ahmad, Mohd Azhardin Ganayee and Zubair Ahmad, Solid-oxide fuel cells: A critical review of materials for cell components, *MRS Communications* 13, (2023). https://doi.org/10.1557/s43579-023-00371-0

[3] Joseph Paul Baboo, Ewa Jakubczyk, Mudasir A Yatoo, Matthew Phillips, Sean Grabe, Matthew Dent, Steven J Hinder, John F Watts, Constantina Lekakou, Investigating battery-supercapacitor material hybrid configurations in energy storage device cycling at 0.1 to 10C rate, *Journal of Power Sources*, 561, (2023) 232762 https://doi.org/10.1016/j.jpowsour.2023.232762

[4] Mudasir A Yatoo, Zhihong Du, Zhang Yang, Hailei Zhao and Stephen J Skinner, $La_xPr_{4-x}Ni_3O_{10-\delta}$: Mixed A-Site Cation Higher-Order Ruddlesden-Popper Phase Materials as Intermediate-Temperature Solid Oxide Fuel Cell Cathodes, *Crystals*, 10 (6) (2020), 428. https://www.mdpi.com/2073-4352/10/6/428

[5] Mudasir A Yatoo, Ieuan D Seymour, Stephen J Skinner, Neutron diffraction and DFT studies of oxygen defect and transport in higher-order Ruddlesden–Popper phase materials, *RSC Advances*, 2023, 13, 13786-13797. https://doi.org/10.1039/D3RA01772A

[6] Mudasir A Yatoo and Stephen J Skinner, Oxygen Transport in Higher-Order Ruddlesden-Popper Phase Materials, ECS Transactions, 111 (2023) 2405. https://doi.org/10.1149/11106.2405ecst

[7] Y. Li, X. Han, T. Yi, Y. He, X. Li, Review and the prospect of NiCo2O4-based composite materials for supercapacitor electrodes, *Journal of Energy Chemistry*, 31 (2018) 54–78.

[8] Mohd Arif Dar, S Dinagaran, D Govindarajan, S Rafi Ahamed, Faiza Habib, C Siva, Annasaheb V Moholkar, Zubair Ahmad and Mudasir A Yatoo, Snx-0MnxS nanomaterial-based electrodes for future-generation supercapacitor and data storage devices, *Journal of Alloys and Compounds*, 958, (2023), 170523. https://doi.org/10.1016/j.jallcom.2023.170523

[9] Q. Li, S. Zheng, Y. Xu, H. Xue, H. Pang, Ruthenium-based materials as electrode materials for supercapacitors, Chem. Eng. J. 333 (2018) 505–518.

[10] A. Aricò, P. Bruce, B. Scrosati, J. Tarascon and W. Schalkwijk, Nanostructured materials for advanced energy conversion and storage devices, Nat. Mater. 4, (2005) 366-377.

[11] F. Liu, S. Song, D. Xue and H. Zhang, Folded Structured Graphene Paper for High-Performance Electrode Materials, Adv. Mater. 24, (2012) 1089-1094.

[12]P. Simon and Y. Gogotsi, Materials for electrochemical capacitors, Nat. Mater. 7, (2008) 845-854.

[13] J. Liu, H. Xia, D. Xue and L. Lu, Double-Shelled Nanocapsules of V_2O_5-Based Composites as High-Performance Anode and Cathode Materials for Li-Ion Batteries, J. Am. Chem. Soc. 131, (2009) 12086-12087.

[14] P. E. Lokhande, U. S. Chavan, S. Bhosale, A. Kalam, S. Deokar, In Flexible Supercapacitor Nanoarchitectonics (Eds.: Inamuddin; Ahamed, M. I.; Boddula, R.; Altalhi, T.), Wiley, 2021, pp. 277–313.

[15] S. Fleischmann, J. B. Mitchell, R. Wang, C. Zhan, D. Jiang, V. Presser, V. Augustyn, Pseudocapacitance: From Fundamental Understanding to High Power Energy Storage Materials Chem. Rev. 2020, 120, 6738-6782.

[16] L. Sinha, P.M. Shirage, Surface oxygen vacancy formulated energy storage application: a pseudocapacitor-battery trait of $W_{18}O_{49}$ nanorods, J. Electrochem. Soc. 166 (14) (2019) A3496.
[17] A. Afif, S.M. Rahman, A.T. Azad, J. Zaini, M.A. Islan, A.K. Azad, Advanced materials and technologies for hybrid supercapacitors for energy storage–A review, J. Energy Storage 25 (2019), 100852.
[18] Y. Liu, X. Xu, Z. Shao and S. P. Jiang, Metal-organic frameworks derived porous carbon, metal oxides and metal sulfides-based compounds for supercapacitors application, Energy Storage Mater., 2020, 26,1 –22.
[19]S. Sanati, R. Abazari, J. Albero, A. Morsali, H. Garc´ ıa, Z. Liang and R. Zou, Metal-Organic Framework Derived Bimetallic Materials for Electrochemical Energy Storage, Angew. Chem., Int. Ed., 2021, 60, 11048–11067.
[20] G.Yilmaz, K.M.Yam, C.Zhang, H.J.Fan and G.W.Ho, In Situ Transformation of MOFs into Layered Double Hydroxide Embedded Metal Sulfides for Improved Electrocatalytic and Supercapacitive Performance, Adv. Mater., 2017, 29, 1606814.
[21] Y.B. Pottathara, H.R. Tiyyagura, Z. Ahmad, K.K. Sadasivuni, Graphene-based aerogels: fundamentals and applications as supercapacitors, J. Energy Storage 30 (2020), 101549.
[22] S. Sanati, Z. Rezvani, g-C3N4 nanosheet@ CoAl-layered double hydroxide composites for electrochemical energy storage in supercapacitors, Chem. Eng. J. 362 (2019) 743–757.
[23] P. Yang, P. Sun, W. Mai, Electrochromic energy storage devices, Mater. Today 19 (7) (2016) 394–402.
[24] C.C. Ji, M.W. Xu, S.J. Bao, C.J. Cai, R.Y. Wang, D.Z. Jia, Effect of alkaline and alkaline–earth cations on the supercapacitor performance of MnO2 with various crystallographic structures, J. Solid State Electrochem. 17 (5) (2013) 1357–1368.
[25] C. Merlet, C. P´ean, B. Rotenberg, P.A. Madden, B. Daffos, P.L. Taberna, *et al.*, Highly confined ions store charge more efficiently in supercapacitors, Nat. Commun. 4 (1) (2013) 1–6.
[26] M. Winter, R.J. Brodd, What are batteries, fuel cells, and supercapacitors? Chem. Rev. 104 (10) (2004) 4245–4270.
[27] X. Zhang, N. Qu, S. Yang, D. Lei, A. Liu, Q. Zhou, Cobalt induced growth of hollow MOF spheres for high-performance supercapacitors, Mater. Chem. Front. 5 (1) (2021) 482–491.
[28] O.M. Yaghi, M. O'Keeffe, N.W. Ockwig, H.K. Chae, M. Eddaoudi, J. Kim, Reticular synthesis and the design of new materials, Nature 423 (6941) (2003) 705–714, https://doi.org/10.1038/nature01650.
[29] M. Eddaoudi, J. Kim, N. Rosi, D. Vodak, J. Wachter, M. O'Keeffe, O.M. Yaghi, Systematic design of pore size and functionality in isoreticular MOFs and their application in methane storage, Science 295 (2002) 469–472, https:// doi.org/10.1126/science.1067208.
[30] M. Safaei, M.M. Foroughi, N. Ebrahimpoor, S. Jahani, A. Omidi, M. Khatami, A review on metal-organic frameworks: synthesis and applications, TrAC, Trends Anal. Chem. 118 (2019) 401–425, https://doi.org/10.1016/ j.trac.2019.06.007.
[31] M. Esmaeilzadeh, A composite prepared from a metal-organic framework of type MIL-101 (Fe) and morin-modified magnetite nanoparticles for extraction and speciation of vanadium (IV) and vanadium (V), Microchim. Acta 186 (2019) 1-7, https://doi.org/10.1007/s00604-018-3093-y.
[32] X.S. Xing, Z.H. Fu, N.N. Zhang, X.Q. Yu, M.S. Wang, G.C. Guo, High proton conduction in an excellent water-stable gadolinium metal-organic framework, Chem. Commun. 55 (2019) 1241–1244, https://doi.org/ 10.1039/C8CC08700H.
[33] H. Yang, J. Bright, S. Kasani, P. Zheng, T. Musho, B. Chen, L. Huang, N. Wu, Metal-organic framework coated titanium dioxide nanorod array p-n heterojunction photoanode for

solar water-splitting, Nano Res. 12 (2019) 643–650, https://doi.org/10.1007/s12274-019-2272-4.
[34] P.Howlader, P. S. Mukherjee, Solvent directed synthesis of a molecular cage and metal-organic framework of copper (II) paddlewheel cluster, Isr. J. Chem. 59 (2019) 292–298, https://doi.org/10.1002/ijch.201800155.
[35] M.Y. Chao, J. Chen, Z.M. Hao, X.Y. Tang, L. Ding, W.H. Zhang, D.J. Young, J.P. Lang, A single-crystal to single-crystal conversion scheme for a twodimensional metal-organic framework bearing linear Cd3 secondary building units, Cryst. Growth Des. 19 (2018) 724–729, https://doi.org/ 10.1021/acs.cgd.8b01311.
[36] S. Soni, P.K. Bajpai, C. Arora, A review on the metal-organic framework: synthesis, properties and application, Characterization Appl. Nanomater. 3 (2020) 87– 106. https://doi.org/10.24294/can.v3i2.551.
[37] K. Sumida, D.L. Rogow, J.A. Mason, T.M. McDonald, E.D. Bloch, Z.R. Herm, T.H. Bae, J.R. Long, Carbon dioxide capture in metal-organic frameworks, Chem. Rev. 112 (2012) 724–781, https://doi.org/10.1021/cr2003272.
[38] G. Chakraborty, I.H. Park, R. Medishetty, J.J. Vittal, Two-dimensional metalorganic framework materials: synthesis, structures, properties and applications, Chem. Rev. 121 (2021) 3751–3891, https://doi.org/10.1021/ acs.chemrev.0c01049.
[39] P.S. Sharanyakanth, M. Radhakrishnan, Synthesis of metal-organic frameworks (MOFs) and its application in food packaging: a critical review, Trends Food Sci. Technol. 104 (2020) 102–116, https://doi.org/10.1016/j. tifs.2020.08.004.
[40] N. Stock, S. Biswas, Synthesis of metal-organic frameworks (MOFs): routes to various MOF topologies, morphologies, and composites, Chem. Rev. 112 (2012) 933–969, https://doi.org/10.1021/cr200304e.
[41] S. Bhattacharjee, J.-S. Choi, S.-T. Yang, S.B. Choi, J. Kim, W.-S. Ahn, Solvothermal synthesis of Fe-MOF-74 and its catalytic properties in phenol hydroxylation, J. Nanosci. Nanotech. 10 (1) (2010) 135–141.
[42] A. Rabenau, The role of hydrothermal synthesis in preparative chemistry, Angew. Chem. Int. Ed. 24 (1985) 1026–1040, https://doi.org/10.1002/ anie.198510261.
[43] D.J. Tranchemontagne, J.R. Hunt, O.M. Yaghi, Room temperature synthesis of metal-organic frameworks: MOF-5, MOF-74, MOF-177, MOF-199, and IRMOF-0, Tetrahedron 64 (2008) 8553–8557, https://doi.org/10.1016/j. tet.2008.06.036.
[44] J. Cravillon, S. Münzer, S.-J. Lohmeier, A. Feldhoff, K. Huber, M. Wiebcke, Rapid room-temperature synthesis and characterization of nanocrystals of a prototypical zeolitic imidazolate framework, Chem. Mater. 21 (8) (2009) 1410–1412, https://doi.org/10.1021/cm900166h.
[45] Y. Chen, X. Mu, E. Lester, T. Wu, High efficiency synthesis of HKUST-1 under mild conditions with high BET surface area and CO2 uptake capacity, Prog. Nat. Sci.: Mater. Int. 28 (2018) 584–589, https://doi.org/10.1016/j. pnsc.2018.08.002.
[46] S. Tanaka, Y. Tanaka, A simple step toward enhancing hydrothermal stability of ZIF-8, ACS Omega 4 (2019) 19905–19912, https://doi.org/10.1021/ acsomega.9b02812.
[47] S. Bauer, N. Stock, Implementation of a temperature-gradient reactor system for high-throughput investigation of phosphonate-based inorganic-organic hybrid compounds, Angew. Chem. Int. Ed. 46 (2007) 6857–6860, https://doi. org/10.1002/anie.200701575.
[48] P.M. Forster, N. Stock, A.K. Cheetham, A high-throughput investigation of the role of pH, temperature, concentration, and time on the synthesis of hybrid inorganic-organic materials, Angew. Chem. Int. Ed. 44 (2005) 7608–7611, https://doi.org/10.1002/anie.200501766.

[49] E. Biemmi, S. Christian, N. Stock, T. Bein, High-throughput screening of synthesis parameters in the formation of the metal-organic frameworks MOF-5 and HKUST-1, Microporous Mesoporous Mater. 117 (2009) 111–117, https://doi.org/10.1016/j.micromeso.2008.06.040.
[50] J. Klinowski, F.A.A. Paz, P. Silva, J. Rocha, Microwave-assisted synthesis of metal-organic frameworks, Dalton Trans. 40 (2011) 321–330, https://doi.org/ 10.1039/C0DT00708K.
[51] R. Vakili, S. Xu, N. Al-Janabi, P. Gorgojo, S.M. Holmes, X. Fan, Microwave-assisted synthesis of zirconium-based metal-organic frameworks (MOFs): optimization and gas adsorption, Microporous Mesoporous Mater. 260 (2018) 45–53. https://doi.org/10.1016/j.micromeso.2017.10.028.
[52] S.H. Jhung, J.H. Lee, J.S. Chang, Microwave synthesis of a nanoporous hybrid material, chromium trimesate, Bull. Korean Chem. Soc. 26 (2005) 880–881, https://doi.org/10.5012/bkcs.2005.26.6.880.
[53] S.H. Jhung, J.H. Lee, J.W. Yoon, C. Serre, G. Férey, J.S. Chang, Microwave synthesis of chromium terephthalate MIL-101 and its benzene sorption ability, Adv. Mater. 19 (2007) 121–124, https://doi.org/10.1002/ adma.200601604.
[54] N.A. Khan, I.J. Kang, H.Y. Seok, S.H. Jhung, Facile synthesis of nano-sized metal-organic frameworks, chromium-benzene dicarboxylate, MIL-101, Chem. Eng. J. 166 (2011) 1152–1157, https://doi.org/10.1016/j. cej.2010.11.098.
[55] K.M.L. Taylor-Pashow, J.D. Rocca, Z. Xie, S. Tran, W. Lin, Postsynthetic modifications of iron-carboxylate nanoscale metalorganic frameworks for imaging and drug delivery, J. Am. Chem. Soc. 131 (2009) 14261–14263, https://doi.org/10.1021/ja906198y.
[56] Z. Ni, R.I. Masel, Rapid production of metalorganic frameworks via microwave-assisted solvothermal synthesis, J. Am. Chem. Soc. 128 (38) (2006) 12394–12395, https://doi.org/10.1021/ja0635231.
[57] F. Zou, R. Yu, R. Li, W. Li, Microwave-assisted synthesis of HKUST-1 and functionalized HKUST-1-@H3PW12O40: selective adsorption of heavy metal ions in water analyzed with synchrotron radiation, ChemPhysChem 14 (2013) 2825–2832, https://doi.org/10.1002/cphc.201300215.
[58] J.-S. Lee, S.B. Halligudi, N.-H. Jang, D.-W. Hwang, J.-S. Chang, Y.-K. Hwang, Microwave synthesis of a porous metal-organic framework, Nickel(II) dihydroxyterephthalate and its catalytic properties in the oxidation of cyclohexene, Bull. Korean Chem. Soc. 31 (6) (2010) 1489–1495.
[59] A.M. Joaristi, J. Juan-Alcañiz, P. Serra-Crespo, F. Kapteijn, J. Gascon, Electrochemical synthesis of some archetypical Zn2+, Cu 2+, and Al3+ metal-organic frameworks, Cryst. Growth Des. 12 (2012) 3489–3498, https://doi. org/10.1021/cg300552w.
[60] W. Cao, Y. Liu, F. Xu, J. Li, D. Li, G. Du, N. Chen, In situ electrochemical synthesis of Rod-Like Ni-MOFs as a battery-type electrode for high-performance hybrid supercapacitor, J. Electrochem. Soc. 167 (5) (2020) 050503.
[61] U. Mueller, M. Schubert, F. Teich, H. Puetter, K. Schierle-Arndt, J. Pastre, Metal-organic frameworks-prospective industrial applications, J. Mater. Chem. 16 (2006) 626–636, https://doi.org/10.1039/B511962F.
[62] O.J.L. Neto, A.C.O. Frós, B.S. Barros, A.F.F. Monteiro, J. Kulesza, Rapid and efficient electrochemical synthesis of a zinc-based nano-MOF for Ibuprofen adsorption, New J. Chem. 43 (2019) 5518–5524, https://doi.org/10.1039/ C8NJ06420B.

[63]J.Z. Wei, F.X. Gong, X.J. Sun, Y. Li, T. Zhang, X.J. Zhao, F.M. Zhang, Rapid and low-cost electrochemical synthesis of UiO-66-NH2 with enhanced fluorescence detection performance, Inorg. Chem. 58 (2019) 6742–6747, https://doi.org/10.1021/acs.inorgchem.9b00157.
[64] J.F. Fernandez-Bertran, Mechanochemistry: an overview, Pure Appl. Chem.71 (1999) 581–586, https://doi.org/10.1351/pac199971040581.
[65] A. Pichon, A. Lazuen-Garay, S.L. James, Solvent-free synthesis of a microporous metal-organic framework, CrystEngComm 8 (2006) 211–214, https://doi.org/10.1039/B513750K.
[66] Q. Zhang, J. Zhang, X. Wang, L. Li, Y.F. Li, W.L. Dai, In-N-In sites boosting interfacial charge transfer in carbon-coated hollow tubular In2O3/ZnIn2S4 heterostructure derived from In-MOF for enhanced photocatalytic hydrogen evolution, ACS Catal. 11 (2021) 6276–6289, https://doi.org/10.1021/ acscatal.0c05520.
[67] Y. Gao, S. Li, Y. Li, L. Yao, H. Zhang, Accelerated photocatalytic degradation of the organic pollutant over metal-organic framework MIL-53(Fe) under visible LED light mediated by persulfate, Appl. Catal. B 202 (2017) 165–174, https:// doi.org/10.1016/j.apcatb.2016.09.005.
[68] A. Pichon, S.L. Anne James, An array-based study of reactivity under solvent-free mechanochemical conditions-insights and trends, CrystEngComm 10 (2008) 1839–1847, https://doi.org/10.1039/B810857A.
[69] A.L. Garay, A. Pichon, S.L. James, Solvent-free synthesis of metal complexes, Chem. Soc. Rev. 36 (2007) 846–855, https://doi.org/10.1039/B600363J.
[70] T. Frišc ˇic ´, D.G. Reid, I. Halasz, R.S. Stein, R.E. Dinnebier, M.J. Duer, Ion- and liquid-assisted grinding: improved mechanochemical synthesis of metalorganic frameworks reveals salt inclusion and anion templating, Angew. Chem. 122 (2010) 724–727, https://doi.org/10.1002/ange.200906583.
[71] W. Yuan, T. Frišc ˇic ´, D. Apperley, S.L. James, High reactivity of metal-organic frameworks under grinding conditions: parallels with organic molecular materials, Angew. Chem. Int. Ed. 49 (2010) 3916–3919, https://doi.org/ 10.1002/anie.200906965.
[72] H. Chun, D.N. Dybtsev, H. Kim, K. Kim, Synthesis, X-ray crystal structures, and gas sorption properties of pillared square grid nets based on paddle-wheel motifs: implications for hydrogen storage in porous materials, Chem. -A Eur. J. 11 (2005) 3521–3529, https://doi.org/10.1002/chem.200401201.
[73] J. 11 (2005) 3521–3529, https://doi.org/10.1002/chem.200401201. [146] K.S. Suslick, S.-B. Choe, A.A. Cichowlas, M.W. Grinstaff, Sonochemical synthesis of amorphous iron, Nature 353 (6343) (1991) 414–416.
[74] Y.R. Lee, J. Kim, W.S. Ahn, Synthesis of metal-organic frameworks: a mini-review, Korean J. Chem. Eng. 30 (2013) 1667–1680, https://doi.org/10.1007/ s11814-013-0140-6.
[75] J. Theerthagiri, J. Madhavan, S.J. Lee, M.Y. Choi, M. Ashokkumar, B.G. Pollet, Sonoelectrochemistry for energy and environmental applications, Ultrason. Sonochem. 63 (2020), https://doi.org/10.1016/j.ultsonch.2020.104960 104960.

[76]N. Stock, S. Biswas, Synthesis of metal-organic frameworks (MOFs): routes to various MOF topologies, morphologies, and composites, Chem. Rev. 112 (2012) 933–969, https://doi.org/10.1021/cr200304e.
[77]K.S. Suslick, D.A. Hammerton, R.E. Cline, Sonochemical hot spot, J. Am. Chem. Soc. 108 (1986) 5641–5642, https://doi.org/10.1021/ja00278a055.
[78] W.J. Son, J. Kim, J. Kim, W.S. Ahn, Sonochemical synthesis of MOF-5, Chem. Commun. 47 (2008) 6336–6338, https://doi.org/10.1039/B814740J.
[79] Z.Q. Li, L.G. Qiu, T. Xu, Y. Wu, W. Wang, Z.Y. Wu, X. Jiang, Ultrasonic synthesis of the microporous metal-organic framework Cu3(BTC)2 at ambient temperature and pressure: an efficient and environmentally friendly method, Mater. Lett. 63 (2009) 78–80, https://doi.org/10.1016/ j.matlet.2008.09.010.
[80] T. Chalati, P. Horcajada, R. Gref, P. Couvreur, C. Serre, Optimisation of the synthesis of MOF nanoparticles made of flexible porous iron fumarate MIL88A, J. Mater. Chem. 21 (2011) 2220–2227, https://doi.org/10.1039/ C0JM03563G.
[81] A.A. Tehrani, V. Safarifard, A. Morsali, G. Bruno, H.A. Rudbari, Ultrasound-assisted synthesis of metal-organic framework nanorods of Zn-HKUST-1 and their templating effects for facile fabrication of zinc oxide nanorods via solid-state transformation, Inorg. Chem. Commun. 59 (2015) 41–45, https://doi. org/10.1016/j.inoche.2015.06.028.
[82] N.A. Khan, S.H. Jhung, Synthesis of metal-organic frameworks (MOFs) with microwave or ultrasound: rapid reaction, phase-selectivity, and size reduction, Coord. Chem. Rev. 285 (2015) 11–23, https://doi.org/10.1016/j. ccr.2014.10.008.
[83] H.Y. Cho, J. Kim, S.N. Kim, W.S. Ahn, High yield 1-L scale synthesis of ZIF-8 via a sonochemical route, Microporous Mesoporous Mater. 169 (2013) 180–184, https://doi.org/10.1016/j.micromeso.2012.11.012.
[84] J. Zhang, T. Wu, S. Chen, P. Feng, X. Bu, Versatile structure-directing roles of deep-eutectic solvents and their implication in the generation of porosity and open metal sites for gas storage, Angew. Chem. Int. Ed. 48 (2009) 3486–3490, https://doi.org/10.1002/anie.200900134.
[85] Z. Lin, A.M. Slawin, R.E. Morris, Chiral induction in the ionothermal synthesis of a 3-D coordination polymer, J. Am. Chem. Soc. 129 (2007) 4880–4881.
https://doi.org/10.1021/ja070671y.
[86] K. Jin, X. Huang, L. Pang, J. Li, A. Appel, S. Wherland, [Cu(I)(bpp)]BF4: the first extended coordination network prepared solvothermally in an ionic liquid solvent, Chem. Commun. 22 (2002) 2872–2873, https://doi.org/ 10.1039/B209937N.
[87] K.Lu,A.L.Peláez,L.C.Wu,Y.Cao, C. H. Zhu, H. Fu, Ionothermal synthesis of five keggin-type polyoxometalate-based metal-organic frameworks, Inorg. Chem. 58 (2019) 1794–1805, https://doi.org/10.1021/acs.inorgchem.8b02277.
[88] J. Liu, X. Zou, C. Liu, K. Cai, N. Zhao, W. Zheng, W.G. Zhu, Ionothermal synthesis and proton-conductive properties of NH2-MIL-53 MOF nanomaterials, CrystEngComm 18 (2016) 525–528, https://doi.org/10.1039/ C5CE02141C.

[89] Z.F. Wu, B. Hu, M.L. Feng, X.Y. Huang, Y.B. Zhao, Ionothermal synthesis and crystal structure of a magnesium metal-organic framework, Inorg. Chem. Commun. 14 (2011) 1132–1135, https://doi.org/10.1016/j. inoche.2011.04.006.
[90] Z.H. Zhang, L. Xu, H. Jiao, Ionothermal synthesis, structures, properties of cobalt-1,4-benzene dicarboxylate metal-organic frameworks, J. Solid-State Chem. 238 (2016) 217–222, https://doi.org/10.1016/j.jssc.2016.03.028.
[91] D. Witters, N. Vergauwe, R. Ameloot, S. Vermeir, D.D. Vos, R. Puers, B. Sels, J. Lammertyn, Digital microfluidic high-throughput printing of single metalorganic framework crystals, Adv. Mater. 24 (2012) 1316–1320, https://doi. org/10.1002/adma.201104922.
[92] M. Faustini, J. Kim, G.Y. Jeong, J.Y. Kim, H.R. Moon, W.S. Ahn, D.P. Kim, Microfluidic approach toward continuous and ultrafast synthesis of metalorganic framework crystals and heterostructures in confined microdroplets, J. Am. Chem. Soc. 135 (2013) 14619–14626, https://doi.org/ 10.1021/ja4039642.
[93] W. Xu, J. Dong, J. Li, J. Li, F. Wu, A novel method for the preparation of zeolite ZSM-5, J. Chem. Soc., Chem. Commun. 10 (1990) 755–756, https://doi.org/ 10.1039/C39900000755.
[94] Q. Shi, Z. Chen, Z. Song, J. Li, J. Dong, Synthesis of ZIF-8 and ZIF-67 by steam-assisted conversion and an investigation of their tribological behaviours, Angew. Chem. 50 (2011) 672–675, https://doi.org/10.1002/anie.201004937.
[95] I. Ahmed, J. Jeon, N.A. Khan, S.H. Jhung, Synthesis of a metal-organic framework, iron-benezenetricarboxylate, from dry gels in the absence of acid and salt, Cryst. Growth Des. 12 (2012) 5878–5881, https://doi.org/ 10.1021/cg3014317.
[96]G.L. Denisov, P.V. Primakov, A.A. Korlyukov, V.V. Novikov, Y.V. Nelyubina, Solvothermal synthesis of the metal-organic framework MOF-5 in autoclaves prepared by 3D printing, Russ. J. Coord. Chem. 45 (2019) 836–842.
https:// doi.org/10.1134/S1070328419120030.
[97] C.T. Lee, M.W. Shin, Solvothermal growth of Mg-MOF-74 films on carboxylic functionalized silicon substrate using acrylic acid, Surf. Interfaces 22 (2021), https://doi.org/10.1016/j.surfin.2020.100845 100845.
[98]H.R. Abid, H. Tian, H.M. Ang, M.O. Tade, C.E. Buckley, S. Wang, Nanosize Zrmetal organic framework (UiO-66) for hydrogen and carbon dioxide storage, Chem. Eng. J. 187 (2012) 415–420, https://doi.org/10.1016/j.cej.2012.01.104.
[99]J.S. Choi, W.J. Son, J. Kim, W.S. Ahn, Metal-organic framework MOF-5 prepared by microwave heating: factors to be considered, Microporous Mesoporous Mater. 116 (2008) 727–731, https://doi.org/10.1016/j. micromeso.2008.04.033.
[100]M. Jahan, Z. Liu, K.P. Loh, A graphene oxide and copper-centred metal-organic framework composite as a tri-functional catalyst for HER, OER, and ORR, Adv. Funct. Mater. 23 (2013) 5363–5372, https://doi.org/10.1002/ adfm.201300510.
[101] Y. Fang, X. Li, F. Li, X. Lin, M. Tian, X. Long, X. An, Y. Fu, J. Jin, J. Ma, Selfassembly of cobalt-centred metal-organic framework and multiwalled carbon nanotubes hybrids as a

highly active and corrosion-resistant bifunctional oxygen catalyst, J. Power Sources 326 (2016) 50–59. https:// doi.org/10.1016/j.jpowsour.2016.06.114.
[102]J.H. Park, S.H. Park, S.H. Jhung, Microwave-syntheses of zeolitic imidazolate framework material, ZIF-8, J. Korean Chem. Soc. 53 (2009) 553–559, https:// doi.org/10.5012/jkcs.2009.53.5.553.
[103] M. Schlesinger, S. Schulze, M. Hietschold, M. Mehring, Evaluation of synthetic methods for microporous metal-organic frameworks exemplified by the competitive formation of [Cu2(btc)3(H2O)3] and [Cu2(btc)(OH)(H2O)], Microporous Mesoporous Mater. 132 (2010) 121–127, https://doi.org/ 10.1016/j.micromeso.2010.02.008.
[104] T. Chalati, P. Horcajada, R. Gref, P. Couvreur, C. Serre, Optimisation of the synthesis of MOF nanoparticles made of flexible porous iron fumarate MIL88A, J. Mater. Chem. 21 (2011) 2220–2227, https://doi.org/10.1039/ C0JM03563G.
[105] D.A. Yang, H.Y. Cho, J. Kim, S.T. Yang, W.S. Ahn, CO2 capture and conversion using Mg-MOF-74 prepared by a sonochemical method, Energy Environ. Sci. 5 (2012) 6465–6473, https://doi.org/10.1039/C1EE02234B.
[106] Z. Liang, R. Zhao, T. Qiu, R. Zou, Q. Xu, Metal-organic framework-derived materials for electrochemical energy applications, EnergyChem 1 (1) (2019) 100001, https://doi.org/10.1016/j.enchem.2019.100001.
[107] Y. Xue, S. Zheng, H. Xue, H. Pang, Metal-organic framework composites and their electrochemical applications, J. Mater. Chem. A 7 (2019) 7301–7327, https://doi.org/10.1039/C8TA12178H.
[108] S. Tajik, H. Beitollahi, F.G. Nejad, K.O. Kirlikovali, Q.V. Le, H.W. Jang, R.S. Varma, O.K. Farha, M. Shokouhimehr, Recent electrochemical applications of metal-organic framework-based materials, Cryst. Growth Des. 20 (2020) 7034–7064, https://doi.org/10.1021/acs.cgd.0c00601.
[109] X. Cao, C. Tan, M. Sindoro, H. Zhang, Hybrid micro-/nano-structures derived from metal-organic frameworks: preparation and applications in energy storage and conversion, Chem. Soc. Rev. 46 (2017) 2660–2677, https://doi. org/10.1039/C6CS00426A.
[110] X. Wei, X. Wang, X. Tan, Q. An, L. Mai, Nanostructured conversion-type negative electrode materials for low-cost and high-performance sodium-ion batteries, Adv. Funct. Mater. 28 (2018) 1804458, https://doi.org/10.1002/ adfm.201804458.
[111] M. Zheng, H. Tang, L. Li, Q. Hu, L. Zhang, H. Xue, H. Pang, Hierarchically nanostructured transition metal oxides for lithium-ion batteries, Adv. Sci. 5 (2018) 1700592, https://doi.org/10.1002/advs.201700592.
[112] B. He, Q. Zhang, Z. Pan, L. Li, C. Li, Y. Ling, Z.Wang, M. Chen, Z. Wang, Y. Yao, Q. Li, L. Sun, J. Wang, L. Wei, Freestanding metal-organic frameworks and their derivatives: an emerging platform for electrochemical energy storage and conversion, Chem. Rev. 122 (2022) 10087–10125, https://doi.org/10.1021/ acs.chemrev.1c00978.
[113] Z. Zhou, Q. Zhang, J. Sun, B. He, J. Guo, Q. Li, C. Li, L. Xie, Y. Yao, Metal-organic framework derived spindle-like carbon incorporated a-Fe2O3 grown on carbon nanotube fiber as

anodes for high-performance wearable asymmetric supercapacitors, ACS Nano 12 (2018) 9333–9341, https://doi.org/10.1021/ acsnano.8b04336.
[114] H. Gong, T. Wang, H. Xue, X. Lu, W. Xia, L. Song, S. Zhang, J. He, R. Ma, Spatially-controlled porous nanoflake arrays derived from MOFs: an efficiently long-life oxygen electrode, Nano Res. 12 (2019) 2528–2534, https://doi.org/10.1007/s12274-019-2480-y.
[115] X. Wang, J. He, B. Yu, B. Sun, D. Yang, X. Zhang, Q. Zhang, W. Zhang, L. Gu, Y. Chen, $CoSe_2$ nanoparticles embedded MOF-derived Co-NC nanoflake arrays as efficient and stable electrocatalyst for hydrogen evolution reaction, Appl. Catal. B 258 (2019), https://doi.org/10.1016/j.apcatb.2019.117996 117996.
[116] S.C. Sekhar, B. Ramulu, D. Narsimulu, S.J. Arbaz, J.S. Yu, Metal-organic framework-derived $Co_3V_2O_8$@ CuV_2O_6 hybrid architecture as a multifunctional binder-free electrode for Li-Ion batteries and hybrid supercapacitors, Small 16 (2020) 2003983, https://doi.org/10.1002/ smll.202003983.
[117] H.B. Wu, X.W. Lou, Metal-organic frameworks and their derived materials for electrochemical energy storage and conversion: promises and challenges.Sci. Adv. 3(12) (2017): eaap9252. [R165].
[118] X. Liu, L. Zhang, J. Wang, Design strategies for MOF-derived porous functional materials: preserving surfaces and nurturing pores, J. Materiomics 7 (2021) 440–459, https://doi.org/10.1016/j.jmat.2020.10.008.
[119] X.Y.Yu, L.Yu, H.B.Wu, X.W.Lou, Formation of nickel sulfide nanoframes from metal-=organic frameworks with enhanced pseudocapacitive and electrocatalytic properties, Angew. Chem. 127 (2015) 5421–5425, https:// doi.org/10.1002/ange.201500267.
[120] S. Zhang, Z. Yang, K. Gong, B. Xu, H. Mei, H. Zhang, J. Zhang, Z. Kang, Y. Yan, D. Sun, Temperature controlled diffusion of hydroxide ion sin 1D channels of NiMOF-74 for its complete conformal hydrolysis to hierarchical Ni(OH)2 supercapacitor electrodes, Nanoscale 11 (2019) 9598–9607, https://doi.org/ 10.1039/C9NR02555C.
[121] Y. Xue, S. Zheng, H. Xue, H. Pang, Metal-organic framework composites and their electrochemical applications, J. Mater. Chem. A 7 (2019) 7301–7327.
https://doi.org/10.1039/C8TA12178H.
[122] L. Zhang, Z. Su, F. Jiang, L. Yang, J. Qian, Y. Zhou, W. Li, M. Hong, Highly graphitized nitrogen-doped porous carbon nanopolyhedra derived from ZIF8 nanocrystals as efficient electrocatalysts for oxygen reduction reactions, Nanoscale 6 (2014) 6590–6602, https://doi.org/10.1039/C4NR00348A.
[123] H. Tian, S. Liu, Z. Zhang, T. Dang, Y. Lu, S. Liu, Highly stable polyoxo vanadate-based Zn–MOF with dual active sites as a solvent-free catalyst for C-C bond formation, ACS Sustainable Chem. Eng. 9 (2021) 4660–4667, https://doi.org/ 10.1021/acssuschemeng.1c00389.
[124]C. Hu, X. Hu, R. Li, Y. Xing, MOF derived ZnO/C nanocomposite with enhanced adsorption capacity and photocatalytic performance under sunlight, J. Hazard. Mater. 385 (2020), https://doi.org/10.1016/j.jhazmat.2019.121599 121599.

[125] M.Z. Hussain, G.S. Pawar, Z. Huang, A.A. Tahir, R.A. Fischer, Y. Zhu, Y. Xia, Porous ZnO/Carbon nanocomposites derived from metal-organic frameworks for highly efficient photocatalytic applications: a correlational study, Carbon 146 (2019) 348–363, https://doi.org/10.1016/j.carbon.2019.02.013.
[126] Z. Liang, R. Zhao, T. Qiu, R. Zou, Q. Xu, Metal-organic framework-derived materials for electrochemical energy applications, EnergyChem 1 (1) (2019) 100001, https://doi.org/10.1016/j.enchem.2019.100001.
[127] H.B. Wu, B.Y. Xia, L. Yu, X.Y. Yu, X.W.D. Lou, Porous molybdenum carbide nano-octahedrons synthesized via confined carburization in metal-organic frameworks for efficient hydrogen production, Nat. Commun. 6 (2015) 1–8, https://doi.org/10.1038/ncomms7512.
[128] L. Shang, H. Yu, X. Huang, T. Bian, R. Shi, Y. Zhao, G.I.N. Waterhouse, L.Z. Wu, C.H. Tung, T. Zhang, Well-dispersed ZIF-derived Co, N-Co-doped carbon nanoframes through mesoporous-silica-protected calcination as efficient oxygen reduction electrocatalysts, Adv. Mater. 28 (2016) 1668–1674, https://doi.org/10.1002/adma.201505045.
[129] J. Zhang, Z. Li, Y. Chen, S. Gao, X.W.D. Lou, Nickel-iron layered double hydroxide hollow polyhedrons as a superior sulfur host for lithium-sulfur batteries, Angew. Chem. 130 (2018) 11110–11114, https://doi.org/10.1002/ ange.201805972.
[130] B.Y. Guan, L. Yu, X.W. Lou, A dual-metal-organic-framework derived electrocatalyst for oxygen reduction, Energy Environ. Sci. 9 (2016) 3092– 3096, https://doi.org/10.1039/C6EE02171A.
[131] W. Xia, J. Zhu, W. Guo, L. An, D. Xia, R. Zou, Well-defined carbon polyhedrons prepared from nano metal-organic frameworks for oxygen reduction, J. Mater. Chem. A 2 (2014) 11606–11613, https://doi.org/10.1039/ C4TA01656D.
[132] S. Choi, H.J. Lee, M. Oh, Facile synthesis of Au or Ag nanoparticles-embedded hollow carbon microspheres from metal-organic framework hybrids and their efficient catalytic activities, Small, 12 (2016) 2425-2431. https://doi.org/10.1002/smll.201600356.
[133] X. Lu, C. Wang, F. Favier, N. Pinna, Electrospun nanomaterials for supercapacitor electrodes: designed architectures and electrochemical performance, Adv. Energy Mater. 7 (2017) 1601301, https://doi.org/ 10.1002/aenm.201601301.
[134] G. Zhang, X. Xiao, B. Li, P. Gu, H. Xue, H. Pang, Transition metal oxides with one-dimensional/one-dimensional-analogue nanostructures for advanced supercapacitors, J. Mater. Chem. A 5 (2017) 8155–8186, https://doi.org/ 10.1039/C7TA02454A.
[135] P. Pachfule, D. Shinde, M. Majumder, Q. Xu, Fabrication of carbon nanorods and graphene nanoribbons from a metal-organic framework, Nat. Chem. 8 (2016) 718–724, https://doi.org/10.1038/nchem.2515.
[136] L. Zhang, X. Wang, R. Wang, M. Hong, Structural evolution from metalorganic framework to hybrids of nitrogen-doped porous carbon and carbon nanotubes for enhanced oxygen reduction activity, Chem. Mater. 27 (2015) 7610–7618, https://doi.org/10.1021/acs.chemmater.5b02708.

[137] A. Saad, S. Biswas, E. Gkaniatsou, C. Sicard, E. Dumas, N. Menguy, N. Steunou, Metal-organic framework based 1D nanostructures and their superstructures: synthesis, microstructure, and properties, Chem. Mater. 33 (2021) 5825–5849, https://doi.org/10.1021/acs.chemmater.1c01034.
[138] S. Kuyuldar, D.T. Genna, C. Burda, On the potential for nanoscale metalorganic frameworks for energy applications, J. Mater. Chem. A 7 (2019) 21545–21576, https://doi.org/10.1039/C9TA09896H.
[139] B. Mendoza-Sánchez, Y. Gogotsi, Synthesis of two-dimensional materials for capacitive energy storage, Adv. Mater. 28 (2016) 6104–6135, https://doi.org/ 10.1002/adma.201506133.
[140] H. Jin, C. Guo, X. Liu, J. Liu, A. Vasileff, Y. Jiao, Y. Zheng, S.-Z. Qiao, Emerging two-dimensional nanomaterials for electrocatalysis, Chem. Rev. 118 (13) (2018) 6337–6408, https://doi.org/10.1021/acs.chemrev.7b00689.
[141] Z. Wu, J. Qi, W. Wang, Z. Zeng, Q. He, Emerging elemental two-dimensional materials for energy applications, J. Mater. Chem. A 9 (2021) 18793–18817, https://doi.org/10.1039/D1TA03676A.
[142] F.R.Fan, R.Wang, H. Zhang, W. Wu, Emerging beyond-graphene elemental 2D materials for energy and catalysis applications, Chem. Soc. Rev. 50 (2021) 10983–11031, https://doi.org/10.1039/C9CS00821G.
[143] F. Cao, M. Zhao, Y. Yu, B.o. Chen, Y. Huang, J. Yang, X. Cao, Q. Lu, X. Zhang, Z. Zhang, C. Tan, H. Zhang, Cao et al, Synthesis of two-dimensional CoS1.097/ nitrogen-doped carbon nanocomposites using metal-organic framework nanosheets as precursors for supercapacitor application, J. Am. Chem. Soc. 138 (22) (2016) 6924–6927, https://doi.org/10.1021/jacs.6b02540.
[144] H.X. Zhong, J. Wang, Y.W. Zhang, W.L. Xu, W. Xing, D. Xu, Y.F. Zhang, X.B. Zhang, ZIF-8 derived graphene-based nitrogen-doped porous carbon sheets as highly efficient and durable oxygen reduction electrocatalysts, Angew. Chem. Int. Ed. 53 (2014) 14235–14239, https://doi.org/10.1002/ anie.201408990.
[145] Y. Xue, G. Zhao, R. Yang, F. Chu, J. Chen, L. Wang, X. Huang, 2Dmetal–organic framework-based materials for electrocatalytic, photocatalytic and thermocatalytic applications, Nanoscale 13 (2021) 3911–3936, https://doi. org/10.1039/D0NR09064F.
[146] M. Zhao, Y. Huang, Y. Peng, Z. Huang, Q. Ma, H. Zhang, Two-dimensional metal-organic framework nanosheets: synthesis and applications, Chem. Soc. Rev. 47 (2018) 6267–6295, https://doi.org/10.1039/C8CS00268A.
[147] Q. Jiang, C. Zhou, H. Meng, Y. Han, X. Shi, C. Zhan, R. Zhang, Two-dimensional metal-organic framework nanosheets: synthetic methodologies and electrocatalytic applications, J. Mater. Chem. A, 8 (2020) 15271–15301, https://doi.org/10.1039/D0TA00468E.
[148] M. Zhao, Q. Lu, Q. Ma, H. Zhang, Two-dimensional metal-organic framework nanosheets, Small Methods 1 (2017) 1600030, https://doi.org/10.1002/ smtd.201600030.

[149] K. Zhao, S. Liu, G.Ye, Q.Gan, Z. Zhou, Z.He, High-yield bottom-up synthesis of 2D metal-organic frameworks and their derived ultrathin carbon nanosheets for energy storage, J. Mater. Chem. A 6 (2018) 2166–2175, https://doi.org/ 10.1039/C7TA06916B.
[150] J. Cong, H. Xu, M. Lu, Y. Wu, Y. Li, P. He, J. Gao, J. Yao, S. Xu, Two-dimensional Co@N-carbon nanocomposites facilely derived from metal-organic framework nanosheets for efficient bifunctional electrocatalysis, Chem.Asian J. 13 (2018) 1485–1491, https://doi.org/10.1002/asia.201800319.
[151] C. Cao, X.u. Qiang, Q.-L. Zhu, Ultrathin two-dimensional metallenes for heterogeneous catalysis, Chem Catalysis 2 (2022) 693–723, https://doi.org/ 10.1016/j.checat.2022.01.021.
[152] Y. Liu, K.N. Dinh, Z. Dai, Q. Yan, Metallenes: recent advances and opportunities in energy storage and conversion applications, ACS Mater. Lett. 2 (2020) 1148–1172, https://doi.org/10.1021/acsmaterialslett.0c00280.
[153] C. Cao, D.D. Ma, J.F. Gu, X. Xie, G. Zeng,X. Li, S.G. Han, Q.T. Zhu, X.T. Wu, Q.Xu, Metal–organic layers leading to atomically thin bismuthene for efficient carbon dioxide electro reduction to liquid fuel, Angew. Chem. Int. Ed. 59 (2020) 15014–15020, https://doi.org/10.1002/anie.202005577.
[154] C. Cao, D.D. Ma, J. Jia, Q. Xu, X.T. Wu, Q.L. Zhu, Divergent paths, same goal: a pair-electrosynthesis tactic for cost-efficient and exclusive formate production by metal-organic-framework-derived 2D electrocatalysts, Adv. Mater. 33 (2021) 2008631, https://doi.org/10.1002/adma.202008631.
[155] G. Zeng, Y. He, D.-D. Ma, S. Luo, S. Zhou, C.Cao, X.Li, X.-T. Wu, H.-G. Liao, Q.-L. Zhu, Reconstruction of ultrahigh-aspect-ratio crystalline bismuth-organic hybrid nanobelts for selective electrocatalytic CO2 reduction to formate, Adv. Funct. Mater. 32 (30) (2022) 2201125.
[156] C. Zhu, H. Li, S. Fu, D. Du, Y. Lin, Highly efficient nonprecious metal catalysts towards oxygen reduction reaction based on three-dimensional porous carbon nanostructures, Chem. Soc. Rev. 45 (2016) 517–531, https://doi.org/ 10.1039/C5CS00670H.
[157] Q.L. Zhu, W. Xia, T. Akita, R. Zou, Q. Xu, Metal-organic framework-derived honeycomb-like open porous nanostructures as precious-metal-free catalysts for highly efficient oxygen electro reduction, Adv. Mater. 28 (2016) 6391–6398, https://doi.org/10.1002/adma.201600979.
[158] Y. Qian, A. Tao, K.E. Birgersson, Z. Liu, D. Zhao, Web-like interconnected carbon networks from NaCl-assisted pyrolysis of ZIF-8 for highly efficient oxygen reduction catalysis, Small 14 (2018) 1704169, https://doi.org/ 10.1002/smll.201704169.
[159]R. Zhao, W. Xia, C. Lin, J. Sun, A. Mahmood, Q. Wang, B. Qiu, H. Tabassum, R. Zou, A pore-expansion strategy to synthesize hierarchically porous carbon derived from a metal-organic framework for enhanced oxygen reduction, Carbon 114 (2017) 284–290, https://doi.org/10.1016/j.carbon.2016.12.027.
[160] X.Xu, T.Yang, Q.Zhang, W.Xia, Z.Ding, K.Eid, A.M.Abdullah, M.S.A.Hossain, S. Zhang, J. Tang, L. Pan, Y. Yamauchi, Ultrahigh capacitive deionization performance by 3D interconnected MOF-derived nitrogen-doped carbon tubes, Chem. Eng. J. 390 (2020), https://doi.org/10.1016/j.cej.2020.124493 124493.

[161] Q. Yang, Y. Liu, C. Deng, M. Yan, W. Shi, MOF-derived 3D hierarchical nanoarrays consisting of NiCoZn-S nanosheets coupled with granular NiCo2S4 nanowires for high-performance hybrid supercapacitors, J. Mater. Chem. A 7 (2019) 26131–26138, https://doi.org/10.1039/C9TA09692B.
[162] .T. Ren, G.G. Yuan, C.C. Weng, Z.Y. Yuan, Rationally designed Co3O4–C nanowire arrays on ni foam derived from the metal-organic framework as reversibleoxygenevolutionelectrodeswithenhancedperformanceforZn-air batteries, ACS Sustainable Chem. Eng. 6 (2018) 707–718, https://doi.org/ 10.1021/acssuschemeng.7b03034.
[163] Y. Liu, G. Li, J. Fu, Z. Chen, X. Peng, Strings of porous carbon polyhedrons as self-standing cathode host for high-energy-density lithium-sulphur batteries, Angew. Chem. Int. Ed. 129 (2017) 6272–6276, https://doi.org/10.1002/ ange.201700686.
[164]O.M. Yaghi, H. Li, Hydrothermal Synthesis of a Metal-Organic Framework Containing Large Rectangular Channels, J. Am. Chem. Soc. 117 (41) (1995) 10401–10402.
[165] O.M. Yaghi, G. Li, Li Hailian, Selective binding and removal of guests in a microporous metal-organic framework, Nature 378 (1995) 703–706.
[166] H. Li, M. Eddaoudi, T.L. Groy, O.M. Yaghi, Establishing microporosity in open metal-organic frameworks: Gas sorption isotherms for Zn(BDC) (BDC = 1,4- benzene-dicarboxylate)
[167] G. Frey, Hybrid porous solids: past, present, future, Chem. Soc. Rev. 37 (2008) 191–214, https://doi.org/10.1039/B618320B.
[168] Z. Wang, S.M. Cohen, Postsynthetic modification of metal-organic frameworks, Chem. Soc. Rev. 38 (2009) 1315, https://doi.org/10.1039/b802258p.
[169] B.F. Hoskins, R. Robson, Infinite polymeric frameworks consisting of three-dimensionally linked rod-like segments, J. Am. Chem. Soc. 111 (1989) 5962–5964, https://doi.org/10.1021/ja00197a079.
[170] B.F. Hoskins, R. Robson, Design and Construction of a New Class of Scaffolding- like Materials Comprising Infinite Polymeric Frameworks of 3D-Linked Molecular Rods. A Reappraisal of the Zn(CN)2 and Cd(CN)2 Structures and the Synthesis and Structure of the Diamond-Related Framework, J. Am. Chem. Soc. 112 (1990) 1546–1554, https://doi.org/10.1021/ja00160a038.
[171] M. Kondo, T. Yoshitomi, K. Seki, H. Matsuzaka, S. Kitagawa, Three-Dimensional Framework with Channeling Cavities for Small Molecules: {[M2(4,4′-by)3(NO3) 4]·xH2O}n (M = Co, Ni, Zn), Angew. Chemie (International Ed. English). 36 (1997) 1725–1727. https://doi.org/10.1002/anie.199717251.
[172] S.S.-Y. Chui, S.M.-F. Lo, J.P.H. Charmant, A.G. Orpen, I.D. Williams, A Chemically Functionalised Nanoporous Material, Science (80-.). 283 (1999) 1148–1150. https://doi.org/10.1126/science.283.5405.1148.
[173] H. Li, M. Eddaoudi, M. O'Keeffe, O.M. Yaghi, Design and synthesis of an exceptionally stable and highly porous metal-organic framework, Nature 402 (1999) 276–279, https://doi.org/10.1038/46248.

[174] K. Barthelet, J. Marrot Dr., D. Riou Prof. Dr., G. F´erey Prof. Dr., A Breathing Hybrid Organic-Inorganic Solid with Very Large Pores and High Magnetic Characteristics, Angew. Chemie Int. Ed. 41 (2002) 281–284. https://doi.org/ 10.1002/1521-3773.
[175] C. Serre, C. Mellot-Draznieks, S. Surbl´e, N. Audebrand, Y. Filinchuk, G. F´erey, Role of solvent-host interactions that lead to very large swelling of hybrid frameworks, Science (80-.). 315 (2007) 1828–1831, https://doi.org/10.1126/ science.1137975.
[176] C. Serre, F. Millange, C. Thouvenot, M. Nogu`es, G. Marsolier, D. Lou¨er, G. F´erey, Very large breathing effect in the first nanoporous chromium(III)-based solids: MIL-53 or CrIII(OH)·{O2C-C6H4- CO2}·{HO2C-C6H4 -CO2H}x·H2Oy, J. Am. Chem. Soc. 124 (2002) 13519–13526, https://doi.org/10.1021/ja0276974.
[177] P. Silva, S.M.F. Vilela, J.P.C. Tom´e, F.A. Almeida Paz, Multifunctional metal-organic frameworks: from academia to industrial applications, Chem. Soc. Rev. 44 (2015) 6774–6803, https://doi.org/10.1039/C5CS00307E.
[178] M.H. Yap, K.L. Fow, G.Z. Chen, Synthesis and applications of MOF-derived porous nanostructures, Green Energy Environ. 2 (2017) 218–245, https://doi.org/ 10.1016/j.gee.2017.05.003.
[179] Changyoon Jeong, Mohd Zahid Ansari, Abdul Hakeem Anwer, Soo-Hyun Kim, Abu Nasar, Mohd Shoeb, Fouzia Mashkoor, A review on metal-organic frameworks for the removal of hazardous environmental contaminants, Separation and Purification Technology 305 (2023) 122416.
[180] O.M. Yaghi, United States Patent (19), 1997.
[181] M. Kondo, T. Yoshitomi, H. Matsuzaka, S. Kitagawa, K. Seki, Three-Dimensional Framework with Channeling Cavities for Small Molecules:{[M2(4,4′-bpy)3(NO3) 4]·xH2O}n(M = Co, Ni, Zn), Angew. Chemie Int. Ed. English. 36 (1997) 1725–1727. https://doi.org/10.1002/anie.199717251.
[182] U. Mueller, M. Schubert, F. Teich, H. Puetter, K. Schierle-Arndt, J. Pastr´e, Metal-organic frameworks—prospective industrial applications, J. Mater. Chem. 16 (2006) 626–636, https://doi.org/10.1039/B511962F
[183] Z. Ni, R.I. Masel, Rapid production of metal-organic frameworks via microwave-assisted solvothermal synthesis, J. Am. Chem. Soc. 128 (2006) 12394–12395, https://doi.org/10.1021/ja0635231.
[184] S.-H. Jhung, J.-S. Chang, Y.-K. Hwang, C. Serre, G. Ferey, United States Patent (10), Patent No. US7855299B2 (2010).
[185] S. Ramanayaka, M. Vithanage, A. Sarmah, T. An, K.-H. Kim, Y.S. Ok, Performance of metal-organic frameworks for the adsorptive removal of potentially toxic elements in a water system: a critical review, RSC Adv. 9 (2019) 34359–34376.
https://doi.org/10.1039/C9RA06879A.
[186] A.L. Garay, A. Pichon, S.L. James, Solvent-free synthesis of metal complexes, Chem. Soc. Rev. 36 (2007) 846, https://doi.org/10.1039/b600363j.

[187] A. Demessence, D.M. D'Alessandro, M.L. Foo, J.R. Long, Strong CO 2 binding in a water-stable, triazolate-bridged metal-organic framework functionalized with ethylenediamine, J. Am. Chem. Soc. 131 (2009) 8784–8786, https://doi.org/ 10.1021/ja903411w.
[188] S. Wang, E.V. Alekseev, J. Diwu, W.H. Casey, B.L. Phillips, W. Depmeier, T. E. Albrecht-Schmitt, NDTB-1: A super tetrahedral cationic framework that removes TcO4 − from solution, Angew. Chemie Int. Ed. 49 (2010) 1057–1060, https://doi.org/10.1002/anie.200906397.
[189] A. Carn´e-S´anchez, K.C. Stylianou, C. Carbonell, M. Naderi, I. Imaz, D. Maspoch, Protecting metal-organic framework crystals from hydrolytic degradation by spray-dry encapsulating them into polystyrene microspheres, Adv. Mater. 27 (2015) 869–873, https://doi.org/10.1002/adma.201403827.
[190] J. Park, A.C. Hinckley, Z. Huang, D. Feng, A.A. Yakovenko, M. Lee, S. Chen, X. Zou, Z. Bao, Synthetic routes for a 2D semiconductive copper hexahydroxybenzene metal-organic framework, J. Am. Chem. Soc. 140 (2018) 14533–14537, https://doi.org/10.1021/jacs.8b06666.
[191] Y. Luo, S. Bag, O. Zaremba, A. Cierpka, J. Andreo, S. Wuttke, P. Friederich, M. Tsotsalas, MOF synthesis prediction enabled by automatic data mining and machine learning, Angew. Chemie Int. Ed. 61 (2022), https://doi.org/10.1002/ anie.202200242.
[192] Y. Gao, S. Li, Y. Li, L. Yao, H. Zhang, Accelerated photocatalytic degradation of the organic pollutant over metal-organic framework MIL-53(Fe) under visible LED light mediated by persulfate, Appl. Catal. B 202 (2017) 165–174, https:// doi.org/10.1016/j.apcatb.2016.09.005.
[193] Y.L. Wu, X. Li, Y.S. Wei, Z. Fu, W. Wei, X.T. Wu, Q.L. Zhu, Q. Xu, Ordered macroporous superstructure of nitrogen-doped nanoporous carbon implanted with ultrafine Ru nanoclusters for efficient pH-universal hydrogen evolution reaction, Adv. Mater. 33 (2021) 2006965, https://doi. org/10.1002/adma.202006965.
[194] C.B. Hong, X. Li, W.B. Wei, X.T. Wu, Q.L. Zhu, Nano-engineering of Ru-based hierarchical porous nanoreactors for highly efficient pH-universal overall water splitting, Appl. Catal. B 294 (2021), https://doi.org/10.1016/j. apcatb.2021.120230 120230.
[195] Y.L. Wu, N. Xie, X.F. Li, Z.M. Fu, X.T. Wu, Q.L. Zhu, MOF-derived hierarchical hollow NiRu-C nanohybrid for efficient hydrogen evolution reaction, Chin. J. Struct. Chem 40 (2021) 1346. https://doi.org/10.14102/j.cnki.0254-5861. 2011-3153.
[196] Liyuan Qu, Hiroaki Iguchi, Shinya Takaishi, Faiza Habib, Chanel F. Leong, Deanna M. D'Alessandro, Takefumi Yoshida, Hitoshi Abe, Eiji Nishibori, and Masahiro Yamashita, Porous Molecular Conductor: Electrochemical Fabrication of Through-Space Conduction Pathways among Linear Coordination Polymers, *J. Am. Chem. Soc.* 141, 17, (2019) 6802–6806. https://doi.org/10.1021/jacs.9b01717
[197] X. Chen, D.D. Ma, B. Chen, K. Zhang, R. Zou, X.T. Wu, Q.L. Zhu, Metal-organic framework-derived mesoporous carbon nanoframes embedded with atomically dispersed Fe-Nx active sites for efficient bifunctional oxygen and carbon dioxide electro-reduction, Appl. Catal. B 267 (2020), https://doi.org/ 10.1016/j.apcatb.2020.118720 118720.
[198] X. Li, Q.-L. Zhu, MOF-based materials for photo-and electrocatalytic CO2 reduction, Energy Chem 2 (3) (2020) 100033.

[199] Faiza Habib, Derek A Tocher, Neil J Press and Claire J Carmalt, *Microporous and Mesoporous Materials*, 308, (2020) 110548. https://doi.org/10.1016/j.micromeso.2020.110548
[200] Faiza Habib, Derek A Tocher, Claire J Carmalt, Applications of the crystalline sponge method and developments of alternative crystalline sponges, *Materials Today: Proceedings* 56, (2022) 3766-3773. https://doi.org/10.1016/j.matpr.2022.01.018
[201] H. Li, L. Li, R.-B.Lin, W.Zhou, Z.Zhang, S.Xiang, B.Chen, Porous metal-organic frameworks for gas storage and separation: status and challenges, EnergyChem 1 (1) (2019) 100006, https://doi.org/10.1016/j.enchem.2019.100006.
[202] Y. Yang, Z. Lun, G. Xia, F. Zheng, M. He, Q. Chen, Non-precious alloy encapsulated in nitrogen-doped graphene layers derived from MOFs as an active and durable hydrogen evolution reaction catalyst, Energy Environ. Sci. 8 (2015) 3563–3571, https://doi.org/10.1039/C5EE02460A.
[203] X.Y. Yu, Y. Feng, B. Guan, X.W.D. Lou, U. Paik, Carbon coated porous nickel phosphides nanoplates for highly efficient oxygen evolution reaction, Energy Environ. Sci. 9 (2016) 1246–1250, https://doi.org/10.1039/C6EE00100A.
[204] C. Petit, T.J. Bandosz, MOF-graphite oxide composites: combining the uniqueness of graphene layers and metal-organic frameworks, Adv. Mater. 21 (2009) 4753–4757, https://doi.org/10.1002/adma.200901581.
[205] Z. Xiang, Z. Hu, D. Cao, W. Yang, J. Lu, B. Han, W. Wang, Metal-organic frameworks with incorporated carbon nanotubes: improving carbon dioxide and methane storage capacities by lithium doping, Angew. Chemie Int. Edition 123 (2011) 491–494, https://doi.org/10.1002/ange.201004537.
[206] X.F. Lu, Y. Fang, D. Luan, X.W.D. Lou, Metal-organic frameworks derived functional materials for electrochemical energy storage and conversion: a mini-review, Nano Lett. 21 (2021) 1555–1565, https://doi.org/10.1021/ acs.nanolett.0c04898.
[207] L. Sun, M.G. Campbell, M. Dinca ˇ, Electrically conductive porous metal-organic frameworks, Angew. Chemie Int. Ed. 128 (2016) 3628–3642, https://doi.org/ 10.1002/anie.201506219.
[208] Q. Li, J. Zhou, S. Zhao, Y. Li, C. Chen, K. Tao, *et al.*, Hollow and hierarchical cobalt–metal-organic framework@ CoCr2O4 microplate array as a battery-type electrode for high-performance hybrid supercapacitors, ChemElectroChem 7 (2) (2020) 437–444.
[209] Y. Seo, P.A. Shinde, S. Park, S.C. Jun, Self-assembled bimetallic cobalt–manganese metal-organic framework as a highly efficient, robust electrode for asymmetric supercapacitors, Electrochim. Acta 335 (2020), 135327.
[210] N. Xin, Y. Liu, H. Niu, H. Bai, W. Shi, In-situ construction of metal-organic frameworks derived Co/Zn–S sandwiched graphene film as free-standing electrodes for ultra-high energy density supercapacitors, J. Power Sources 451 (2020), 227772.
[211] R. Rajak, R. Kumar, S.N. Ansari, M. Saraf, S.M. Mobin, Recent highlights and future prospects on mixed-metal MOFs as emerging supercapacitor candidates, Dalton Trans. 49 (34) (2020) 11792–11818.

[212] S. Ghosh, C.K. Maity, G.C. Nayak, H.P. Nayek, A cobalt(II) metal-organic framework featuring supercapacitor application, J. Solid State Chem. 282 (2020), 121093.
[213] D. Han, J. Wei, Y. Zhao, Y. Shen, Y. Pan, Y. Wei, *et al.*, Metal-organic framework derived petal-like Co3O4@CoNi2S4 hybrid on carbon cloth with enhanced performance for supercapacitors, Inorg. Chem. Front. 7 (6) (2020) 1428–1436.
[214] V. Elayappan, P.A. Shinde, G.K. Veerasubramani, S.C. Jun, H.S. Noh, K. Kim, *et al.*, Metal-organic-framework-derived hierarchical Co/CoP-decorated nanoporous carbon polyhedra for robust high-energy storage hybrid supercapacitors, Dalton Trans. 49 (4) (2020) 1157–1166.
[215] J. Cherusseri, D. Pandey, K. Sambath Kumar, J. Thomas, L. Zhai, Flexible supercapacitor electrodes using metal-organic frameworks, Nanoscale 12 (34) (2020) 17649–17662.
[216] C.S. Lee, J. Moon, J.T. Park, J.H. Kim, Highly interconnected nanorods and nanosheets based on a hierarchically layered metal-organic framework for a flexible, high-performance energy storage device, ACS Sustain. Chem. Eng. 8 (9) (2020) 3773–3785.
[217] C. Miao, X. Xiao, Y. Gong, K. Zhu, K. Cheng, K. Ye, *et al.*, Facile synthesis of metal-organic framework-derived CoSe2 nanoparticles embedded in the N-doped carbon nanosheet array and application for supercapacitors, ACS Appl. Mater. Interfaces 12 (8) (2020) 9365–9375.
[218] M. Wang, H. Shi, P. Zhang, Z. Liao, M. Wang, H. Zhong, *et al.*, Phthalocyanine- based 2D conjugated metal-organic framework nanosheets for high-performance micro-supercapacitors, Adv. Funct. Mater. 30 (30) (2020), 2002664.
[219] S. Zheng, Q. Li, H. Xue, H. Pang, Q. Xu, A highly alkaline-stable metal oxide@ metal-organic framework composite for high-performance electrochemical energy storage, Natl. Sci. Rev. 7 (2) (2020) 305–314.
[220] S. Chen, L. Zhao, W. Wei, Y. Li, L. Mi, A novel strategy to synthesize NiCo layered double hydroxide nanotube from metal-organic framework composite for high-performance supercapacitor, J. Alloy. Compd. 831 (2020), 154794.
[221] F. Xu, N. Chen, Z. Fan, G. Du, Ni/Co-based metal-organic frameworks rapidly synthesized in an ambient environment for high energy and power hybrid supercapacitors, Appl. Surf. Sci. 528 (2020), 146920.
[222] J. Sun, X. Yu, S. Zhao, H. Chen, K. Tao, L. Han, Solvent-controlled morphology of amino-functionalized bimetal metal-organic frameworks for asymmetric supercapacitors, Inorg. Chem. 59 (16) (2020) 11385–11395.
[223] K.B. Wang, R. Bi, Z.K. Wang, Y. Chu, H. Wu, K.B. Wang, Metal-organic frameworks with different spatial dimensions for supercapacitors, New J. Chem. 44 (8) (2020) 3147–3167.
[224] Y. Zhong, X. Cao, L. Ying, L. Cui, C. Barrow, W. Yang, *et al.*, Homogeneous nickel metal-organic framework microspheres on reduced graphene oxide as novel electrode material for supercapacitors with outstanding performance, J. Colloid Interface Sci. 561 (2020) 265–274.
[225] Z. Andikaey, A.A. Ensafi, B. Rezaei, Synthesis of engineered graphene nanocomposites coated with NiCo metal-organic frameworks as electrodes for high-quality supercapacitor, Int. J. Hydrog. Energy 45 (56) (2020) 32059–32071.

[226] J. Kim, S.-J. Park, S. Chung, S. Kim, Preparation and capacitance of Ni metal-organic framework/reduced graphene oxide composites for supercapacitors as nano architectonics, J. Nanosci. Nanotechnol. 20 (5) (2019) 2750–2754.
[227] M.S. Javed, M.K. Aslam, S. Asim, S. Batool, M. Idrees, S. Hussain, *et al.*, High-performance flexible hybrid-supercapacitor enabled by pairing binder-free ultrathin Ni–Co–O nanosheets and metal-organic framework derived N-doped carbon nanosheets, Electrochim. Acta 349 (2020), 136384.
[228] F. Ran, X. Xu, D. Pan, Y. Liu, Y. Bai, L. Shao, Ultrathin 2D metal-organic framework nanosheets in situ interpenetrated by functional CNTs for hybrid energy storage device, Nano Micro Lett. 12 (1) (2020) 1–13.
[229] X. Shi, J. Yu, Q. Liu, L. Shao, Y. Zhang, Z. Sun, H. Huang, *et al.*, Metal-organic-framework-derived N-, P-, and O-codoped nickel/carbon composites homogeneously decorated on reduced graphene oxide for energy storage, ACS Appl. Nano Mater. 3 (6) (2020) 5625–5636.
[230] R. Hou, M. Miao, Q. Wang, T. Yue, H. Liu, H.S. Park, *et al.*, Integrated conductive hybrid architecture of metal-organic framework nanowire array on polypyrrole membrane for all-solid-state flexible supercapacitors, Adv. Energy Mater. 10 (1) (2020) 1–9.
[231] N. Wu, H. Wu, J. Zhang, Y. Zhang, D. Cao, L. Bai, *et al.*, Cu2O/Cu@C nanosheets derived from one novel Cu (II) metal-organic framework for high-performance supercapacitors, J. Alloy. Compd. 856 (2021), 157466.
[232] A.M. Zardkhoshoui, S.S.H. Davarani, Ultra-high energy density supercapacitors based on a metal-organic framework derived yolk–shell Cu–Co–P hollow nanospheres and CuFeS2 nanosheet arrays, Dalton Trans. 49 (10) (2020) 3353–3364.
[233] Y.F. Wang, S.Y. Yang, Y. Yue, S.W. Bian, Conductive copper-based metal-organic framework nanowire arrays grown on graphene fibres for flexible all-solid-state supercapacitors, J. Alloy. Compd. 835 (2020), 155238.
[234] A. Ehsani, M. Bigdeloo, F. Assefi, M. Kiamehr, R. Alizadeh, Ternary nanocomposite of conductive polymer/chitosan biopolymer/metal-organic framework: synthesis, characterization and electrochemical performance as effective electrode materials in pseudocapacitors, Inorg. Chem. Commun. 115 (2020), 107885.
[235] Y. Gu, L. Miao, Y. Yin, M. Liu, L. Gan, L. Li, Highly N/O co-doped ultramicroporous carbons derived from a nonporous metal-organic framework for high-performance supercapacitors, Chin. Chem. Lett. 32 (4) (2021) 1491–1496.
[236] M. Lan, X. Wang, R. Zhao, M. Dong, L. Fang, L. Wang, Metal-organic framework-derived porous MnNi2O4 micro flower as an advanced electrode material for high-performance supercapacitors, J. Alloy. Compd. 821 (2020), 153546.
[237] S. Hong, Y. Kim, Y. Kim, K. Suh, M. Yoon, K. Kim, Hierarchical porous carbon materials prepared by direct carbonization of metal-organic frameworks as an electrode material for supercapacitors, Bull. Korean Chem. Soc. 42 (2) (2021) 309–314.

[238] X. Xu, C. Zhao, X. Liu, Y. Liu, P. Dong, C. Itani, Metal-organic framework-derived ZnMoO4 nanosheet arrays for advanced asymmetric supercapacitors, J. Mater. Sci. Mater. Electron. 31 (4) (2020) 3631–3641.
[239] P.A. Shinde, Y. Seo, S. Lee, H. Kim, Q.N. Pham, Y. Won, *et al.*, Layered manganese metal-organic framework with high specific and areal capacitance for hybrid supercapacitors, Chem. Eng. J. 387 (2020), 122982.
[240] M. Majumder, R.B. Choudhary, A.K. Thakur, A. Khodayari, M. Amiri, R. Boukherroub, *et al.*, Aluminum based metal-organic framework integrated with reduced graphene oxide for improved supercapacitive performance, Electrochim. Acta 353 (2020), 136609.
[241] C. Wang, G.Y. Qiao, J.S. Qin, J. Yu, Discrete nanographene implanted in zirconium metal-organic framework for electrochemical energy storage, J. Solid State Chem. 287 (2020), 121377.
[242] R. Govindan, X. Hong, P. Sathishkumar, Y. Cai, Electrochimica Acta Construction of metal-organic framework-derived CeO2/C integrated MoS2 hybrid for high- performance asymmetric supercapacitor, Electrochim. Acta 353 (2020), 136502.
[243] X. Li, Y. Xu, H. Wu, X. Qian, L. Chen, L.Y. Dan, *et al.*, Porous Fe3O4/C nano aggregates by the carbon polyhedrons as templates derived from the metal-organic framework as battery-type materials for supercapacitors, Electrochim. Acta 337 (2020), 135818.
[244] S. Xiong, X. Lin, S. Liu, S. Weng, S. Jiang, Y. Jiao, *et al.*, Metal-organic framework derived α-Fe2O3 nano-octahedron with oxygen vacancies for realizing outstanding energy storage performance, Vacuum 182 (2020), 109692.
[245] Q. Li, J. Zhou, S. Zhao, Y. Li, C. Chen, K. Tao, *et al.*, Hollow and hierarchical cobalt–metal-organic framework@ CoCr2O4 microplate array as a battery-type electrode for high-performance hybrid supercapacitors, ChemElectroChem 7 (2) (2020) 437–444.
[246] D. Chen, L. Wei, J. Li, Q. Wu, Nanoporous materials derived from a metal-organic framework for supercapacitor application, J. Energy Storage 30 (2020), 101525.
[247] N. Xin, Y. Liu, H. Niu, H. Bai, W. Shi, In-situ construction of metal-organic frameworks derived Co/Zn–S sandwiched graphene film as free-standing electrodes for ultra-high energy density supercapacitors, J. Power Sources 451 (2020), 227772.
[248] X. Du, J. Zhang, H. Wang, Z. Huang, A. Guo, L. Zhao, *et al.*, Solid-solid interface growth of conductive metal-organic framework nanowire arrays and their supercapacitor application, Mater. Chem. Front. 4 (1) (2020) 243–251.
[249] L. Wang, X. Feng, L. Ren, Q. Piao, J. Zhong, Y. Wang, H. Li, Y. Chen, and B. Wang, Flexible Solid-State Supercapacitor Based on a Metal-Organic Framework Interwoven by Electrochemically-Deposited PANI, J. Am. Chem. Soc., 137, (2015) 4920-4923.
[250] L. Shao, Q. Wang, Z. Ma, Z. Ji, X. Wang, D. Song, Y. Liu, and N. Wang, A high-capacitance flexible solid-state supercapacitor based on polyaniline and Metal-Organic Framework (UiO-66) composites, J. Power Sources, 379 (2018) 350-361.
[251] Q. Wang, L. Shao, Z. Ma, J. Xu, Y. Li, and C. Wang, Hierarchical porous PANI/MIL-101 nanocomposites based solid-state flexible supercapacitor**,** Electrochim. Acta, 281, (2018) 582-593.

[252] R. Hou, M. Miao, Q. Wang, T. Yue, H. Liu, H. S. Park, K. Qi, and B. Y. Xia, Integrated Conductive Hybrid Architecture of Metal–Organic Framework Nanowire Array on Polypyrrole Membrane for All-Solid-State Flexible Supercapacitors, Adv. Energy Mater., 10, 1901892 (2020).
[253] X. Xu, J. Tang, H. Qian, S. Hou, Y. Bando, M. S. A. Hossain, L. Pan, and Y. Yamauchi, Three-Dimensional Networked Metal–Organic Frameworks with Conductive Polypyrrole Tubes for Flexible Supercapacitors, ACS Appl. Mater. Interfaces, 9, (2017) 38737-38744.
[254] D. Tian, N. Song, M. Zhong, X. Lu, and C. Wang, Bimetallic MOF Nanosheets Decorated on Electrospun Nanofibers for High-Performance Asymmetric Supercapacitors**,** ACS Appl. Mater. Interfaces, 12, 1280 (2020).
[255]Y.-Z. Zhang, T. Cheng, Y. Wang, W.-Y. Lai, H. Pang, and W. Huang, A Simple Approach to Boost Capacitance: Flexible Supercapacitors Based on Manganese Oxides@MOFs via Chemically Induced In Situ Self-Transformation, Adv. Mater., 28, 5242 (2016).
[256] H. Duan, Z. Zhao, J. Lu, W. Hu, Y. Zhang, S. Li, M. Zhang, R. Zhu, and H. Pang, When Conductive MOFs Meet MnO_2: High Electrochemical Energy Storage Performance in an Aqueous Asymmetric Supercapacitor, ACS Appl. Mater. Interfaces, 13, (2021) 33083-33090.
[257] L. Kong, J. Zhu, W. Shuang, and X.-H. Bu, Nitrogen-Doped Wrinkled Carbon Foils Derived from MOF Nanosheets for Superior Sodium Storage**,** Adv. Energy Mater., 8, 1801515 (2018).
[258] W. Shuang, H. Huang, L. Kong, M. Zhong, A. Li, D. Wang, Y. Xu, and X.-H. Bu, Nitrogen-doped carbon shell-confined Ni_3S_2 composite nanosheets derived from Ni-MOF for high-performance sodium-ion battery anodes, Nano Energy, 62 (2019) 154-163.
[259] L. Kong, M. Zhong, W. Shuang, Y. Xu, and X.-H. Bu, Electrochemically active sites inside crystalline porous materials for energy storage and conversion, Chem. Soc. Rev., 49, (2020) 2378-2407.
[260] R. R. Salunkhe, Y. V. Kaneti, J. Kim, J. H. Kim, and Y. Yamauchi, Nanoarchitectures for Metal–Organic Framework-Derived Nanoporous Carbons toward Supercapacitor Applications, Acc. Chem. Res., 49 (2016) 2796-2806.
[261] Y. Liu, X. Xu, Z. Shao, and S. P. Jiang, Metal-organic frameworks derived porous carbon, metal oxides and metal sulfides-based compounds for supercapacitors application, Energy Storage Mater., 26, (2020) 1-22.
[262] N. L. Torad, R. R. Salunkhe, Y. Li, H. Hamoudi, M. Imura, Y. Sakka, C.-C. Hu, and Y. Yamauchi, Electric Double-Layer Capacitors Based on Highly Graphitized Nanoporous Carbons Derived from ZIF-67, Chem. Eur. J., 20, 7895 (2014).
[263] W. Chaikittisilp, M. Hu, H. Wang, H.-S. Huang, T. Fujita, K. C. W. Wu, L.C. Chen, Y. Yamauchi, and K. Ariga, Nanoporous carbons through direct carbonization of a zeolitic imidazolate framework for supercapacitor electrodes, Chem. Comm., 48, (2012) 7259-7261.

[264] J. Tang, R. R. Salunkhe, J. Liu, N. L. Torad, M. Imura, S. Furukawa, and Y. Yamauchi, Thermal Conversion of Core-Shell Metal-Organic Frameworks: A New Method for Selectively Functionalized Nanoporous Hybrid Carbon, J. Am. Chem. Soc., 137, (2015) 1572-1580.

[265] R. Yuksel *et al.*, Necklace-like Nitrogen-Doped Tubular Carbon 3D Frameworks for Electrochemical Energy Storage, Adv. Fun. Mater., 30, 1909725 (2020).

[266] P. Pachfule, D. Shinde, M. Majumder, and Q. Xu, Fabrication of carbon nanorods and graphene nanoribbons from a metal-organic framework, Nat. Chem., 8, (2016) 718-724.

[267] R. R. Salunkhe, Y. V. Kaneti, and Y. Yamauchi, Metal-Organic Framework-Derived Nanoporous Metal Oxides toward Supercapacitor Applications: Progress and Prospects, ACS Nano, 11, (2017) 5293-5308.

[268] W. Meng *et al.*, Porous Fe_3O_4/carbon composite electrode material prepared from metal-organic framework template and effect of temperature on its capacitance, Nano Energy, 8, (2014) 133-140.

[269] Z. Zhou, Q. Zhang, J. Sun, B. He, J. Guo, Q. Li, C. Li, L. Xie, and Y. Yao, Metal-Organic Framework Derived Spindle-like Carbon Incorporated α-Fe_2O_3 Grown on Carbon Nanotube Fiber as Anodes for High-Performance Wearable Asymmetric Supercapacitors, ACS Nano, 12, (2018) 9333-9341.

[270]K. Wang, Z. Wang, J. Liu, C. Li, F. Mao, H. Wu, and Q. Zhang, Tuning Oxygen Redox Reaction through the Inductive Effect with Proton Insertion in Li-Rich Oxides, ACS Appl. Mater. Interfaces, 12 (2020)7277-7284.

[271] X. Wei, Y. Song, L. Song, X. D. Liu, Y. Li, S. Yao, P. Xiao, and Y. Zhang, Phosphorization Engineering on Metal–Organic Frameworks for Quasi-Solid-State Asymmetry Supercapacitors, Small, 17 (2021) 2007062.

[272] S. He, F. Guo, Q. Yang, H. Mi, J. Li, N. Yang, and J. Qiu, Design and Fabrication of Hierarchical NiCoP–MOF Heterostructure with Enhanced Pseudocapacitive Properties, Small, 17(2021) 2100353.

[273] Q. Wang, Y. Luo, R. Hou, S. Zaman, K. Qi, H. Liu, H. S. Park, and B. Y. Xia, Redox Tuning in Crystalline and Electronic Structure of Bimetal–Organic Frameworks Derived Cobalt/Nickel Boride/Sulfide for Boosted Faradaic Capacitance, Adv. Mater., 31, 1905744 (2019).

[274] W. Zhao, G. Yan, Y. Zheng, B. Liu, D. Jia, T. Liu, L. Cui, R. Zheng, D. Wei, and J. Liu, Bimetal-organic framework derived $Cu(NiCo)_2S_4/Ni_3S_4$ electrode material with hierarchical hollow heterostructure for high-performance energy storage, J. Colloid Interface Sci., 565 (2020) 295-304.

[275] Q. Yang, Q. Wang, Y. Long, F. Wang, L. Wu, J. Pan, J. Han, Y. Lei, W. Shi, and S. Song, In Situ Formation of Co_9S_8 Quantum Dots in MOF-Derived Ternary Metal Layered Double Hydroxide Nanoarrays for High-Performance Hybrid Supercapacitors, Adv. Energy Mater., 10, 1903193 (2020).

[276] L. Wang, D. Jia, L. Yue, K. Zheng, A. Zhang, Q. Jia, and J. Liu, In Situ Fabrication of a Uniform Co-MOF Shell Coordinated with $CoNiO_2$ to Enhance the Energy Storage Capability of NiCo-LDH via Vapor-Phase Growth, ACS Appl. Mater. Interfaces, 12, (2020) 47526-47538.

[277] C. Zhong, Y. Deng, W. Hu, J. Qiao, L. Zhang, J. Zhang, A review of electrolyte materials and compositions for electrochemical supercapacitors, Chem. Soc. Rev. 44 (21) (2015) 7484–7539.
[278] B. Pal, S. Yang, S. Ramesh, V. Thangadurai, R. Jose, Electrolyte selection for supercapacitive devices: a critical review, Nanoscale Adv. 1 (10) (2019) 3807–3835.
[279] R. Rajak, M. Saraf, S.M. Mobin, Mixed-ligand architected unique topological heterometallic sodium/cobalt-based metal-organic framework for high-performance supercapacitors, Inorg. Chem. 59 (3) (2020) 1642–1652.
[280] G. Hasegawa, K. Kanamori, T. Kiyomura, H. Kurata, T. Abe, K. Nakanishi, Hierarchically porous carbon monoliths comprising ordered mesoporous nanorod assemblies for high-voltage aqueous supercapacitors, Chem. Mater. 28 (11) (2016) 3944–3950.
[281] L. Suo, O. Borodin, T. Gao, M. Olguin, J. Ho, X. Fan, *et al.*, Water-in-salt" electrolyte enables high-voltage aqueous lithium-ion chemistries, Science 350 (6263) (2015) 938–943.
[282] Y. Yamada, K. Usui, K. Sodeyama, S. Ko, Y. Tateyama, A. Yamada, Hydrate-melt electrolytes for high-energy-density aqueous batteries, Nat. Energy 1 (10) (2016) 1–9.
[283] M. Yu, D. Lin, H. Feng, Y. Zeng, Y. Tong, X. Lu, Boosting the energy density of carbon-based aqueous supercapacitors by optimizing the surface charge, Angew. Chem. 129 (20) (2017) 5546–5551.
[284] Z. Zhou, L. Miao, H. Duan, Z. Wang, Y. Lv, W. Xiong, *et al.*, Highly active N, O- doped hierarchical porous carbons for high-energy supercapacitors, Chin. Chem. Lett. 31 (5) (2020) 1226–1230.
[285] Z. Shi, X. Yu, J. Wang, H. Hu, C. Wu, Excellent low-temperature performance electrolyte of spiro-(1, 1′)-bipyrrolidinium tetrafluoroborate by tunable mixtures solvents for electric double layer capacitor, Electrochim. Acta 174 (2015) 215–220.
[286] X. Yu, D. Ruan, C. Wu, J. Wang, Z. Shi, Spiro-(1, 1′)-bipyrrolidinium tetrafluoroborate salt as high voltage electrolyte for electric double layer capacitors, J. Power Sources 265 (2014) 309–316.
[287] Y.K. Ahn, B. Kim, J. Ko, D.J. You, Z. Yin, H. Kim, *et al.*, All solid state flexible supercapacitors operating at 4 V with a cross-linked polymer–ionic liquid electrolyte, J. Mater. Chem. A 12 (4) (2016) 4386–4391.
[288] Y. Cho, C. Hwang, D.S. Cheong, Y. Kim, H. Song, Gel/solid polymer electrolytes characterized by in situ gelation or polymerization for electrochemical energy systems, Adv. Mater. 31 (20) (2019), 1804909.
[289] Z. Song, D. Zhu, L. Li, T. Chen, H. Duan, Z. Wang, *et al.*, Ultrahigh energy density of an N, O codoped carbon nanosphere based all-solid-state symmetric supercapacitor, J. Mater. Chem. A 7 (3) (2019) 1177–1186.
[290] Z. Song, D. Zhu, D. Xue, J. Yan, X. Chai, W. Xiong, *et al.*, Nitrogen-enriched hollow porous carbon nanospheres with tailored morphology and microstructure for all-solid-state symmetric supercapacitors, ACS Appl. Energy Mater. 1 (8) (2018) 4293–4303.

[291] W. Kang, L. Zeng, S. Ling, C. Zhang, 3D printed supercapacitors toward trinity excellence in kinetics, energy density, and flexibility, Adv. Energy Mater. 11 (12) (2021), 2100020.
[292] K. Xu, Nonaqueous liquid electrolytes for lithium-based rechargeable batteries, Chem. Rev. 104 (10) (2004) 4303–4418.
[293] A. Bhide, J. Hofmann, A.K. Dürr, J. Janek, P. Adelhelm, Electrochemical stability of non-aqueous electrolytes for sodium-ion batteries and their compatibility with Na 0.7 CoO2, Phys. Chem. Chem. Phys. 16 (5) (2014) 1987–1998.
[294] A. Ponrouch, E. Marchante, M. Courty, J.M. Tarascon, M.R. Palacín, In search of an optimized electrolyte for Na-ion batteries, Energy Environ. Sci. 5 (9) (2012) 8572–8583.
[295] C.H. Wang, Y.W. Yeh, N. Wongittharom, Y.C. Wang, C.J. Tseng, S.W. Lee, *et al.*, Rechargeable Na/NaO. 44MnO2 cells with ionic liquid electrolytes containing various sodium solutes, J. Power Sources 274 (2015) 1016–1023.
[396]Waris, Abdul HakeemAnwer, Fahad Abdulaziz, Salman Latif, Abdulaziz Alanazi, Saima S ultana [a], Mohammad Zain Khan, Microwave-assisted green synthesis of high capacitive TiO_2 doped rGO nanosheets for supercapacitor applications**,** Materials Science and Engineering: B 291(2023) 116367.